# Biodegradation and electro-assisted biodegradation of 1,4-dioxane under different electron accepting conditions

By

Aryan Samadi

Submitted in partial fulfilment of the requirements for the degree of Doctor of Philosophy

at

Dalhousie University
Halifax, Nova Scotia
August 2023

*To my parents, Mehrangiz and Hossein, and my sister, Aida, who always believed in me and provided me with unconditional support*

## Table of Contents

## List of Tables

## List of Figures

## Abstract

1,4-Dioxane (DX) is an emerging contaminant of concern in water resources. In the past, it was commonly utilized to stabilize chlorinated solvents, and it has now been discovered as a contaminant present in various personal care and food products. DX is also used in many industries including plastics and polymers, adhesiveness and sealants, and pharmaceuticals. Therefore, discharge from industrial processes is the major route of DX release to the water bodies. Once discharged to the environment, DX mostly ends up in groundwaters and is persistent (half-life of 3-5 years) and causes ecological and human health impacts if exposed (a probable carcinogen).

This thesis focuses on developing novel, green and effective processes for removal of 1,4-dioxnae from water. The main objective was to fill the knowledge gaps in the literature about (1) DX biodegradation in low dissolved oxygen concentrations, (2) effect of carrier's properties on growth of DX-degrading biofilm, and (3) mechanisms of electrochemical stimulation of DX biodegradation. In order to answer the related research questions to each gap, experiments were designed systematically and performed in lab-scale batch or continuous reactors using pure culture or microbial community as the inoculation source.

Experiments conducted under low dissolved oxygen concentrations (between 1-3 mg/L) demonstrated that the biodegradation of DX occurred at a very slow rate (0.21 mgDX/L/day) when external sources of oxygen were not provided. As time passed, the overall diversity and richness of the microbial community decreased, though certain genera, such as *Pseudonocardiaceae*, *Xanthobacteraceae*, and *Chitinophagaceae*, were able to thrive by using DX as a carbon source. These findings suggest that the microbial community has the ability to adapt to different electron-accepting conditions, which could be beneficial for in-situ bioremediation or natural attenuation of DX in water resources.

Experiments conducted on delignified porous wood as biofilm carriers demonstrated an improvement in biofilm formation in terms of growth rate and hydrophilicity compared to natural untreated wood as biofilm carriers. This improvement was attributed to the superior physiochemical properties of the treated wood, which exhibited higher porosity, formation of macropores, and an increase in surface roughness and hydrophilicity compared to untreated wood. Moreover, the rate of DX biodegradation increased by 5.33-fold when treated woods were used as carriers compared to untreated woods. These findings shed light on the physiochemical properties of biofilm carriers that contribute to biofilm formation and can be valuable for ongoing research on DX bioremediation.

The experiments on electrochemical stimulation of DX biodegradation in a continuous flow bioelectrochemical reactor revealed that two different mechanisms could be responsible for the observed stimulation at low applied voltages between 1.0-1.2 V. One mechanism was attributed to the production of oxygen as a result of the water electrolysis reaction occurring at 1.2 V. This oxygen could then serve as a source of electron acceptor for aerobic microorganisms in the medium. The other mechanism was linked to an increase in microbial population activity due to electrochemical stimulation at 1.0 V. The analysis of changes in microbial composition revealed the enrichment of *Alistipes* and *Lutispora* at 1.0 V, which was attributed to their ability to directly transfer electrons with a conductive surface. The results can be helpful to issue the challenge of lack of electron acceptors in DX bioremediation.

## List of Abbreviations

| | |
|---|---|
| ABR | Anaerobic baffled reactor |
| AHL | N-acyl homoserine lactone |
| AMO | Ammonia monooxygenase |
| AMS | Ammonium mineral salts |
| ANOVA | Analysis of variance |
| AOPs | Advanced oxidation processes |
| ATP | Adenosine triphosphate |
| BAME | bacterial acid methyl esters |
| BER | bioelectrochemical reactor |
| BFA | branched fatty acids |
| BOD | Biological oxygen demand |
| BSTFA | bis-(trimethyl-silyl)-trifluoroacetamide |
| B5 | *Pseudonocardia benzenivorans* B5 |
| CB1190 | *Pseudonocardia dioxanivorans* CB1190 |
| CDC | cells direct count |
| cDCE | cis-1,2-dichoroethene |
| CEC | Contaminant of emerging concern |
| COD | chemical oxygen demand |
| CrI | Crystallinity index |
| DBT | di-benzothiophene |
| DCM | dichloromethane |
| DO | dissolved oxygen |
| DX | 1,4-dioxane |
| DX-d8 | 1,4-dioxane-d8 |
| DXMO | Dioxane Monooxygenase |
| EPA | Environmental Protection Agency |
| EPS | extracellular polymeric substance |
| FA | fatty acid |
| FAME | fatty acid methyl esters |
| FID | flame ionization detection |
| GC/MS | Gas Chromatography Mass Spectrophotometry |
| GG | graphite granules |
| HA | humic acid |
| HEAA | 2-Hydroxyethoxy acetic acid |
| HFA | hydroxy fatty acids |
| HGT | Horizontal gen transfer |
| HPLC | high-performance liquid chromatography |
| IARC | International Agency for Research on Cancer |
| LLE | liquid-liquid extraction |
| MO | monooxygenase enzyme |
| MS | mineral salts |

| | |
|---|---|
| MTBE | Methyl tert-butyl ether |
| ORP | oxidation reduction potential |
| OUT | operational taxonomic unit |
| PAHs | polycyclic aromatic hydrocarbons |
| PCBs | polychlorinated biphenyls |
| PCR | polymerase chain reaction |
| POPs | persistent organic pollutants |
| QS | Quorum sensing |
| SEM | scanning electron microscopy |
| SFA | saturated fatty acids |
| SHE | standard hydrogen electrode |
| STD | standard deviation |
| TCA | 1,1,1-trichloroethane |
| TCE | trichloroethylene |
| THF | tetrahydrofuran |
| UFA | unsaturated fatty acids |
| VFAs | volatile fatty acids |
| VSS | Volatile suspended solids |
| XRD | X-ray diffraction |
| 1,1-DCE | 1,1-dichloroethene |

## Acknowledgements

I would like to express my heartfelt gratitude to Dr. Azadeh Kermanshahipour, my supervisor, for her unlimited support throughout my PhD journey. She provided invaluable feedback, discussed ideas, and supervised my work. I am also grateful to her for being understanding and supportive during the times when I was not feeling well.

I would also like to extend my appreciation to Dr. Suzanne Budge and Dr. Rob Jamieson for their participation in my supervisory committee and for providing valuable feedback.

Furthermore, I would like to thank Dr. Chunbao Charles Xu and Dr. Ramon Filipe Beims for their support and feedback on the fourth chapter of my thesis. I greatly enjoyed our online meetings and learned a lot from them. Dr. Budge also deserves special thanks for her help with analyzing GC/MS results and metabolite identification procedures. Dr. Yannan Huang's help with bioinformatic analysis and Dr. Stanislav Sokolenko's insights on statistical analysis of the experiments were also greatly appreciated.

Thank you, Julie O'Grady and Paula Colicchio from the PEAS department, and John Pyke for his technical assistance.

I would like to acknowledge the ASPIRE program for providing financial support and opportunities for practical training and professional development. I am also grateful to the SEM facility and IMR center, laboratories of Dr. Jeff Dahn and Dr. Su-Ling Brooks, and protein assembly research team at Dalhousie University for providing equipment and assisting with measurements and analysis.

My colleagues in the biorefinery and remediation laboratory, Pawan Kumar, Jianan Lin, Khashayar Bahri and Lauren MacEachern, were very helpful to me as they made my PhD experience enjoyable. They were always available to offer help and support, and made the lab feel like a second home. Finally, special thanks to Leila Rezaei for her constant encouragement and support during the most challenging moments.

# Chapter 1 Introduction

## 1.1 1,4-dioxane

1,4-dioxane ($C_4H_8O_2$) is a heterocyclic organic compound (**Figure 1-1**) which is considered as a contaminant of emerging concern (CEC) by United States Environmental Protection Agency (EPA) (EPA, 2017, 2020a). EPA defines CECs as chemicals that are being detected in water resources, which may cause ecological and human health impacts, and are not well regulated under current environmental laws (EPA, 2019). In the EPA's final evaluation report of 1,4-dioxane, no unreasonable risks to the environment, consumers, bystanders, or the general population was found (EPA, 2020b). Additionally, EPA has released the 2023 Draft Revised Risk Determination for 1,4-Dioxane using the information in the 2020 risk evaluation and the 2023 draft supplement (EPA, 2023). Because 1,2- and 1,3-dioxane are rare isomers, 1,4-dioxane is often simply called dioxane (DX hereafter in this document). The maximum acceptable concentration of DX in Canadian drinking water is 0.050 mg/L according to the Health Canada (https://www.canada.ca/en/health-canada/services/publications/healthy-living/water-talk-1-4-dioxane-drinking-water.html). This level protects the health of all Canadians, including the most vulnerable members of society, such as infants and children.

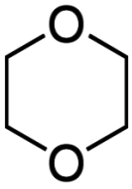


Figure 1-1 Chemical structure of 1,4-dioxane.

DX has been historically used as a stabilizer in chlorinated solvents, especially in 1,1,1-trichloroethane (TCA) (Mohr et al., 2020). In addition, it is used in the production of pesticides, paints, dyes, plasticizers, cosmetics, and personal care products (Zhang et al., 2017). Improper disposal regulations caused huge amount of release to the environment. In the United States for instance, approximately 617,000 pounds

was released to the industrial wastewaters in 2017 (Pollitt et al., 2019). Most of the industrial wastewater treatment plants are not capable of DX treatment (Stepien et al., 2014). In addition, DX can be released into air through volatilization of paints and dyes, and to soil through dispose of cosmetics and food packaging into landfills.

The dimensionless Henry's Law constant of DX is $H' = 1.96 \times 10^{-4}$ which has been reported by EPA as an experimentally measured value (EPA-DSSTox, 2021). Given this Henry's Law constant, DX is considered as a slightly volatile compound according to the classification presented by Allen and Shonnard (Allen and Shonnard, 2001). Thus, the occurrence of DX in the atmosphere is not a major concern. Its occurrence in soil is also negligible due to its low soil organic carbon distribution coefficient, $K_{OC}$=17 $L.kg^{-1}$, which has also been reported by EPA as an experimentally measured value (EPA-DSSTox, 2021). According to the classification based on log $K_{OC}$ presented by Allen and Shonnard (2001), DX is a compound with a negligible partitioning into soil compared to aqueous phase, indicating higher mobility of DX in the wet soils compared to dry soil. Therefore, it easily leaches to water resources mainly groundwaters. Groundwaters are the main concern for occurrence of DX because of its high solubility, $S_w$=11.35 M or 1000 $g.L^{-1}$, which has been reported by EPA as an experimentally measured value (EPA-DSSTox, 2021). According to the classification of Allen and Shonnard based on water solubility, DX is a very soluble compound (Allen and Shonnard, 2001). Furthermore, its octanol-water partition coefficient is experimentally measured at log $K_{OW}$=-0.27, according to EPA (EPA-DSSTox, 2021). The reported experimental value of octanol-water partition coefficient is classified as low bioaccumulation potential according to Allen and Shonnard's guideline (Allen and Shonnard, 2001; EPA-DSSTox, 2021), indicating higher potential of DX to partition into groundwater compared to organic matter and tissue of organisms.

DX is considered as a non-biodegradable compound under traditional wastewater treatment plants (Stepien et al., 2014). Although DX has not been added to the list of persistent organic pollutants (POPs) so far (Nadal et al., 2015), its extreme persistency in groundwater (3-5 years half-life) has made it one of

the most prevalent contaminants in public water supplies (Pollitt et al., 2019). A study on more than 2000 sites in California's groundwaters demonstrated that 194 sites were contaminated with DX with the median concentration of 365 $\mu g.L^{-1}$ (Adamson et al., 2014). Moreover, according to the data collected by Unregulated Contaminant Monitoring Rule, DX was detected in 21% of the measured samples of 4915 public drinking water systems in the United States with highest detected concentration of 34 $\mu g.L^{-1}$ (Adamson et al., 2017). These values are several orders of magnitude higher than health risk guideline level of 0.35 $\mu g.L^{-1}$ which has been announced by EPA (EPA, 2017).

DX adversely affects the environment and causes health problems for living organisms. Although bioaccumulation of DX in living organisms' bodies is not a major concern because of its low $K_{OW}$ and accordingly low bioconcentration factor (log BCF=0.501, an experimental value reported by EPA, EPA-DSSTox (2021)), its chronic exposure results in severe health consequences. For instance, studies on rats have proved the carcinogenic effects of DX in drinking water. Sixteen weeks of exposure to high concentration levels of DX (200-5000 ppm) was enough for damage to the DNA of the liver cells in rats (Gi et al., 2018). Furthermore, DX is exposed to human through several ways including consumption of contaminated water and food, being in contact with consumer products that contain DX, and inhalation of the contaminated air (Bilal and Iqbal, 2019). However, epidemiological studies have not been yet conducted on the exact health effects of DX on human. Based on the extensive studies on carcinogenic effects of DX on animals and lack of studies on humans, the International Agency for Research on Cancer (IARC) have classified DX in group B2 as a possible carcinogenic chemical (Stepien et al., 2014).

Different remediation approaches have been studied for treatment of DX including biological, chemical and physical methods (Zhang et al., 2017). Although it has been indicated by several studies that chemical technologies such as advanced oxidation processes (AOPs) are highly efficient for removal of DX (Boving et al., 2014; Zhao et al., 2014), introduction of active chemical reagents such as hydrogen peroxide or ozone to the environment can have adverse effects on the environment, limiting the application of these

technologies. Furthermore, application of these technologies generates exceeding costs due to the high energy demand and chemical consumption. A general concern with the physical remediation methods is transferring the organic contaminants from one media to the other, without any degradation. In addition, they are not considered as appropriate remediation methods for DX because of its low octanol water partition coefficient, high solubility and low Henry's law constant (Zhang et al., 2017). Therefore, physical technologies such as air-stripping and adsorption by activated carbon have not been reported as efficient methods for DX treatment (Pollitt et al., 2019). Biological remediation methods, on the other hand, consume less energy and are generally less expensive compared to abiotic remediation methods such as chemical oxidation or adsorption. Furthermore, they are more environmentally friendly methods because they are conducted in ambient condition and do not require addition of active materials into the environmental media (Nancharaiah and Venugopalan, 2019). Bioremediation of DX is a promising approach which has been the focus of research on DX treatment in recent years (Zhang et al., 2017). However, certain challenges are remaining in DX bioremediation systems including scarcity of DX-degrading microorganisms, lack of electron acceptors and co-contaminant effects of chlorinated solvents.

Use of biofilm engineered systems have been studied for bioremediation of emerging and persistent organic contaminants (Edwards and Kjellerup, 2013). These systems have some advantages over suspended biomass bioremediation processes and, in general, over other remediation technologies. Low cost, retention of biomass in the system, higher resistance to environmental stresses and toxic chemicals, and increased bioavailability are all among advantages of biofilm-mediated bioremediation systems (Rittmann and McCarty, 2001). Furthermore, biofilm can respond to the environmental condition changes and different organic pollutants through intrinsic processes such as quorum sensing and chemotaxis (Nancharaiah and Venugopalan, 2019). Coupling electrochemical stimulation with biofilm-mediated bioremediation systems is an emerging and promising approach for overcoming the limitations of emerging contaminant remediation in groundwaters (Li and Yu, 2015). Electrocatalytic biofilm is formed

on the electrodes when exoelectrogenic microbial species cooperate with the polarized electrodes for electron transfer of their metabolism. Electro-assisted bioremediation enhances the contaminant removal process through several mechanisms, including direct supply of electron donor/acceptor by electrodes, electrokinetic enhancement of the environment around the electrodes by inducing electromigration and electrophoresis processes, and increasing the bioavailability by adsorption of pollutant and enrichment of biofilm on the electrodes (Li and Yu, 2015). Since electro-assisted bioremediation is a new technology with mostly unrevealed processes, microbial-electrode, microbial-pollutant and microbial-microbial interactions need to be investigated thoroughly in these systems.

## 1.2 Research objectives

The overall goal of this research is to investigate the feasibility of integrating bioremediation system with electrochemical stimulation to overcome the most important challenge in DX biodegradation (i.e., lack of electron acceptors). Therefore, the following objectives are considered in this research to meet the overall goal:

- Investigation of DX biodegradation in different electron accepting conditions, temperatures and presence of co-contaminant (Chapter 3)
- Understanding the responses of the microbial community in different electron accepting conditions (Chapter 3)
- Identification of the DX-degrading genera in the microbial community (Chapter 3)
- Investigation of the biofilm-mediated bioremediation: effective parameters on the biofilm formation and characterization of the DX-degrading biofilm (Chapter 4)
- Comparison of the DX biodegradation rate between the biofilm and suspended cultures (Chapter 4)

- Evaluation of the electrical stimulation on DX biodegradation by biofilm on conductive carriers in a bioelectrochemical reactor (BER) (Chapter 5)
- Developing understanding on the responses of the microbial community to the electrical stimulation (Chapter 5)
- Evaluation of the BER performance in DX removal in different voltages. (Chapter 5)

## 1.3 Scope

In this section, the focus, boundaries, and limitations of the performed experiments in each chapter have been discussed.

Research chapter 3 aims to explore the potential of a native digestate microbial community for the biodegradation of DX under low dissolved oxygen (DO) concentrations. The focus of the study is to evaluate the ability of this microbial community to break down DX when exposed to varying conditions, including different electron acceptors, co-substrates, co-contaminants, and temperatures.

The investigation specifically examines the biodegradation of DX at an initial concentration of 25 mg/L. The microbial community's behavior is studied under low DO concentrations ranging from 1 to 3 mg/L, without the provision of external aeration. Additionally, the study considers various electron-accepting conditions, including unamended flasks, nitrate-amended conditions, and aerated environments. Furthermore, the research investigates the influence of co-substrates and co-contaminants on the DX biodegradation process. The identification of oxalic acid as a common metabolite during DX biodegradation is a significant aspect of the study. The impact of temperature on DX biodegradation is also investigated, with a focus on two specific temperatures: 30 ˚C and ambient conditions (20-25 ˚C). The comparison between these two temperatures provides insights into how temperature affects the efficiency of DX biodegradation by the native digestate microbial community. The study also monitors the transition of the microbial community during the DX biodegradation period.

Despite the valuable insights provided by the research, it is important to acknowledge certain limitations. The study focuses on a specific initial concentration of DX (25 mg/L), and its findings may not be fully representative of the microbial community's behavior at other concentrations. Additionally, the exploration of DX biodegradation is limited to low DO concentrations (1-3 mg/L), and the community's response at higher DO levels remains unexplored. The study also does not comprehensively investigate all possible electron acceptors, co-substrate, and co-contaminant combinations that may be encountered in real-world scenarios. Moreover, while the research examines two temperatures, it may not encompass the entire range of temperature conditions present in different environments. Finally, the study's generalizability may be limited since it focuses on a specific native digestate microbial community, and its applicability to other microbial communities or environments requires cautious consideration.

Research chapter 4 explores the use of delignified porous wood samples as carriers to facilitate biofilm formation of a bacterial consortium capable of degrading DX. The main focus of the study is to investigate how the delignification treatment affects the physical and chemical properties of the wood carriers and, in turn, influences biofilm growth and the biodegradation of DX.

Treated carriers are compared to untreated wood carriers to assess their impact on biofilm development. The delignification treatment affects the wood samples regarding porosity, the formation of macropores, surface roughness, and hydrophilicity, which are the important characteristics of biofilm carriers. Additionally, the study investigates the fatty acid profiles during biofilm formation, which may be linked to the carriers' characteristics and further biodegradation capabilities of the biofilm. In addition, the research employs the Monod model to analyze the DX biodegradation data, enabling a comparison between biodegradation rates by biofilm versus suspended biomass.

While the findings provide valuable insights into the biofilm formation process concerning the physical and chemical properties of carriers, there are certain limitations to consider. The study focuses on a

specific bacterial consortium, and the results may not be directly applicable to other microbial communities. Moreover, the batch lab-scale experiments cannot capture long-term effects or steady-state conditions in DX biodegradation. Additionally, while the Monod model helps in understanding growth rates, it may not fully capture the complexities of biofilm behavior and DX degradation kinetics. Furthermore, the initial concentration of 100 mg/L of DX is not representative of the bioavailability limiting factor, which is sometimes important in real word situations.

Research chapter 5 explores the application of bioelectrochemical degradation as an environmentally friendly, cost-effective, and controllable method for enhancing the biodegradation of DX. To achieve this, a continuous-flow bioelectrochemical reactor (BER) is developed and utilized to investigate the potential of two different approaches: the use of *Pseudonocardia dioxanivorans* CB1190 (CB1190) and a microbial community biofilm on both conductive and non-conductive carriers. The primary focus is on examining the effect of low voltages (ranging from 1.0 V to 1.2 V) and currents (<2 mA) on DX removal efficiency. Furthermore, the study investigates possible mechanisms of DX biodegradation enhancement under electro-assisted conditions considering the changes in the microbial composition and activity of the biofilm.

Although the research highlights the potential of low-voltage electro-assisted biodegradation for DX removal, there are certain limitations to consider. The specific strain CB1190 and the microbial community biofilm used in the study may not be directly applicable to other microbial species or consortia. Additionally, while the study identifies the enrichment of specific microbial genera at 1.0 V, the underlying reasons for this enrichment require further investigation. Moreover, other potential electron transfer pathways that could contribute to DX degradation are not extensively explored.

# Chapter 2 Literature review

## 2.1 Bioremediation of DX

### 2.1.1 Fundamentals of bioremediation

Bioremediation is a process that uses living organisms, such as bacteria, fungi, or plants, to detoxify, degrade, or remove pollutants or contaminants from soil, water, or air. It is an environmentally friendly and sustainable approach to cleaning up polluted environments. Biological technologies use living organisms to remove organic pollutants from the environment. They include bacterial degradation, fungal degradation, and phytoremediation. Biodegradation is the most prevalent method among biological technologies, which has been extensively applied for remediation of organic pollutants (Rittmann and McCarty, 2012). Biodegradation refers to the breakdown or transformation of organic substances into simpler, naturally occurring compounds by the action of living organisms, mainly microorganisms like bacteria and fungi.

In bacterial degradation, bacteria degrade organic pollutants for metabolism. There are several mechanisms for degradation of organic pollutants by bacteria. First, bacteria degrade organic pollutants as electron donors (catabolism) when electrons are received by bacterial electron carrier molecules (e.g., $NAD^+$). In this mechanism, existence of an electron acceptor such as oxygen or nitrate is also necessary to receive the electron from electron carriers (Rittmann and McCarty, 2001). This class of bacteria is called aerobic bacteria since oxygen is usually the electron acceptor. For instance, Parales et al. (1994) reported for the first time that DX can be aerobically degraded by *Pseudonocardia dioxanivorans* CB1190 when $CO_2$ is the carbon source of the bacterium. The half reactions of DX oxidation are presented in equations 1 and 2 which provides energy for the bacterial metabolism.

Donor: $$\frac{1}{20}C_4H_8O_2 + \frac{3}{10}H_2O \rightarrow \frac{1}{5}CO_2 + H^+ + e^- \quad (1)$$

Acceptor: $\frac{1}{4}O_2 + H^+ + e^- \rightarrow \frac{1}{2}H_2O$ (2)

In the second mechanism, organic pollutants can be reduced by receiving electrons from bacterial electron carrier molecules (Rittmann and McCarty, 2001). In this mechanism, existence of another chemical such as hydrogen or acetate is necessary to be the electron donor. This class of bacteria is called anaerobic bacteria because the mechanism is conducted in the absence of oxygen. For instance, He et al. (2005) isolated a bacterium identified as *Dehalococcoides* sp. strain FL2, which anaerobically degrades trichloroethylene (TCE) when hydrogen serves as the electron donor and acetate as the carbon source for growth of the bacterium. The half reactions of TCE reductive dechlorination are presented in equations 3 and 4, which provides energy for metabolism of the bacterium.

Donor: $\frac{1}{2}H_2 \rightarrow H^+ + e^-$ (3)

Acceptor: $\frac{1}{6}C_2HCl_3 + \frac{1}{2}H^+ + e^- \rightarrow \frac{1}{6}C_2H_4 + \frac{1}{2}Cl^-$ (4)

There is another mechanism of biodegradation called co-metabolic degradation. In this mechanism, bacteria degrade a more easily degradable compound such as methane or glucose for growth. The enzyme produced by bacteria to degrade the first substrate (easily degradable compound), simultaneously degrades the target pollutant (second substrate). For instance, Oldenhuis et al. (1989) used a methanotrophic bacterium, *Methylosinus trichosporium* OB3b, which uses methane as the sources of carbon and energy for growth to co-metabolically degrade TCE. The bacterium produces methane monooxygenase for catabolism of methane, which also degrades TCE. The half reactions of methane and TCE oxidation are presented in equations 5 to 7.

Donors: $\frac{1}{8}CH_4 + \frac{1}{4}H_2O \rightarrow \frac{1}{8}CO_2 + H^+ + e^-$ (5)

$\frac{1}{6}C_2HCl_3 + \frac{2}{3}H_2O \rightarrow \frac{1}{3}CO_2 + \frac{1}{2}Cl^- + \frac{3}{2}H^+ + e^-$ (6)

Acceptor: $\frac{1}{2}O_2 + 2H^+ + 2e^- \rightarrow H_2O$ (7)

All of these mechanisms can be applied in situ and ex situ, and in all environments such as water, soil and sediments for bioremediation of the organic pollutants (Gaur et al., 2018). The success of microbial degradation process mainly depends on utilization of the right kind of bacteria, suitability of temperature and pH, availability of the required nutrients and moisture, presence of the necessary electron donors and acceptors, non-existence of co-contaminants, and bioavailability of the organic pollutants to the bacteria (Tyagi et al., 2011). Therefore, these are the main challenges to be addressed in design of any bioremediation process.

### 2.1.2 Non-aerated bioremediation of DX

Almost all studies in the literature on DX biodegradation include use of aerobic species (Zhang et al., 2017). However, a few studies have reported the possibility of DX biodegradation in low dissolved oxygen concentrations, where no external aeration is provided. These studies are summarized in **Table 2-1**.

Shen et al. (2008) reported biodegradation of DX by iron (III) reducing microorganisms. They used anaerobic sludge of a municipal wastewater treatment plant for the initial inoculation. Experiments were conducted in 250 mL flasks containing 150 mL MS medium that was boiled and fluxed by $N_2$ to remove the dissolved oxygen. Medium was amended with Fe(III)-EDTA as the electron acceptor of the biodegradation process. They also indicated that addition of Humic acid as the co-substrate positively affects degradation of the DX. In presence of Fe(III)-EDTA (30 mM) and Humic acid (0.5 g/L), and 10 g/L sludge inoculation, they achieved to around 90% removal of 13 mg/L initial DX in 40 days. This is the most remarkable anaerobic degradation of DX reported in the literature.

Ramalingam and Cupples (2020) investigated biodegradation of DX by indigenous cultures from several sources including 3 samples from uncontaminated agricultural soils, 2 samples from uncontaminated river

sediments, and 2 samples from contaminated sites (not mentioned what the sites were) in California and Maine. Experiments were conducted in 70 mL flasks containing 55 mL medium inoculated by 20 g/L (soil/sediment) of samples. They added Fe(III)-EDTA, nitrate salt and sulfate salt to the flasks as the electron acceptors, or added no electron acceptor to the control flasks reaching the total flask numbers to 18. DX concentration in days 20, 40, 200 and 300 after the start day of experiments was measured. In almost all the flasks, no noticeable degradation percentage was reported even after 300 days of the start of experiment except in one flask (around 50 % removal after 300 days) which had not been amended with electron acceptors and contained the inoculum from contaminated site in Maine. Initial concentration of DX was in the range of 4-6 mg/L in all the flasks.

Lee et al. (2014) investigated biodegradation of DX in an anaerobic digestion process. They developed a pilot-scale (3 $m^3$) CSTR reactor for anaerobic digestion of a chemical fiber manufacturing wastewater that contained 11,480 mg/L COD and 252 mg/L DX. The mixed liquor suspended solids inside the anaerobic digestion reactor was reported to be 14,480 mg/L and it included a sludge recycle system. When no specific amendment was added for DX biodegradation, 40-50% removal was reported in the reactor with hydraulic retention time (HRT) of 1.5 to 9.2 days. They speculated that DX is degraded when the produced acetic acid during acidogenesis stage of anaerobic digestion works as the co-substrate of the DX biodegradation process based on a previous study that proposed this biodegradation mechanism for DX (Raj et al., 1997).

Table 2-1 Studies reported biodegradation of DX using anaerobic microorganisms.

| Type and origin of microorganism | Environmental condition | Reference |
|---|---|---|
| Origin: municipal wastewater treatment sludge<br><br>Type: Fe(III)-reducing bacterium | Media: MS medium<br>Electron donor: DX<br>Electron acceptor: Fe(III)-EDTA<br>Co-substrate: Humic acid/none<br>Co-contaminant: N/A<br>Metabolites: $CO_2$<br>Degradation pathway: N/A | (Shen et al., 2008) |

| | | |
|---|---|---|
| | Flask condition: 250 mL, 10 g/L sludge, pH: 7.2, 30 ˚C<br>Range of DX, time, and degradation: 10-60 ppm, 40-120 days, 10-100 %removal | |
| Origin: uncontaminated agricultural soil / uncontaminated river sediment / contaminated sites (with DX and chlorinated solvents)<br><br>Type:<br>Phylotype: *Comamonadaceae (unclassified) / 3 genus incertae sedis*<br>Genus: *Pseudomonas and Rhodanobacter* | Media: Basal salts media/none<br>Electron donor: DX<br>Electron acceptor: Iron/nitrate/sulfate/none<br>Co-substrate: Lactate/none<br>Co-contaminant: N/A<br>Metabolites: N/A<br>Degradation pathway: N/A<br>Flask condition: 70 mL, 20 g soil/sediment, 200 rpm, 20 ˚C<br>Range of DX, time, and degradation: 4-6 ppm, 340 days, <50 %removal | (Ramalingam and Cupples, 2020) |
| Origin: chemical fiber manufacturing wastewater<br><br>Type: not mentioned specifically but the process is anaerobic digestion of the wastewater | Media: Wastewater itself<br>Electron donor: DX<br>Electron acceptor: none<br>Co-substrate: acetic acid produced in the acidogenesis stage of the anaerobic digestion<br>Co-contaminant: N/A<br>Metabolites: N/A<br>Degradation pathway: N/A<br>Flask condition: continuous in a 18 L reactor, 18.5 mg/L SS, 80 rpm, 35 ˚C<br>Range of DX, time, and degradation: 252 ppm, 30-40 days, 40-50 %removal | (Lee et al., 2014) |

### 2.1.3 Aerated bioremediation of DX

DX was initially considered as a non-biodegradable organic pollutant (Zhang et al., 2017). However, in past decades, studies have indicated the capability of bacteria to biodegrade DX. Mahendra and Alvarez-Cohen (2006) showed that 13 monooxygenase-expressing bacterial strains were able to aerobically transform DX. Two bacterial strains, *Pseudonocardia dioxanivorans* CB1190 (CB1190) and *Pseudonocardia benzenivorans* B5 (B5), degraded DX metabolically and used it as their growth substrate. It was found that DX biodegradation rate by CB1190 was significantly higher than its rate by B5, respectively 0.19 and 0.01 $mg.h^{-1}.mg\ protein^{-1}$. The other bacterial strains degraded DX co-metabolically by the expression of monooxygenase enzyme (MO). Several growth substrates including tetrahydrofuran (THF), toluene,

methane, propane and tryptone were consumed by different co-metabolic degrading bacterial strains. DX biodegradation rate by these bacterial strains varied from 0.06 to 0.40 $mg.h^{-1}.mg\ protein^{-1}$.

Zhang et al. (2017) have demonstrated metabolic biodegradation pathway of DX by *Mycobacterium* sp. PH-06, *Acinetobacter baumannii* DD1, and *Pseudonocardia dioxanivorans* CB1190, and its co-metabolic biodegradation pathway by *Pseudonocardia* sp. strain ENV478 and *Pseudomonas mendocina* KR1 (**Figure 2-1**). The metabolic bacterial strains degrade DX to ethylene glycol by monooxygenation, which further goes under TCA cycle for complete mineralization. However, CB1190 has a unique degradation pathway indicated in the yellow box. Co-metabolic biodegradation of DX by the mentioned bacterial strains ends up in formation of 2-Hydroxyethoxy acetic acid (HEAA) which is indicated by * in **Figure 2-1**.

Because of high rate of DX metabolic degradation reported by CB1190 species, $0.19 \pm 0.007\ mg.h^{-1}.mg\ protein^{-1}$ (Mahendra and Alvarez-Cohen, 2006), it has been used by several further studies in both batch and continuous systems (**Table 2-2**) (Mahendra and Alvarez-Cohen, 2006; Myers et al., 2018; Zhao et al., 2018). These studies have reported high DX removal efficiencies (often > 90%) in modest times (2-17 days) for initial concentrations lower than $100\ mg.L^{-1}$ (**Table 2-2**) in diverse systems including suspended batch reactor, continuous packed biofilm reactor, and electrochemical assisted biofilm reactor, indicating high potential of CB1190 for DX biodegradation in variety of systems. **Table 2-2** also includes studies which reported DX biodegradation using different bacterial species such as *Afipia* sp. strain D1 and *Mycobacterium vaccae* JOB5 (Hand et al., 2015; Isaka et al., 2016). While *Afipia* sp. strain D1 consumed DX as the source of carbon and energy (metabolic biodegradation), *Mycobacterium vaccae* JOB5 relies on propane as the primary substrate for co-metabolic DX biodegradation (**Table 2-2**).

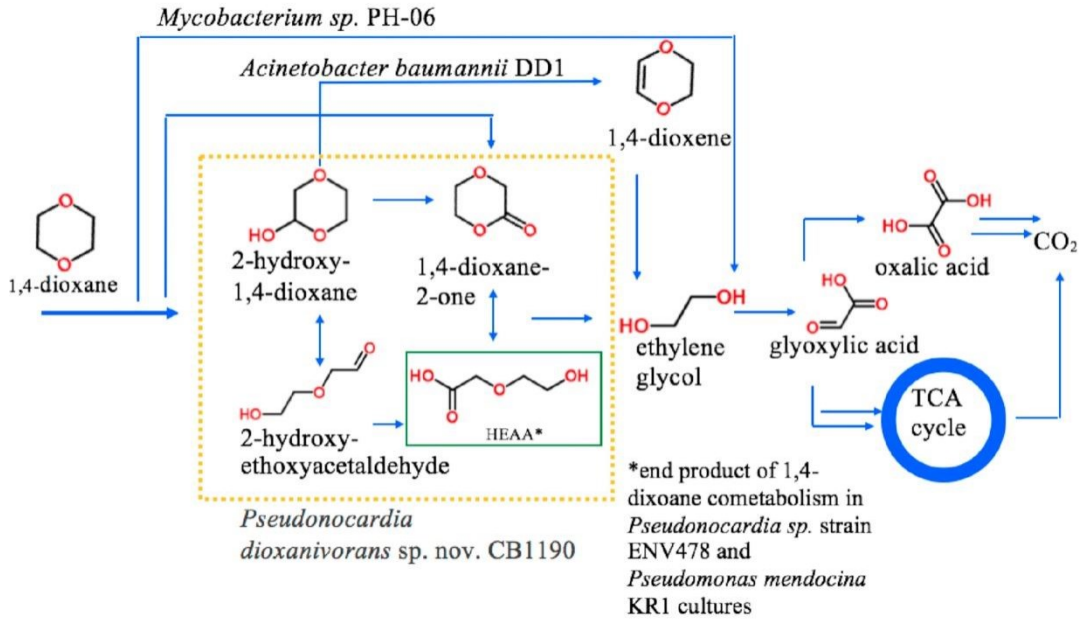


Figure 2-1 Metabolic biodegradation pathway of DX by Mycobacterium sp. PH-06, *Acinetobacter baumannii* DD1, and *Pseudonocardia dioxanivorans* CB1190, and its co-metabolic biodegradation pathway by *Pseudonocardia sp*. ENV478 and *Pseudomonas mendocina* KR1, adapted from Zhang et al. (2017).

Table 2-2 Studies reported DX aerobic biodegradation by different bacterial species and in different conditions.

| **Contaminant** | **Bacterial species** | **Co-substrate** | **DX Initial conc.** | **Retention time** | **Removal** | **Removal rate** | **Reactor condition** | **Reference** |
|---|---|---|---|---|---|---|---|---|
| DX | *P. dioxanivorans* CB1190 | None | 50 mg/L | N/A | N/A | 0.19 mg/h/mg protein | Batch 26 mL | (Mahendra and Alvarez-Cohen, 2006) |
| DX | *Mycobacterium vaccae* JOB5 | propane | 20 mg/L | 72 h | 87% | N/A | Batch 40 mL | (Hand et al., 2015) |
| DX | *Afipia* sp. strain D1 | None | 252 mg/L | 29-41 h | >99% | 0.3-0.4 g/L/d | Continuous 120 L | (Isaka et al., 2016) |
| DX | *P. dioxanivorans* CB1190 | None | 3-10 mg/L | 78 h | 80-90% | N/A | Continuous 50 mL | (Zhao et al., 2018) |
| DX | *P. dioxanivorans* CB1190 | None | 100 mg/L | 48 h | 95-98% | N/A | Batch 250 mL | (Myers et al., 2018) |

### 2.1.4 Co-contaminant effect of chlorinated solvents

DX is mainly used as a chlorinated solvent's stabilizer. Consequently, it is often found in groundwaters co-contaminated with chlorinated solvents such as trichloroethene (TCE) and 1,1-dichloroethene (1,1-DCE) (Adamson et al., 2014). The occurrence of chlorinated solvents as co-contaminants significantly reduces

efficiency of DX biodegradation by reversible or competitive inhibition mechanisms (Mahendra et al., 2013). In the reversible inhibition mechanism, chlorinated solvents deactivate the enzyme produced by DX-degrading microorganisms. In the competitive mechanism, chlorinated solvents limit the bioavailability of DX to the enzyme produced by DX-degrading microorganisms. It has been indicated that metabolic degradation of DX is limited by the reversible inhibition, and its co-metabolic degradation is limited by competitive inhibition (Mahendra et al., 2013).

Recent studies have mostly focused on overcoming the co-contaminant effects of chlorinated solvents on biodegradation of DX. These studies have been conducted both in batch and continuous modes. Generally, batch studies have achieved higher removal efficiencies due to the fact that control of bioremediation process, e.g., growth of microorganisms, is easier in these systems. On the other hand, continuous systems more realistically simulate the real condition of contaminated groundwaters presenting a better understanding of the real remediation process (Zhao et al., 2018). In the following, studies both conducted in batch and continuous systems are discussed, all of which have tried to overcome the co-contaminant effect of chlorinated solvents.

Zhang et al. (2016) has separately investigated co-contaminant effect of chlorinated solvents including trichloroethylene (TCE), 1,1,1-trichloroethane (TCA), 1,1-dichloroethene (1,1-DCE) and cis-1,2-dichoroethene (cDCE) on DX biodegradation. The experiments were conducted in 120 mL batch flasks containing samples from a contaminated groundwater amended with ammonium mineral salts (AMS) medium, and bioaugmented with CB1190. The spiked concentration of DX was 1000 $\mu g.L^{-1}$ and concentrations of 0.5, 5 or 50 $mg.L^{-1}$ of chlorinated solvents were added to the experimental runs to investigate the co-contaminant effects. 1,1-DCE was the only chlorinated solvent that inhibited DX biodegradation at concentration of 0.5 $mg.L^{-1}$ of chlorinated solvents. The experiments with concentration of 0.5 $mg.L^{-1}$ of TCE, TCA and cDCE, or solvent free mediums showed no co-contaminant effect (i.e., complete degradation in less than a day). 1,1-DCE and cDCE inhibited the DX biodegradation in

concentration of 5 mg.$L^{-1}$, and all except TCA inhibited the DX biodegradation in concentration of 50 mg.$L^{-1}$ (**Table 2-3**). They concluded that the order of DX biodegradation inhibition by chlorinated solvents is 1,1-DCE > cDCE > TCE > TCA. This order of inhibition was attributed to the structural properties of chlorinated solvents such as electron density distribution, polarity, and hydrophobicity of the molecules. For instance, 1,1-DCE and cDCE are more polar solvents than TCE and TCA resulting in a more abundant binds to cell membranes. They inactivate the cells by changing the composition of cell membranes. The other explanation is that the unsaturated carbon-carbon bonds in 1,1-DCE, cDCE and TCE render higher reactivity than the saturated carbon-carbon bond in TCA (Zhang et al., 2016).

A major problem in simultaneous biodegradation of DX and chlorinated solvents is that aerobic condition is favored by DX-degrading bacteria, while TCE is best dechlorinated under anaerobic condition (Polasko et al., 2018). These opposing conditions limit the efficiency of simultaneous biodegradation of DX and TCE. To overcome this challenge, Polasko et al. (2018) developed a mixture of bacterial strains capable of surviving in a wide range of redox potential and applied a sequential anaerobic/aerobic condition for biodegradation of DX and TCE as the initial co-contaminants. The mixture included an anaerobic chlorinated ethene degrading consortium KB-1, dominated by *Dehalococcoides* genus which has been found to be capable of complete reductive dichlorination of TCE to ethene (Aulenta et al., 2007), and the aerobic DX-degrading bacterial strain, CB1190. Complete mineralization (100 % biodegradation) of initial concentrations of DX (3500 µg.$L^{-1}$) and TCE (1250 µg.$L^{-1}$) was achieved in about 6 days (**Table 2-3**). They concluded that combination of KB-1 and CB1190 is a promising bacterial mixture for in-situ bioremediation of DX. However, effectiveness of this idea has not been investigated in a field-scale study.

Zhao et al. (2018) used a continuous pack reactor with quartz sand or soil, and bioaugmented with CB1190 to overcome the inhibitory effects of co-contaminants including TCE, 1,1-DCE and $Cu^{2+}$ on DX removal. A simulated contaminated groundwater with initial concentration of 100 mg.$L^{-1}$ DX was entered to the reactor with flow rate of 0.01 mL.$min^{-1}$ providing the residence time of 6-7 days. For the quartz sand

packed bioreactor, DX removal efficiency of 5-10% was reported both in presence and absence of 25 mg/L TCE (**Table 2-3**). However, in a similar quartz packed column, removal percentage of DX decreased from 35-40% in absence of co-contaminants to 15-20% in presence of 1 mg/L 1,1-DCE (**Table 2-3**). For the soil packed bioreactor, DX removal efficiency of was reported to be a little lower in the presence of 5-10 mg/L 1,1-DCE (80-90%) compared to DX removal efficiency in absence of co-contaminants (90-95%) (**Table 2-3**). Their hypothesis was that sorption of chlorinated solvents onto the particles could lead to a decreased bioavailability of co-contaminants to the bioaugmented CB1190. Thus, TCE or 1,1-DCE imposed less inhibitory effects on CB1190 cells. However, $Cu^{2+}$ caused more inhibitory effects and reduced the removal percentage from 90-95% in soil packed column to around 50-60% (**Table 2-3**). The reason of strong inhibitory effect of $Cu^{2+}$ was explained through changes in the enzymatic pathway of bacteria according to the direct interaction of $Cu^{2+}$ with microbial organelles.

Jasmann et al. (2017) used electrochemical-enhanced biodegradation to overcome the inhibitory effects of TCE as the co-contaminant on biodegradation of DX. They used a continuous aerobic 10 cm diameter x 45 cm long clear PVC column reactor with two permeable, disc-shaped $Ti/IrO_2–Ta_2O_5$ mesh electrodes for the electrochemical-enhanced biodegradation process (**Figure 2-2**). 8-12 mesh silica sand (1.68-2.38 mm) was used in the reactor to maintain the microbial density required for biodegradation of the organic pollutants. The system was bioaugmented with the aerobic DX-degrading bacterial strain, CB1190. Over 20% removal of 100 $mg.L^{-1}$ initial concentration of DX in the presence of 5 $mg.L^{-1}$ TCE at the flow rate of 1.07 $mL.min^{-1}$ (**Table 2-3**). Several causes can be attributed to the low removal efficiency of DX. First, TCE has been only degraded 41% when the applied voltage is at the optimum value (3 V) for DX degradation. It indicates that the electrochemical treatment was not able to completely remove co-contaminant effect of TCE. The underlying reasons for this could be low surface area of the electrodes and non-use of ion exchange membrane which separates reactants present around the two electrodes (**Figure 2-2**) (Aulenta et al., 2011). Another reason was drastic reduction of pH around the anode (4.7 compared to 6-7 in other

parts of the reactor) which was deadly for CB1190 (Jasmann et al., 2017). The underlying reason for the pH reduction could also be low surface area of the electrodes causing all oxidation reactions to occur in a small area (**Figure 2-2**) (Jasmann et al., 2017).

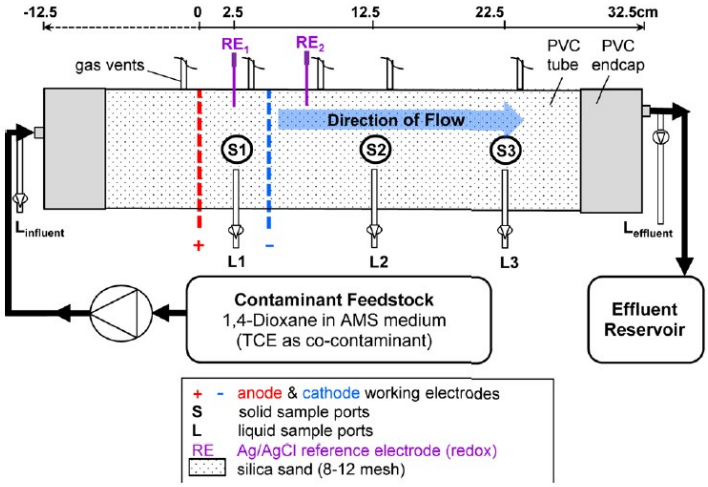


Figure 2-2 The schematic overview of an aerobic bioelectrochemical reactor developed to overcome inhibitory effects of chlorinated solvents on biodegradation of DX (Jasmann et al., 2017).

Table 2-3 Selected studies on co-contaminant effect of chlorinated solvents on DX biodegradation.

| **Bacterial species** | **DX Initial conc.** | **Co-contaminant, Initial conc.** | **DX Removal without co-contaminant** | **DX Removal with co-contaminant** | **Reactor condition** | **Reference** |
|---|---|---|---|---|---|---|
| *P. dioxanivorans* CB1190 | 1 mg/L | DCE, 0.5 mg/L<br>cDCE, 5 mg/L<br>TCE, 50 mg/L | 100% in 12 h | 60% in 12 h<br>50% in 12 h<br>35% in 12 h | Batch<br>120 mL | (Zhang et al., 2016) |
| *P. dioxanivorans* CB1190 & *Dehalococcoides* species | 3.5 mg/L | TCE, 1.25 mg/L | --- | 100% in 4 days | Batch<br>60 mL | (Polasko et al., 2018) |
| *Mycobacterium vaccae* JOB5 | 20 mg/L | TCE, 5 mg/L | 2.2 mg/d/mg protein | 1.6 mg/d/mg protein | Batch<br>40 mL | (Hand et al., 2015) |
| *P. dioxanivorans* CB1190 | 100 mg/L | 1,1-DCE, 10 mg/L | 94% | 82% | Soil-packed<br>Continuous<br>50 mL | (Zhao et al., 2018) |
| *P. dioxanivorans* CB1190 | 100 mg/L | TCE, 25 mg/L | 5-10% | 5-10% | Quartz sand-packed<br>Continuous<br>50 mL | (Zhao et al., 2018) |
| *P. dioxanivorans* CB1190 | 100 mg/L | TCE, 5 mg/L | 169 mg/h/$m^2$ | 98.4 mg/h/$m^2$ | Electro-assisted<br>Continuous<br>3.5 L | (Jasmann et al., 2017) |

## 2.2 Biofilm-mediated bioremediation

Biofilm is the aggregation of microbial communities and extracellular polymer substances produced by them on a solid surface. There are several reasons for the tendency of microorganisms to form biofilms. First, different species of bacteria live together in the microcolonies of a biofilm, which allows them to interact with each other to transfer substrates and genes (Nancharaiah and Venugopalan, 2019). Second, they create a favorable condition (e.g., pH, electron acceptors and donors, substrates, etc.) in biofilm microcolonies, which provides them a better environment for growth than the bulk liquid (Rittmann and McCarty, 2001). Third, biofilm formation can be considered a defense mechanism of microorganisms since it increases their tolerance to physical forces, pH changes, nutrient depletion, active chemicals, and xenobiotics (Jefferson, 2004). Besides, the solid surface can improve the biofilm's microenvironment by providing electron donors such as $Fe^{2+}$ and increasing microorganisms' resistance by adsorbing the toxic chemicals. Finally, biofilms are usually formed near the substrate source, ensuring a continuous exposure of the fresh substrate to the microcolonies (Rittmann and McCarty, 2001).

Biofilms have extensive applications in the engineering systems used for wastewater treatment, such as trickling filters, biological towers, rotating biological contactors, and granular-media filters (Rittmann and McCarty, 2001). The stability and retention of biomass, as well as no need to use biomass separation devices, are essential advantages of these systems compared to the suspended microbial systems. Bioremediation of hazardous contaminants such as petrochemicals, pesticides, pharmaceuticals, and persistent organic pollutants has been conducted in the past decades through biofilm mediated systems (Edwards and Kjellerup, 2013). This topic is discussed in section 2.2.3 Applications of biofilm in bioremediation. Furthermore, the use of electrocatalytic biofilm in remediation systems is an emerging technology for treating contaminants in the environment, especially contaminated groundwaters (Li and Yu, 2015). This topic is discussed in detail in section 2.3.2 Electrocatalytic biofilm.

### 2.2.1 Biofilm formation

The formation of biofilm on a solid surface includes a few sequential steps (Costerton et al., 1995). The initial attachment of bacteria to the surface is a reversible attachment when they are attached to the surface only by weak forces such as van der Waals forces and hydrophobicity. In this stage, the organic and inorganic compounds secreted by the organisms condition the surface providing a more suitable surface for settlement of other cells (Nancharaiah and Venugopalan, 2019). Then, using cell adhesion structures (e.g., pilus), microorganisms attach to the conditioned surface irreversibly to form microcolonies. In the next stage, the attached microorganisms multiply and start to produce an extracellular polymeric substance (EPS), which is the fundamental component of a biofilm. EPS helps the microcolonies to form a mature biofilm, which has a complex structure that consisted of polysaccharides, proteins, and lipids (Costerton et al., 1995). Finally, part of the mature biofilm is dispersed in the bulk liquid repeating the biofilm formation cycle on a new surface area. **Figure 2-3** shows the steps of biofilm formation.

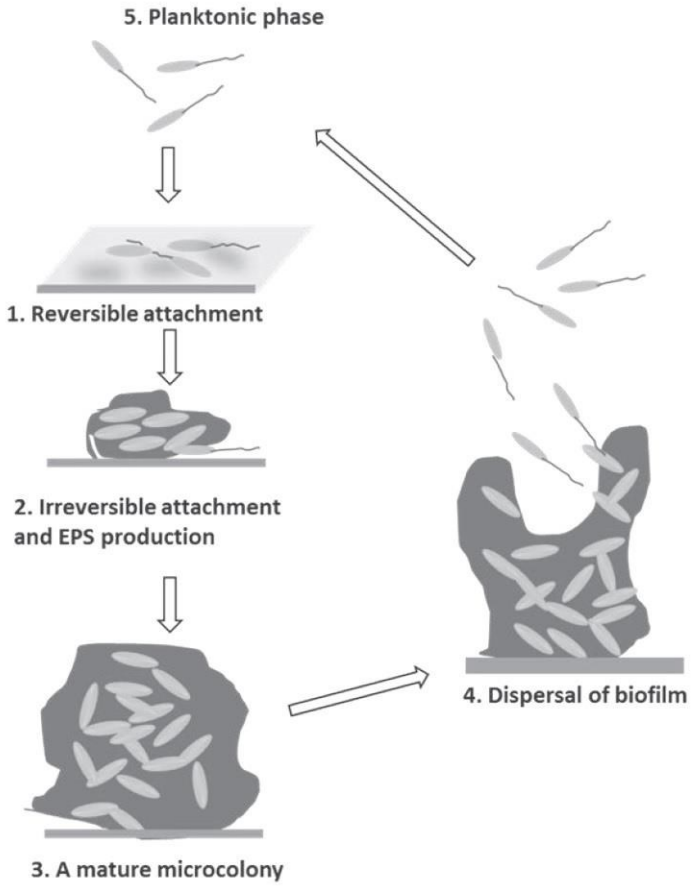


Figure 2-3 Steps of biofilm formation, adapted from Nancharaiah and Venugopalan (2019).

### 2.2.2 Biofilm components

As mentioned earlier, EPS is the fundamental component of a biofilm. It is mainly composed of polysaccharides secreted by the attached microorganisms. It also contains DNA, lipids, and other hydrophobic or hydrophilic materials, making the biofilm flexible in attaching different surfaces and interacting with the bulk liquid (Costerton et al., 1995). The produced EPS protects the microorganisms from environmental stresses such as desiccation, acidification, predation, etc. Moreover, EPS plays an essential role in the biofilm-mediated bioremediation processes. It works as a matrix where organic contaminants have high solubilities due to the adsorption and hydrophobicity effects (Wolfaardt et al., 1995). This and high cell density in this matrix work synergistically to enhance the bioremediation processes in the biofilm. It has been reported that the percentage of EPS in the biofilm has a positive

correlation with the degradation rate of polycyclic aromatic hydrocarbons using a consortium of microorganisms consisted of ten bacterial strains (Mangwani et al., 2016).

Quorum sensing (QS) is a biofilm regulatory component through which microorganisms communicate to control cell density and EPS production of a biofilm. This is conducted by secretion of signaling molecules such as N-acyl homoserine lactone (AHL) (Sakuragi and Kolter, 2007). Although QS significantly affects the growth and resistance of a biofilm, it is not observed in all biofilm-forming species (usually observed in gram-negative species) (Nancharaiah and Venugopalan, 2019). It has been reported that the presence of AHL in a biofilm increases the degradation rate of polycyclic aromatic hydrocarbons (Mangwani et al., 2016). The QS has also been indicated to influence the production of extracellular enzymes in the biofilm, such as monooxygenase, dioxygenase, and hydrolyase (Shukla et al., 2014). These enzymes usually are employed by microorganisms in the biodegradation process of organic contaminants. In addition, EPS provides a matrix for the immobilization of these enzymes, which further improves the degradation process (Nancharaiah and Venugopalan, 2019).

Chemotaxis is the movement of microorganisms toward the chemicals in response to the gradient in their concentrations. Since chemicals need to diffuse into biofilms, the formation of a concentration gradient in biofilms is usual. Therefore, chemotaxis is an essential regulatory component of biofilms, enabling microorganisms to overcome the scarcity of substrates and nutrients in the beneath layers (Costerton et al., 1995). The flagellum is the significant organ in microorganisms for chemotaxis. It has been reported that the species with this ability can overcome the bioavailability limitations of organic contaminants in the biofilms leading to higher degradation rates of polycyclic aromatic hydrocarbons (Law and Aitken, 2003).

Horizontal gen transfer (HGT) is a common phenomenon among microorganisms of a biofilm. It is conducted through gene release and transformation between bacterial strains that form a union together

to exchange genetic materials (conjugation) (Nancharaiah and Venugopalan, 2019). HGT enables the bacterial communities to exchange the genetic codes for catabolism of different compounds, including organic contaminants. It has been indicated that the genetic code for catabolism of several xenobiotics (e.g., 3-chlorobenzoate) is encoded on the plasmid, an extrachromosomal DNA molecule, which was an essential component of the contaminant degrading biofilm (Springael et al., 2002). It has also been shown that the potential of HGT is 600 times higher in biofilms compared to the planktonic microorganisms (Nancharaiah and Venugopalan, 2019).

Finally, biosurfactant is another critical component of microbial biofilms formed by cells to increase organic compounds' bioavailability. The produced extracellular biosurfactants are hydrophilic and hydrophobic, enabling them to solubilize organic compounds for microbial degradation (Costerton et al., 1995). For example, it has been reported that biosurfactants can improve the biodegradation of polycyclic aromatic hydrocarbons by desorption of them from soil particles in contaminated groundwaters resulting in more bioavailability (Makkar and Rockne, 2003).

### 2.2.3 Applications of biofilm in bioremediation

As mentioned earlier, biofilms are resistant to environmental stresses such as pH change, lack of nutrients and electron donors/acceptors, and the existence of toxic chemicals. These advantages gain significance in bioremediation systems where microorganisms are exposed to contaminants for long times, with many environmental conditions variations (Edwards and Kjellerup, 2013). Moreover, the low cost and ease of operation of biofilm systems compared to suspended bioremediation systems, and generally compared to other remediation methods, resulted in many biofilm applications in bioremediation during the past few decades (Nancharaiah and Venugopalan, 2019).

Edwards and Kjellerup (2013) have reviewed the past two decades studies on biofilm mediated bioremediation of polycyclic aromatic hydrocarbons (PAHs), chlorinated ethenes, polychlorinated

biphenyls (PCBs) and dioxins, and pharmaceutical and personal care products. A variety of biofilm systems have been used, including bioactive granular activated carbon, biofilm on the sand aquifer and porous rocks, membrane biofilm, packed biofilm, and moving-bed biofilm reactors. Besides, pure bacterial strains or a consortium of species can be developed on those systems capable of degrading organic contaminants. Promising results have been reported for removal percentages of PAHs such as phenanthrene (97-99%), pyrene (99.9%), naphthalene (94-100%), and acenaphthene (>99%) in the ranges of time from days to months. However, lower efficiencies have been reported for PCBs (33-56%) in 120-200 days. Low bioavailability, high toxicity, and lack of electron donors are the main reasons for low efficiencies in PCBs' removal (Edwards and Kjellerup, 2013). It shows that adding some sort of biostimulation to these systems can help remove persistent organic pollutants.

The growth of biofilm on various solid surfaces, including polytetrafluoroethylene filters, glass beads, granular activated carbon, fiber membranes, and natural rivers, shows biofilms' flexibility to grow on different materials because of the existence of hydrophobic and hydrophilic materials in the structure of biofilm, as discussed earlier (Nancharaiah and Venugopalan, 2019). In addition, both pure bacterial strains and microbial consortium are used as biofilms' microorganisms.

## 2.3 Electro-assisted bioremediation

### 2.3.1 Electrochemical stimulation

Lack of electron donors and acceptors is one of the main challenges in any bioremediation process. For instance, concentration of dissolved oxygen usually is not enough in groundwaters to provide the electron acceptor required by bacteria for degradation of organic pollutants (Rivett and Thornton, 2008). Biostimulation is a way to overcome this problem by injection of oxygen producing chemicals such as superoxide ($O_2^-$), chlorate ($ClO_3^-$), and perchlorate ($ClO_4^-$), or by provision of the oxygen molecules mechanically. However, it needs periodical supplement of chemicals or continuous transfer of oxygen to

the contaminated groundwater, which exert high expenses to the in-situ bioremediation. In addition, control of these processes is hard since they might cause secondary contamination to the groundwater (Li and Yu, 2015). Electrochemical stimulation is an alternative way of providing electron donors and acceptors which has several advantages including controllability, environmentally benign nature and removal efficiency.

The main idea of electro-assisted bioremediation is to install electrodes into contaminated environments (usually groundwaters) and apply electric potentials to the electrodes stimulating the microbial metabolism (Li and Yu, 2015). The stimulation of microorganisms to degrade contaminants occurs in several mechanisms. In the first mechanism, the electrodes work directly as the electron donors or acceptors of the microbial metabolism (**Figure 2-4**). This is extremely significant in environments where the availability of electron acceptors such as oxygen, sulfate, and nitrate are minimal. Since groundwaters are usually located in empty spaces between rocks, soils, and sediments, they lack a good mixing condition, which results in depletion of electron acceptors (Anneser et al., 2010). Electron transfer between the cells and the electrode can occur directly, as discussed in the electrocatalytic biofilm section (2.1.3). It can also happen through redox mediators (e.g., methyl viologen) in the aqueous medium (Aulenta et al., 2009). Another way is the hydrolysis of water caused by the polarized electrode, which results in the formation of oxygen that serves as an electron acceptor (Jasmann et al., 2017). The higher potential is generally applied to the anode where oxidation of organic contaminant (electron donors) occurs. On the other hand, a lower potential is used on the cathode, which stimulates the dechlorination of halogenated organic contaminants such as PCBs (Yu et al., 2017).

Another mechanism of electrochemical stimulation is the enhanced mixing condition around the electrode caused by the electrode's electric field (Gill et al., 2014). This mechanism of stimulation is referred to as electrokinetic enhancement (**Figure 2-4**). In the created electric field, all materials including soil particles, organic contaminant and bacteria are partially charged, leading to their movement

(electromigration) (Lohner et al., 2008). These movements cause the pore water to flow (electroosmosis) and transfer bacteria and contaminants with itself (electrophoresis) (Lohner et al., 2008). These movements enhance the proximity of electron donors/acceptors (electrodes or redox compounds), bacteria, and contaminants, leading to stimulated bioremediation. The other mechanism is the adsorption of bacteria and organic contaminants on the electrode surface (**Figure 2-4**), and enrichment of bacteria on the electrode surface (i.e., biofilm formation), which increases both bioavailability of contaminants and microbial density. Furthermore, other stimulation methods have been suggested by the literature, such as the increase of temperature due to electrochemical processes that induce the microbial activity, or removal of toxic compounds for microbial activity such as heavy metals by electrochemical processes (Gill et al., 2014).

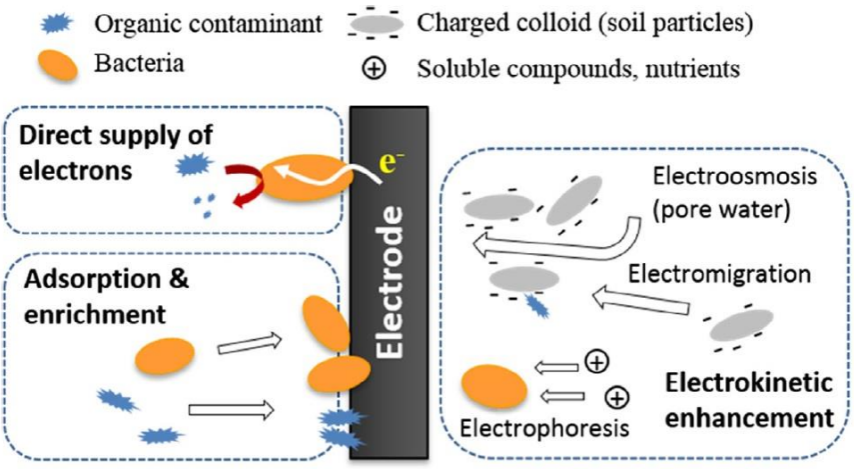


Figure 2-4 Mechanisms of microbial stimulation by a polarized electrode, adapted from Li and Yu (2015).

To conduct the electrochemical stimulation by the explained mechanisms, an electrolytic cell must be created. Electrolytic cell is a type of electrochemical cell that uses electrical energy to drive a non-spontaneous redox reaction (Lund and Hammerich, 2001). For instance, an external voltage of at least 1.23 V is needed to electrolyze water into oxygen and hydrogen molecules in the standard temperature, pressure, and pH. The half reactions of water electrolysis are presented in equations 8 and 9.

Anode (oxidation): $2H_2O \rightarrow O_2 + 4H^+ + 4e^-$ E°=+1.23 V (8)

Cathode (reduction): $2H^+ + 2e^- \rightarrow H_2$ E°=0.00 V (9)

Two electrodes are required: an anode (working electrode), which contacts the analyte (DX) and a cathode (auxiliary or counter electrode), which balances the charge removed by the working electrode. In such a system, potential of the counter electrode must be a constant value so potential of the working electrode will be determined. However, it is impossible for the counter electrode to both have a constant potential and balances the redox events at the working electrode. Therefore, another electrode (reference electrode) is added to the system to be the electrode with constant potential which enables us to determine the potential of the working electrode. In the three-electrode system, the counter electrode is used only to return the charge removed by the working electrode to the electrolytic solution (Das, 2018).

Three-electrode systems are controlled by an electronic hardware called potentiostat. Potentiostat is electronically connected to the working, contour and reference electrodes. It includes an electric circuit, which enables it to measure the current between the working and counter electrodes, and to adjust its internal resistance in a way that voltage between the working and reference electrodes remains constant. These parameters are related to each other by Ohm's law (equation 10):

$$I_o = {}^{E_c}/_{R_v} \quad (10)$$

where $I_o$ is the output electric current of the potentiostat, $E_c$ is the voltage that is kept constant, and $R_v$ is the electrical resistance that varies.

### 2.3.2 Electrocatalytic biofilm

Another significant challenge in a successful bioremediation process is bioavailability of organic contaminant to the bacteria. Generally, two types of systems are used to provide the organic contaminants to the bacteria. The first one is the use of bacteria in the planktonic way. In a planktonic system, substrate and bacteria are put in vicinity of each other floating in the aqueous phase. The second

one is the use of microorganisms in the sessile way. In a sessile system, bacteria form a biofilm on a solid surface such as packings and are exposed to the substrate when it penetrates through the formed layer of bacteria (Marshall, 2006). Sessile systems generally have several advantages over planktonic systems. They are more robust since the accumulated population of bacteria can survive in harder conditions. Moreover, stability and retention of biomass, as well as no need to use biomass separation devices, are other advantages of these systems compared to the suspended microbial systems (Rittmann and McCarty, 2001). Furthermore, it simulates the real growth condition of microorganisms in the groundwater where water exists among porous soils (Li and Yu, 2015).

The process of biofilm formation on the electrodes is very similar to the general process of biofilm formation (Nancharaiah and Venugopalan, 2019). In the initial step, few planktonic cells are adsorbed to the surface of an electrode (anode or cathode based on the system mechanism) forming the microcolonies. In the next step, the attached microorganisms multiply and start to produce EPS, which is the fundamental component of a biofilm. EPS helps the microcolonies to form a mature biofilm, which has a complex structure that consisted of polysaccharides, proteins, and lipids (Costerton et al., 1995). Finally, part of the biofilm is dispersed, attaching to the electrode's new surface and extending the biofilm. During the process of microorganisms' attachment to the electrode and biofilm growth, the phenotype of microorganisms changes to adapt them to the affinity of a conductive surface (Babauta et al., 2012). This results in microorganisms' capability to metabolically cooperate with the electrode as the direct electron donor or acceptor. The adapted microorganisms with this ability to exchange electrons from their metabolic pathway to an external electrode, are called exoelectrogens (Gorby et al., 2006).

**Figure 2-5** indicates a biofilm formation on an anode of a 2-electrode galvanic cell and the direct electron transfer mechanism from the microbial exoelectrogenic metabolism to the anode. In the metabolic pathway shown in **Figure 2-5**, electrons are released during the glycolysis process of glucose (electron donor) to pyruvate. The microorganisms use the high energy adenosine triphosphate (ATP) molecule

produced during this process, and the emitted electrons are transferred directly to the anode. The produced pyruvate goes under the citric acid cycle, resulting in more ATP production and electrons. The protons produced during the microbial metabolism process are transferred to the cathodic cell through an ion exchange membrane, working as a salt bridge for the galvanic cell. The received electrons by the anode are transmitted through the external circuit from the anode to the cathode. In the cathodic cell, oxygen is reduced to water, completing the electron transfer cycle and neutralizing the transferred protons to the cathodic cell (**Figure 2-5**). In summary, the following reactions (11-13) describe the processes at the anode and the cathode:

Anode (oxidation): $C_6H_{12}O_6 \xrightarrow{Microoranisms} CO_2 + H^+ + e^-$ (11)

Cathode (reduction): $O_2 + H^+ + e^- \rightarrow H_2O$ (12)

Total reaction: $C_6H_{12}O_6 + 6O_2 \rightarrow 6CO_2 + 6H_2O$ (13)

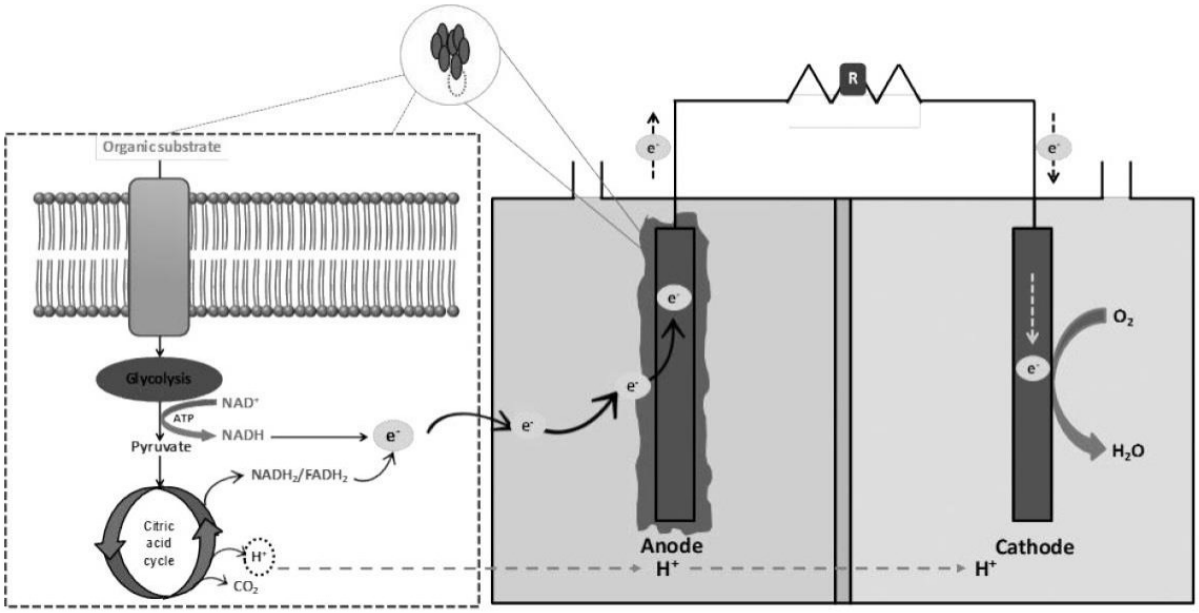


Figure 2-5 Biofilm formation on the anode of a 2-electrode galvanic cell and direct electron transfer from microbial exoelectrognic metabolism to the anode, adapted from Nancharaiah and Venugopalan (2019).

Many parameters affect the interaction of biofilm with an electrode. These parameters include the available microbial species in the biofilm, the structure, material and surface of the electrode, and the operating environmental parameters such as pH, hydrodynamics of the system, and the aqueous medium (Nancharaiah and Venugopalan, 2019). Many bacteria can interact with electrodes known as electrocatalytic bacteria. The electrocatalytic bacteria mostly include species from genera *Geobacter* and *Shewanella*. However, other species such as *Proteus Vulgaris*, *Pseudomonas spp*., *Klebsiella pneumoniae*, *Bacillus subtilis* and *Corynebacterium spp.* can form electrocatalytic biofilm too (Kumar et al., 2017). It has been reported that pilus is an important organ of microorganisms for the formation of biofilm on electrodes. For instance, a highly conductive pilus of genus *Geobacter* results in a long-range direct electron transfer between the cells and the electrode (Reguera et al., 2006). *Shewanella* species, on the other hand, secretes flavins, which interact with the cell's membrane to ease electron transfer across the membrane leading to enhanced exoelectrogenic metabolism (Ringeisen et al., 2006).

The electrode itself significantly affect the biofilm formation. The electrode surface's roughness is an important parameter since it increases both the available surface for the biofilm formation and the thickness of the biofilm-forming on the electrode (Artyushkova et al., 2015). Although microorganisms tend to attach to the hydrophobic and non-polar surfaces such as plastics, the hydrophobic and hydrophilic materials secreted by microorganisms overcome the metal's repellent forces, causing irreversible attachment of microorganisms to the electrode surface (Artyushkova et al., 2015).

As mentioned earlier, operating environmental parameters are also important in biofilm formation on the electrode surface. The exoelectrogenic metabolism of biofilm includes proton release, which affects the medium's pH around the electrode. Mutually, the pH of the medium affects the metabolism rate of microorganisms and biofilm formation. It has been reported that the optimum range of pH for biofilm preservation is 6-9, while the growth rate of biofilm at pH 7 was twice its rate at pH 6 or 8 (Rozendal et al., 2008). Similar to the formation of biofilm on plastic or natural surfaces, the medium's flow velocity

adversely affects the thickness of the biofilm and its layered structure (Rozendal et al., 2008). In addition, medium characteristics such as nutrients level, electrolyte concentration, and temperature all affect the biofilm formation on an electrode. While the existence of ions can improve the electron transfer rate, some cations such as sodium can disturb the attachment of the bacterial cells to the electrode by stimulating charge accumulation on the cell's surface, creating a repulsive force between the cells and the electrode (Rozendal et al., 2008).

### 2.3.3 Electro-assisted bioremediation

During the last decade, several studies have worked on electro-assisted bioremediation of persistent and emerging organic contaminants such as PCBs, chlorinated ethenes, DX and PAHs (**Table 2-4**) (Aulenta et al., 2011; Rodrigo et al., 2014; Jasmann et al., 2017; Yu et al., 2017). Due to the limited research on electro-assisted bioremediation of contaminants, examples regarding all the contaminants are provided in this section instead of only DX.

As also mentioned in the co-contaminant effect section (2.1.4), Jasmann et al. (2017) developed a continuous reactor (3.5 L) packed with *Pseudonocardia dioxanivorans* CB1190 bioaugmented silica and electrochemically stimulated with Ti/$IrO_2$–$Ta_2O_5$ electrodes for removal of DX. The removal rate reported for the electro-assisted biodegradation (169 mg/h/$m^2$) was about 3 times more than the removal rate by only biodegradation (68.7 mg/h/$m^2$) indicating the significance of electrochemical stimulation (**Table 2-4**). DX removal rate was decreased when the applied voltage to the electrodes was increased from 3 V to 8 V. At the applied voltage 8 V, drastic drop of pH from 7 to around 4 (because of formation of protons at high positive potential, reaction 8) was reported as the main reason of decrease in removal rate which made a fatal condition for microorganisms. However, measurement of both biofilm and planktonic cell concentrations indicated that only concentration of planktonic cell decreased from $10^8$ cells/mL to $10^4$

cells/mL, while the biofilm cell concentration was stable, showing resistance of the formed biofilm to the drastic pH drop (Jasmann et al., 2017).

The other studies summarized in **Table 2-4** also support the importance of electrochemical stimulation on the bioremediation process. Use of electrochemical stimulation (-0.5 V versus standard calomel electrode, SCE) in the cathodic chamber of a two-chamber batch reactor (each chamber 110 mL) increased dechlorination percentage of PCB 61 from 41 % to 72.6 % in 180 days by the indigenous microorganisms of a contaminated sediment (**Table 2-4**) (Yu et al., 2017). The polymerase chain reaction (PCR) of 16S rRNA gene of the microbial community showed the dominance of dechlorinating genera such as *Dechloromonas*, *Desulfovibrio* and *Ahromobacter* in the biofilm formed on the sediments of the cathodic chamber after 180 days of experiment (Yu et al., 2017). Aulenta et al. (2011) reported that dechlorination percentage of trichloroethylene (TCE) in the cathodic chamber of a two-chamber (each ~1 L) continuous reactor filled with *Dehalococcoides spp.* bioaugmented graphite granules was more than 90% at the applied voltage of -750 mV versus standard hydrogen electrode (**Table 2-4**). It was around 7 times of dechlorination percentage (13 %) in the open circuit (0 V) bioaugmented system indicating the great effect of electrochemical stimulation on the bioremediation process. The increase of cell concentration from 0.6 millions of cells/mL at 0 V to 2.5 millions of cells/mL at -750 mV showed the benefit of electrochemical stimulation on the cell growth in the medium filled with graphite granules and thus an enhanced bioremediation process (Aulenta et al., 2011). Finally, Rodrigo et al. (2014) reported that degradation percentage of di-benzothiophene (DBT) increased from 11 % to 50 % in 25 days when the indigenous microorganisms of a contaminated soil were stimulated electrochemically through graphite electrodes in a multi-chamber (each 120 mL) batch reactor (**Table 2-4**). The increase of cells growth in the mixture of soil (50 g) and water (100 mL), and on the graphite anode (3 cm x 3 cm x 0.5 cm) was confirmed visually comparing to same experiments in the sterile soil and without electrochemical stimulation (Rodrigo et al., 2014).

Table 2-4 Studies on electro-assisted biodegradation of organic contaminants including DX, PCBs, chlorinated ethenes and PAHs.

| **Electro-assisted bioremediation system** | **Contaminant** | **Initial concentration** | **Removal by electro-assisted bioremediation** | **Removal by bioremediation** | **Reference** |
|---|---|---|---|---|---|
| A continuous reactor (3.5 L) packed with *Pseudonocardia dioxanivorans* CB1190 bio augmented silica using $Ti/IrO_2–Ta_2O_5$ electrodes | DX | 100 mg/L | 169 mg/h/$m^2$ | 68.7 mg/h/$m^2$ | (Jasmann et al., 2017) |
| A batch reactor (220 mL) by indigenous species using graphite electrodes | PCB 61 | 50 µmol/kg | 72.6 % in 180 days | 41 % in 180 days | (Yu et al., 2017) |
| A continuous reactor (~ 2L) filled with *Dehalococcoides spp.* bioaugmented graphite granules and rod graphite electrodes for the external circuit | Tri-chloroethylene (TCE) | 35 µmol/L | > 90 % from 0.58 L/d contaminated water | ~ 13 % from 0.58 L/d contaminated water | (Aulenta et al., 2011) |
| A batch reactor (240 mL) by indigenous species using graphite electrodes | di-benzothiophene (DBT) | 5 mg/L | 50 % in 25 days | 11 % in 25 days | (Rodrigo et al., 2014) |

# Chapter 3 Biodegradation of 1,4-dioxane by a native digestate microbial community under different electron accepting conditions

This chapter has been published in journal of *Biodegradation*.

Samadi, A., Kermanshahi-pour, A., Budge, S.M., Huang, Y., Jamieson, R., Biodegradation of 1,4-dioxane by a native digestate microbial community under different electron accepting conditions, *Biodegradation* (2023). https://doi.org/10.1007/s10532-023-10019-4

## 3.1 Highlights

- 1,4-dioxane was completely degraded by the native digestate microbial community.
- Biodegradation rate increased in nitrate-amended and aerated conditions.
- Trichloroethylene and temperature affected 1,4-dioxane biodegradation rate.
- Overall richness and diversity of the microbial community decreased.
- *Pseudonocardiaceae*, *Xanthobacteraceae* and *Chitinophagaceae* were DX-degraders.

## 3.2 Graphical abstract

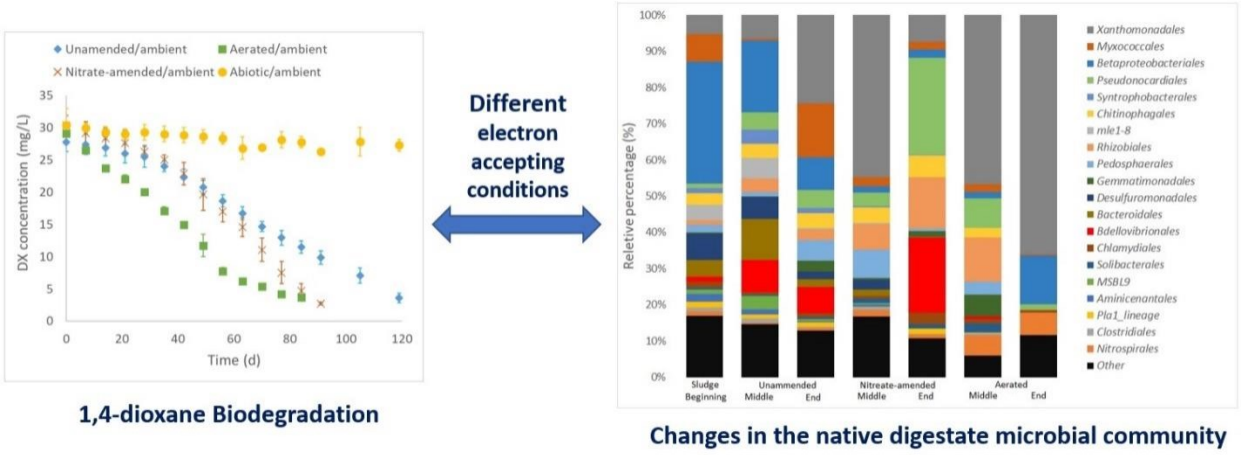


Figure 3-1 Graphical abstract of chapter 3.

## 3.3 Abstract

The potential of a native digestate microbial community for 1,4-dioxane (DX) biodegradation was evaluated under low dissolved oxygen (DO) concentrations (1-3 mg/L) under different conditions in terms of electron acceptors, co-substrates, co-contaminants and temperature. Complete DX biodegradation (detection limit of 0.01 mg/L) of initial 25 mg/L was achieved in 119 days under low DO concentrations, while complete biodegradation happened faster at 91 and 77 days, respectively in nitrate-amended and aerated conditions. In addition, conducting biodegradation at 30 ˚C showed that the time required for complete DX biodegradation in unamended flasks reduced from 119 days in ambient condition (20-25 ˚C) to 84 days. Oxalic acid, which is a common metabolite of DX biodegradation was identified in the flasks under different treatments including unamended, nitrate-amended and aerated conditions. Furthermore, transition of the microbial community was monitored during the DX biodegradation period. While the overall richness and diversity of the microbial community decreased, several families of known DX-degrading bacteria such as *Pseudonocardiaceae*, *Xanthobacteraceae* and *Chitinophagaceae* were able to maintain and grow in different electron-accepting conditions. The results suggested that DX biodegradation under low DO concentrations, where no external aeration was provided, is possible by the digestate microbial community, which can be helpful to the ongoing research for DX bioremediation and natural attenuation.

***Key words:*** 1,4-dioxane, Biodegradation, Electron acceptor, Microbial community, Dissolved oxygen

## 3.4 Introduction

1,4-dioxane (DX) is a heterocyclic organic compound, which is considered as a contaminant of emerging concern (CEC) by the U.S. Environmental Protection Agency (EPA) (2019). DX has been historically used as a stabilizer in chlorinated solvents, and also used in the production of pesticides, paints, dyes, shampoos

and cosmetics (Pollitt et al., 2019). Improper disposal regulations and the limited capacity of wastewater treatment plants to degrade DX cause its release and distribution into the environment (Stepien et al., 2014). When released to the environment, DX can contaminate groundwater because of its low octanol-water partition coefficient, log $K_{OW}$=-0.27 (EPA-DSSTox, 2021), and high solubility, $S_w$=11.35 M (EPA-DSSTox, 2021). Its persistence in groundwater (2-5 years half-life) has made DX one of the most prevalent contaminants in water supplies worldwide (Pollitt et al., 2019). DX has shown carcinogenic effect on animals (Kano et al., 2009) and has been classified in group B2 as a possible carcinogenic material (Stepien et al., 2014; 2018).

Although potential of DX bioremediation has been shown previously (Mahendra and Alvarez-Cohen, 2006; Shen et al., 2008; Hand et al., 2015), only advanced oxidation processes (AOPs) such as UV-hydrogen peroxide and HiPOx (ozone + hydrogen peroxide) have been used for full- and pilot-scale treatment projects for DX-contaminated groundwaters (EPA, 2006; Pollitt et al., 2019). Main challenges in DX bioremediation include limited availability of indigenous DX-degrading microbial species, lack of oxygen in subsurface waters and co-contaminant effects of chlorinated solvents (Jasmann et al., 2017). The majority of the DX biodegradation studies have been conducted in complete aerobic conditions (Zhang et al., 2017), which do not represent many groundwater environments where oxygen is depleted by other microorganisms and reaeration is limited due to the soil matrix (Li and Yu, 2015). The use of microbial communities that can survive in the environments with low dissolved oxygen (DO) concentrations could overcome this challenge for DX bioremediation. However, only a few studies have reported the ability of microbial communities to degrade DX in such conditions (Shen et al., 2008; Ramalingam and Cupples, 2020).

Shen et al. (2008) reported improved DX biodegradation by Fe(III)-reducing bacterium in the presence of humic acid (HA) as an electron transfer mediator. They showed 30% and >99% removal of DX at an initial concentration of 50 mg/L within 70 days by a microbial community obtained from a local wastewater

treatment plant under unamended and Fe(III)EDTA-HA-amended conditions. DX biodegradation metabolites and microbial community identification were not reported in this study. In another study, Ramalingam and Cupples (2020) investigated biodegradation of DX by indigenous cultures from several sources including 3 samples from uncontaminated agricultural soils, 2 samples from uncontaminated river sediments, and 2 samples from DX-contaminated sites in California and Maine. They evaluated the effect of different electron acceptors (nitrate, sulfate, iron) and co-substrates (HA, lactate) on all the microbial sources and showed slow DX biodegradation rates (4-6 mg/L in 295-316 days) or no degradation in most of the conditions. Enrichment of class *Gammaproteobacteria* and order *Xanthomonadales* in the indigenous microbial community was observed.

DX biodegradation under low DO concentrations has been investigated only to a limited extent and there are knowledge gaps about the microbial communities capable of DX biodegradation and the degradation pathways. Moreover, no work has been conducted on the effect of chlorinated solvents on DX biodegradation under low DO concentrations. Presence of chlorinated solvents such as trichloroethylene (TCE) and 1,1-dichloroethene (1,1-DCE) as co-contaminants in DX-contaminated groundwaters is often reported (Adamson et al., 2014; Karges et al., 2018) and is associated with reducing the rate of DX biodegradation (Mahendra et al., 2013; Hand et al., 2015; Zhang et al., 2016). Analysis of DX biodegradation kinetics by metabolic and co-metabolic strains have shown that TCE is involved in enzyme deactivation and competitive inhibition for metabolic and co-metabolic strains, respectively (Mahendra et al., 2013).

The objective of this study was to evaluate DX biodegradation capability of a native digestate microbial community under low DO concentrations (1-3 mg/L), where no external aeration was provided. The digestate microbial community had previously been studied in both aerobic and anaerobic conditions (Sayedin et al., 2018; Sayedin et al., 2020), showed high diversity, and contained orders of bacteria that have been reported to degrade DX such as *Pseudomonadales* and *Rhizobiales* (Parales et al., 1994; Huang

et al., 2014; Guan et al., 2018; Chen et al., 2021a). Therefore, we hypothesized that the digestate microbial community survives in low DO concentrations and might be capable of DX biodegradation under different electron accepting conditions. The effect of different electron acceptors (oxygen, sulfate, nitrate and Fe (III)), co-substrates (glucose, HA), and a co-contaminant (TCE) on DX biodegradation at varying temperatures (30 ˚C and 20-25 ˚C) was examined. We also monitored transition of the microbial community during the biodegradation experiments using next generation sequencing methods. This study provides valuable insight for the research on *in-situ* bioremediation or natural attenuation of DX contaminated groundwaters.

## 3.5 Materials and methods

### 3.5.1 Chemicals and inoculum

DX (99.8%, Sigma-Aldrich), 1,4-dioxane-d8 (DX-d8) (99% and ≥99% Atom D, Sigma-Aldrich), and TCE (99.5%, Sigma-Aldrich) were used to develop internal/external calibration curves and to prepare the initially contaminated medium. Methyl tert-butyl ether (MTBE) (99.8%, Sigma-Aldrich) and dichloromethane (DCM) (99.8%, Sigma-Aldrich) were used as extraction solvents before the GC/MS analysis. Oxalic acid (98%, Sigma-Aldrich) and ethylene glycol (99.8%, Sigma-Aldrich) were used as authentic compounds for the tentative identification of biodegradation metabolites. Chemicals used in preparation of mineral salts (MS) medium, and all other chemicals were purchased from Sigma-Aldrich or VWR. The MS medium was used in the experiments as source of nitrogen, metals, vitamins and trace elements needed by microorganisms. Since, environmental samples were not used in the conducted experiments by this study, the synthesized MS medium was used to serve as a proxy of inorganic ions found in the environment, especially groundwaters (Jasmann et al., 2017). The composition of MS medium is provided in **Section S1** of the supplementary documents (**Appendix B**).

The sludge sample was provided by IGPC Ethanol Inc. (Aylmer, ON, Canada), taken from the methanator used for anaerobic digestion of corn-ethanol by-products. This sludge was used to inoculate an anaerobic baffled reactor (ABR) with 4 compartments (each 6.9 L) for anaerobic digestion of thin stillage (Sayedin et al., 2018; Sayedin et al., 2019). The compartmentalized reactor provided optimum environmental condition for acidogenic and methanogenic microbial populations (Sayedin et al., 2018; Sayedin et al., 2019). These sludge samples had been previously shown flexibility toward different range of DO concentrations (i.e., anaerobic, low DO concentrations and aerobic) (Sayedin et al., 2020), which was aligned with the purpose of this study. Therefore, sludge samples were collected from each compartment of the ABR to evaluate their DX biodegradation capability.

### 3.5.2 Acclimatization stage

MS medium was boiled before the start of experiments to remove DO and was cooled down under a stream of nitrogen (Shen et al., 2008). Flasks were capped by rubber stoppers and flushed with a nitrogen stream during the sampling periods to maintain low dissolved oxygen concentration (1-3 mg/L). Sludge, taken from each compartment of the ABR, was acclimatized to DX at an initial concentration of 25 mg/L in 250 mL flasks containing 200 mL of MS medium, shaking at 200 rpm for a period of 80 days. Relatively higher concentration of DX compared to contaminated groundwaters was used in this study to accelerate the acclimatization process and to see the microbial community change in presence of DX. In addition, higher initial concentration enabled us to monitor DX biodegradation easier through the analytical technique used (GC/MS) and also to make sure that higher DX concentrations do not limit the biodegradation ability of the microbial community. DX concentration was monitored on a weekly basis until its concentration reached to below the usual concentrations in the contaminated groundwaters (<0.01 mg/L). Electron acceptors including Fe (III), nitrate, sulfate and oxygen, as well as a co-substrate such as glucose were added to selected flasks at acclimatization stage (detailed in **Table S1-Appendix B**).

For aerated flasks (oxygen as electron acceptor), conventional shake flask method at 200 rpm was used to supply the medium with oxygen from the air. A foam was used at the head of flask to avoid contamination. DO concentrations of the flasks were measured on a weekly basis to make sure that aerated condition (DO>8 mg/L) is maintained.

Acclimatization was conducted at ambient temperature (20-25 ˚C), (S1-S14), as well as at a controlled elevated temperature of 30 ˚C (S15-S21). The conditions (i.e., electron acceptor, co-substrate) that showed promising DX biodegradation at ambient condition (S1-S12), were further investigated at 30 ˚C (S15-S20) (**Table S1-Appendix B**). Abiotic experiments were conducted at both ambient temperature and 30 ˚C to monitor the possibility of DX removal by abiotic pathways such as volatilization.

### 3.5.3 Biodegradation experiments

Volatile suspended solids (VSS) concentration in the flasks (S1-12) were measured at the end of acclimatization stage (**Table S1-Appendix B**) by the standard method (Baird et al., 2017). Furthermore, the content of flasks S1-12 was centrifuged at 3000 RPM for 10 minutes and supernatant was removed. The settled VSS was collected and suspended in MS medium to bring the volume to 100 mL. The biodegradation stage flasks were inoculated using 100 mg/L VSS of the acclimatization stage flasks to carry out biodegradation experiments using different electron acceptors, co-substrates without the presence or in the presence of TCE as a co-contaminant, and at varying temperatures as shown in **Table 3-1**. Biodegradation experiments were conducted in duplicate. The growth condition with respect to the type of electron acceptor, co-substrate etc. were consistent in the acclimatization and biodegradation stages. For example, the sludge of the biodegradation stage flask, which was amended with nitrate was supplied from the sludge of acclimatization stage flask, amended with nitrate.

The effect of Fe(III) and sulfate was not further investigated in the biodegradation stage because these conditions did not improve DX biodegradation rate at the acclimatization stage compared to the

unamended condition (less than 10% change in the biodegradation rate) (**Figure S1-Appendix B**). The experimental conditions that showed promising biodegradation results (F1, F2, F9, F10, F13 and F14, **Table 3-1**) under ambient temperature were selected to be investigated for further biodegradation study at 30 ˚C. No evidence of DX biosorption was observed at the highest concentration of sludge (19,405 mg/L) comparing to the lowest sludge concentration (90 mg/L) used at the acclimatization stage (**Table S1-Appendix B**). In addition, killed control experiments were conducted in the biodegradation stage with the same sludge concentration (100 mg/L VSS, **Table 3-1**) to rule out the possibility of biosorption. Abiotic control experiments were also conducted at both ambient and 30 ˚C temperatures to evaluate the DX evaporation rate.

DX and TCE concentrations, DO concentration (measured by Vernier Optical DO probe), pH (measured by VWR Benchtop Meter), chemical oxygen demand (COD), nitrate concentration and VSS were monitored during biodegradation. pH was kept in the range of 5-7 by adding sodium bicarbonate to maintain a suitable environment for the digestate microbial community, and low DO concentration was maintained by injecting nitrogen gas when needed. Both DX and TCE concentrations were measured by liquid-liquid extraction (LLE), followed by GC/MS analysis. MTBE and DCM were used as the extraction solvents for DX and TCE, respectively (Jasmann et al., 2017; Vatankhah et al., 2019). In the nitrate-amended flasks, nitrate concentration was also monitored regularly to check possibility of DX biodegradation by nitrate-reducing microorganisms. COD and nitrate were measured respectively by TNTplus 822 and 837 kits (HACH, United States) using DR6000 spectrophotometer (HACH, United States) after filtration of samples through 0.45 µm filters to remove the suspended solids. In the glucose-amended flasks, glucose concentration and volatile fatty acids (VFAs) including acetic acid, butyric acid and propionic acid were also measured regularly to check possibility of co-metabolism of glucose and DX in case DX biodegradation rate was increased in glucose-added flasks. Glucose concentration was measured by high-performance liquid chromatography (HPLC) (Fockink et al., 2018). Concentrations of VFAs in the medium were measured

using GC with flame ionization detection (FID) through the method described by Sayedin et al. (2018). Analytical methods for monitoring DX, TCE, glucose, and VFAs are described in the **Section S2-Appendix B** of the supplementary document.

Table 3-1 Experimental condition of the biodegradation stage flasks.

| Flask | Sludge sample[1]/VSS | DX concentration | Electron acceptor | Co-substrate | Co-contaminant | Temperature |
|---|---|---|---|---|---|---|
| F1 | Comp. 1, 100 mg/L | 25 mg/L | ---------- | --- | ---------- | Ambient |
| F2 | Comp. 1, 100 mg/L | 25 mg/L | ---------- | --- | ---------- | Ambient |
| F3 | Comp. 2, 100 mg/L | 25 mg/L | $O_2$, >8 mg/L | --- | ---------- | Ambient |
| F4 | Comp. 2, 100 mg/L | 25 mg/L | $O_2$, >8 mg/L | --- | ---------- | Ambient |
| F5 | Comp. 3, 100 mg/L | 25 mg/L | ------ | --- | ---------- | Ambient |
| F6 | Comp. 3, 100 mg/L | 25 mg/L | $NO_3$, 10 mM | --- | TCE, 30 mg/L | Ambient |
| F7 | Comp. 4, 100 mg/L | 25 mg/L | $NO_3$, 10 mM | --- | TCE, 30 mg/L | Ambient |
| F8 | Comp. 4, 100 mg/L | 25 mg/L | ---------- | --- | TCE, 30 mg/L | Ambient |
| F9 | 100 mg/L | 25 mg/L | $O_2$, >8 mg/L | --- | TCE, 30 mg/L | Ambient |
| F10 | 100 mg/L | 25 mg/L | $O_2$, >8 mg/L | --- | TCE, 30 mg/L | Ambient |
| F11 | 100 mg/L | 25 mg/L | ------ | Glucose, 200 mg/L | TCE, 30 mg/L | Ambient |
| F12 | 100 mg/L | 25 mg/L | $NO_3$, 10 mM | Glucose, 200 mg/L | | Ambient |
| F13 | 100 mg/L | 25 mg/L | $NO_3$, 10 mM | ------ | | Ambient |
| F14 | 100 mg/L | 25 mg/L | $O_2$, >8 mg/L | HA, 200 mg/L | | Ambient |
| F15 | 100 mg/L | 25 mg/L | $O_2$, >8 mg/L | HA, 200 mg/L | | Ambient |
| F16 | 100 mg/L | 25 mg/L | ------ | ---------- | | Ambient |
| F17 | Killed | 25 mg/L | O2, >8 mg/L | ---------- | | Ambient |
| F18 | Killed | 25 mg/L | $O_2$, >8 mg/L | ---------- | | Ambient |
| F19 | Abiotic | 25 mg/L | $NO_3$, 10 mM | --- | | Ambient |
| F20 | Abiotic | 25 mg/L | $NO_3$, 10 mM | --- | | Ambient |
| F21 | 100 mg/L | 25 mg/L | --------- | | | 30 ˚C |
| F22 | 100 mg/L | 25 mg/L | --- | | | 30 ˚C |
| F23 | 100 mg/L | 25 mg/L | | | | 30 ˚C |
| F24 | 100 mg/L | 25 mg/L | | | | 30 ˚C |
| F25 | 100 mg/L | 25 mg/L | | | | 30 ˚C |
| F26 | 100 mg/L | 25 mg/L | | | | 30 ˚C |
| F27-1 | Abiotic | 25 mg/L | | | | 30 ˚C |
| F27-2 | Abiotic | 25 mg/L | | | | 30 ˚C |
| F27-3 | Abiotic | 25 mg/L | | | | 30 ˚C |
| F27-4 | Abiotic | 25 mg/L | | | | 30 ˚C |
| F28 | 100 mg/L | 25 mg/L | | | | Ambient |
| F29 | 100 mg/L | 25 mg/L | | | | Ambient |
| F30 | 100 mg/L | 25 mg/L | | | | Ambient |
| F31 | 100 mg/L | 25 mg/L | | | | Ambient |
| F32-1 | Abiotic | 25 mg/L | | | | Ambient |
| F32-2 | Abiotic | 25 mg/L | | | | Ambient |

[1]For the biological flasks F9 to F32, sludge obtained from comp. 1 was used since statistical analysis no difference in DX biodegradation rates.

### 3.5.4 Microbial community analysis

Sludge used to inoculate the acclimatization flasks, and sludge at the stage of acclimatization and biodegradation were sampled. Two milliliters of sludge samples from inoculum and acclimatization stage flasks were directly collected in 4 mL cryovials and preserved in a -80 ˚C freezer until analysis. In the case of biodegradation flasks, the fluid at the end of the experiments was centrifuged at 5000 RPM, and the pellet was redissolved in 2 mL of MS medium, added to 4 mL cryovials, and preserved at -80 ˚C. DNA extraction, library preparation, PCR sequencing and bioinformatics analyses were conducted by Integrated Microbiome Resources at Dalhousie University (Halifax, Canada) (https://imr.bio/index.html).

DNA extraction was conducted using QIAGEN PowerWater DNA Kits (Qiagen Inc., Toronto, Ontario, Canada). The V6-V8 regions of the bacterial 16S rRNA gene amplicon was amplified in the PCR step, which was performed using forward primer B969F = ACGCGHNRAACCTTACC and reverse primer BA1406R = ACGGGCRGTGWGTRCAA (Comeau et al., 2011). Illumina MiSeq Paired-End sequencing (~450-500 bp) with 2X depth (max. 100k reads/sample) was performed following the established protocol (Comeau et al., 2011). Bioinformatics Analyses were then conducted on the sequences using the procedure of Microbiome Helper website (https://github.com/LangilleLab/microbiome_helper/wiki) (Comeau et al., 2017).

### 3.5.5 Identification of degradation metabolites

The potential metabolites of DX biodegradation were identified using GC/MS. The samples of day 43 (when DX biodegradation was observed in all the biological flasks) from flasks F1-F16 and abiotic flasks as control were centrifuged for 10 minutes at 10,000 RPM. A sample (200 µL) of the supernatant was collected, and the metabolites were extracted using ethyl acetate (Huang et al., 2014). For silylation of the samples, the procedure described by Kermanshahi Pour et al. (2009) was followed. After evaporation of the solvent under a gentle stream of nitrogen, the residue was silylated using 50 µL of bis-(trimethyl-silyl)-trifluoroacetamide (BSTFA) in 50 µL pyridine in 2 mL glass auto-injector vials. Vials were put in a

digital reactor block (DRB200 HACH) at 40 ˚C for 2 h for the silylation reaction. Then, 1 mL acetone was added to the vials and samples were analyzed by GC (7890B Agilent) connected to MS (5977B Agilent). The GC/MS method is mentioned in **Section S2-Appendix B** of the supplementary document. The peaks of potential metabolites were tentatively identified by the NIST library and were further verified using authentic compounds.

### 3.5.6 Statistical analysis

The DX biodegradation data of unamended/ambient flasks are reported as an average of all unamended flasks (F1-F8, 8 replicates) ± standard deviation (STD). There was no difference in DX biodegradation using sludge from different compartments, as compared by single factor one-way analysis of variance (ANOVA). The mean DX biodegradation rates of unamended conditions and any specific amended condition were compared using T-tests. The difference between flasks were considered significant if the calculated P-values were less than 0.05 according to the null hypothesis.

## 3.6 Results

### 3.6.1 DX biodegradation by sludge samples

DX was completely degraded in unamended/ambient flasks in 119 days and reduced to below detection limit of the samples (0.01 mg/L) (**Figure 3-2**). The biodegradation data are shown after removing the effect of DX abiotic loss by evaporation (0.028 mg/L/d or 11.57% loss due to evaporation, **Table S2-Appendix B**). After a slow DX biodegradation for the first 25 days, DX biodegradation rate increased and remained almost constant (0.25 mg/L/d, **Table 3-2**) until it reached below the detection limit. Since the sludge samples were acclimatized to the DX biodegradation (**Figure S1-Appendix B**), the initial slow biodegradation is presumably attributed to a competitive inhibitory effect of biodegradation of other organic molecules (crude protein, glucan, cellulose, starch, etc.) that existed in the initial sludge samples

(BOD of 54.9±0.5 g/L, Sayedin et al. (2018)). COD measurements of the filtered samples during the biodegradation stage indicated a continuous decrease in all the ambient flasks (**Figure 3-3a**), showing concurrent removal of other carbon resources. The average COD of ambient flasks decreased from 664.5±45.3 mg/L at the beginning day to 169±31.5 mg/L on day 77. In addition, an intensive biomass growth from 107.3±13.4 mg/L to 199.8±15.2 VSS mg/L (average for unamended flasks F1-F8) was observed in approximately the first half time (day 0-42) of the biodegradation stage (**Figure S2-Appendix B**), majorly as the result of degradation of other organic compounds.

Amendment of flasks by glucose as another carbon source did not improve the mean DX biodegradation rate compared to the unamended flasks (P=0.8601). Glucose degradation and production of volatile fatty acids were monitored during the biodegradation stage (**Figure S3-Appendix B**). Acetic acid was produced in the glucose-amended flasks but did not improve the DX biodegradation rate. It was previously reported that the acetic acid produced during the acidogenesis step of anaerobic digestion can possibly be used as co-substrate of DX biodegradation (Lee et al., 2014). Amendment of flasks with nitrate as an electron acceptor, on the other hand, significantly increased the mean DX biodegradation rate (P=0.0008). After the initial slow DX biodegradation rate, the rate increased to 0.38 mg/L/d (**Table 3-2**) and remained almost constant until complete degradation of DX (**Figure 3-2**). Nitrate concentration was dropped to less than 20% of its initial concentration in the first 21 days (**Figure 3-3b**) showing its rapid consumption by the nitrate-reducing bacteria, when no aeration was provided. The fact that faster DX biodegradation occurred after the initial stage (days 0-21) suggests that nitrate-amendment did not directly increase DX biodegradation rate. On the other hand, faster removal of other organic compounds in the nitrate-amended flasks compared to unamended flasks (**Figure 3-3a**) implies that nitrate-amendment may have indirectly contributed to the overall faster DX biodegradation by eliminating the competitive inhibitory effect. In the first 21 days, 58.3±4.31% of COD was removed in the nitrate-amended flasks, while it was 41.69±4.04% for the unamended-flasks. This hypothesis is supported by comparing the DX biodegradation

patterns (**Figure 3-2**) of unamended and nitrate-amended flasks, where faster DX biodegradation was observed in the nitrate-amended flasks mostly after the first 25 days.

The aerated condition that was maintained in flasks F9 and F10 (**Table 3-1**) also significantly increased the mean DX biodegradation rate compared to the unamended flasks (P=0.0008). Unlike unamended and nitrate-amended conditions, no inhibition was observed at the initial stage of DX biodegradation in the aerated condition (**Figure 3-2**). This suggests that DX can be degraded relatively easier in complete aerobic condition (DO > 8 mg/L) as a carbon source. However, DX biodegradation was slowed down when its concentration was less than 5 mg/L, which shows the dependance of DX biodegradation rate to its concentration. The DO concentration of the aerobic condition flasks was above 8 mg/L, while DO concentration of other flasks, in which no external aeration was provided, were mostly in the range of 1-3 mg/L during the biodegradation stage experiments.

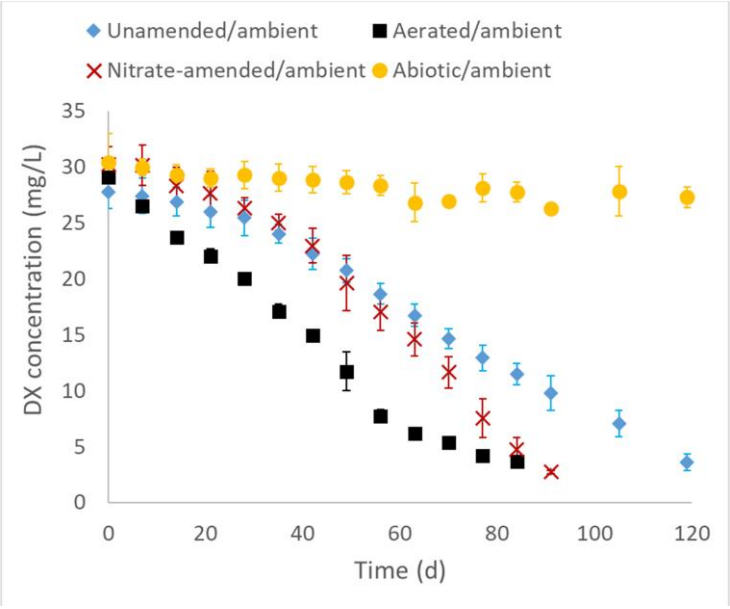


Figure 3-2 DX biodegradation by unamended (8 replicates), nitrate-amended (duplicate) and aerated (duplicate) flasks in ambient (20-25 ˚C) condition after eliminating the effect of evaporation. Final DX concentrations were below the detection limit (<0.01 mg/L), but it shows higher in the figure because DX loss by evaporation has been subtracted. Abiotic (duplicate) flasks containing DX in MS medium are also shown for comparison. No additional DX removal was observed in the control experiments with killed microbial consortia (data not shown). The colorful version is better for demonstration.

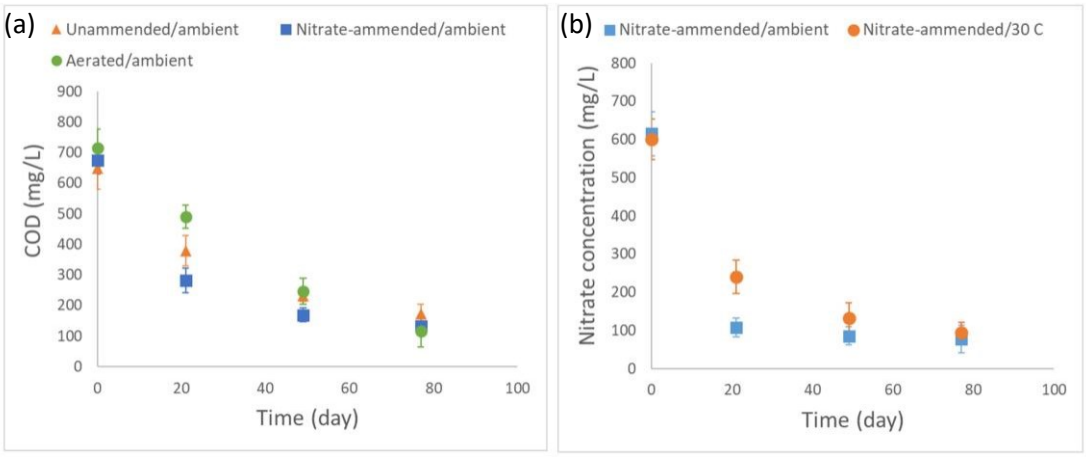


Figure 3-3 (a) COD concentration in the biodegradation stage. Samples (duplicate flasks) were analyzed for COD after 0.45 µm filtration to remove the suspended solids. (b) Nitrate concentration in the nitrate-amended flasks in ambient and 30 ˚C conditions. The colorful version is better for demonstration.

Table 3-2 DX biodegradation rates under low DO conditions, where no external aeration was provided, reported by this and previous studies.

| **Source of microorganisms for DX biodegradation** | **Electron acceptor (EA), co-substrate (CS), co-contaminant (CC) and temperature** | **DX biodegradation rate or percentage** | **Reference** |
|---|---|---|---|
| Municipal wastewater treatment sludge enriched by iron-reducing species | Unamended – 30 ˚C<br>Fe(III) (EA) – HA (CS) – 30 ˚C<br>Fe(III)-EDTA (EA) – HA (CS) – 30˚C | 24% of 58 mg/L in 110 days<br>68% of 59 mg/L in 110 days<br>0.7 mg/L/d | (Shen et al., 2008) |
| Uncontaminated agricultural soil and river sediment, and DX/chlorinated solvents contaminated sites | Unamended – ambient<br>Fe(III)-EDTA (EA) – HA (CS) – ambient<br>$NO_3$ (EA) – ambient<br>Sulfate (EA) – ambient | 22% of ~5 mg/L in ~300 days<br>No DX biodegradation<br>16% of ~5 mg/L in ~300 days<br>7% of ~5 mg/L in ~300 days | (Ramalingam and Cupples, 2020) |
| Sample of DX-contaminated groundwater located in Lansing, Michigan | Oxygen stimulated – without AMS medium<br>Oxygen stimulated – with AMS medium<br>Propane stimulated – without AMS medium<br>Propane stimulated – with AMS medium | 354 to 170 µg/L in 150 days<br>Almost same as without AMS<br>345 to 207 µg/L in 150 days<br>~260 to < 5 µg/L in 60 days | (Miao et al., 2021) |
| Sludge samples from an anaerobic digestion bioreactor used in a previous study (Sayedin et al., 2018) | Unamended – ambient<br>$NO_3$ (EA) – ambient<br>Aerated – ambient<br>Unamended – 30 ˚C<br>$NO_3$ (EA) – 30 ˚C<br>Aerated – 30 ˚C<br>Unamended – TCE (CC) – ambient<br>$NO_3$ (EA) – TCE (CC) – ambient | 0.25[1] mg/L/d<br>0.38[1,2] mg/L/d<br>0.36[1,2] mg/L/d<br>0.31[1] mg/L/d<br>0.36[1,3] mg/L/d<br>0.35[1,3] mg/L/d<br>0.050[1] mg/L/d<br>0.090[1] mg/L/d | This study |

[1]Highest biodegradation rate obtained by analyzing the linear part of the graphs: Unamended-ambient (days 28-119), $NO_3$-ambient (days 21-91), Aerated-ambient (days 0-56), Unamended-30˚C (days 28-84), $NO_3$-30˚C (days 28-77), Aerated-30˚C (days 7-63), Unamended-TCE-ambient (days 0-84) and $NO_3$-TCE-ambient (days 0-84).

[2]Although the highest biodegradation rate between $NO_3$-ambient (0.38 mg/L/d) and aerated-ambient (0.36 mg/L/d) are not significantly different (P>0.05), biodegradation patterns are different; between days 0-21: $NO_3$-ambient (0.18 mg/L/d) < Aerated-ambient (0.35 mg/L/d), between days 21-56: $NO_3$-ambient (0.31 mg/L/d) < Aerated-ambient (0.36 mg/L/d) and between days 56-84: $NO_3$-ambient (0.38 mg/L/d) >> Aerated-ambient (0.14 mg/L/d).

[3] Although the highest biodegradation rate between $NO_3$-30˚ (0.36 mg/L/d) and aerated-30˚C (0.35 mg/L/d) are not significantly different (P>0.05), biodegradation patterns are different; between days 0-21: $NO_3$-30˚C (0.16 mg/L/d) < Aerated-30˚C (0.35 mg/L/d), between days 21-42: $NO_3$-30˚C (0.36 mg/L/d) ≈ Aerated-30˚C (0.35 mg/L/d), and between days 42-63: $NO_3$-30˚C (0.36 mg/L/d) > Aerated-30˚C (0.27 mg/L/d).

### 3.6.2 Effect of temperature and TCE on DX biodegradation

Temperature control at 30 ˚C significantly increased the mean DX biodegradation rate in unamended flasks compared to the ambient (20-25 ˚C) condition flasks (P=0.0023). DX was completely degraded in 84 days in the 30 ˚C unamended flasks, while it took 119 days in the ambient unamended flasks (**Figure 3-4a**). The slow DX biodegradation rate at the initial stage was also observed in the 30˚C experiments. The mean DX biodegradation rate did not significantly increase in the 30 ˚C experiments for nitrate-amended and aerated flasks compared to the ambient condition runs (**Table 3-2**) (nitrate-amended: P=0.2309 and aerated: P=0.4984). Although DX was completely degraded to below the detection limit in shorter times at 30 ˚C (respectively 77 and 63 days for nitrate-amended and aerated) than ambient (respectively 91 and 84 days for nitrate amended and aerobic) (**Figure 3-4b** and **3-4c**), the mean DX biodegradation rates were not different after subtracting the mean DX abiotic removal rates. In other words, greater evaporation rate of DX at 30 ˚C (0.046 mg/L/d, Table S2) than ambient temperature (0.028 mg/L/d, Table S2) caused faster removal of DX in the 30 ˚C nitrate-amended and aerated flasks.

The TCE-contaminated flasks showed a significant slower rate of biodegradation for both unamended and nitrate-amended conditions (respectively P=0.00029 and P=0.00034). Until day 91 of the biodegradation experiments, DX removal percentages were 99, 75, 39 and 27 % for nitrate-amended, unamended, TCE-contaminated-nitrate-amended, and TCE-contaminated-unamended flasks, respectively (**Figure 3-4d**), which shows the significant effect of TCE on reducing DX biodegradation. In addition, the microbial

community was not able to degrade TCE either as the carbon source or co-substrate (**Figure S4-Appendix B**).

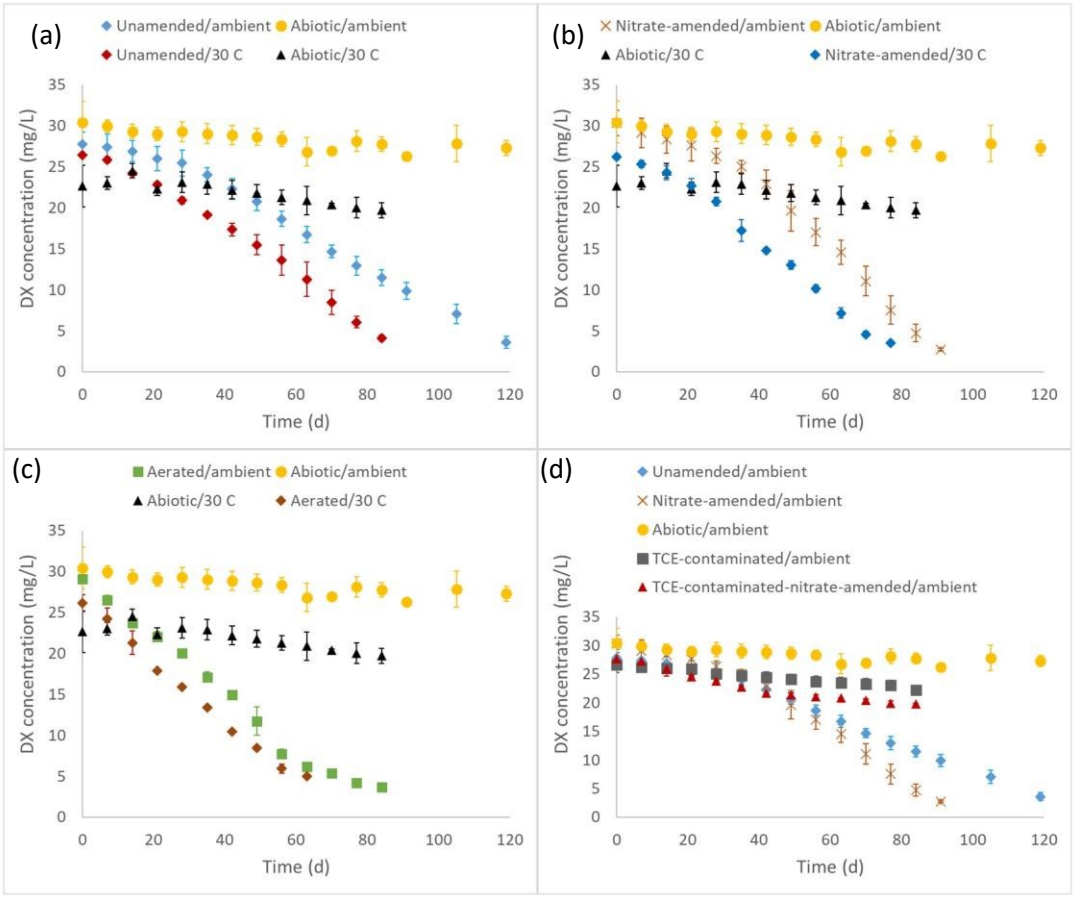


Figure 3-4 Temperature effect on DX biodegradation (ambient versus 30 ˚C) in (a) unamended, (b) nitrate-amended and (c) aerated flasks (duplicate flasks). Data are shown after eliminating the effect of evaporation. Final DX concentrations were below the detection limit (<0.01 mg/L), but it shows higher in the figure because DX loss by evaporation has been subtracted. TCE effect on DX biodegradation in (d) unamended and nitrate-amended flasks (duplicate flasks). The colorful version is better for demonstration.

### 3.6.3 Changes in the microbial community during DX biodegradation

Transition of the microbial population at three stages of the experiments (initial sludge sample, after the acclimatization stage (middle) and at the end of biodegradation stage) were monitored. Because all the existing bacteria in the population were not identified to the family, genus or species levels, the microbial population has been shown at the order level (**Figure 3-5**). The initial sludge sample was dominated by *Betaproteobacteriales* (33.65%) followed by *Myxococcales* (7.72%) and *Desulfuromonadales* (7.23%).

However, these orders lost their dominance during the experiments in all three unamended, nitrate-amended and aerated flasks. This indicates that these groups of microorganisms were not able to persist with DX as the main carbon source in the flasks (especially from middle to end, where other possible carbon sources were depleted). In general, the richness and diversity of the microbial population decreased during the experiments, shown by operational taxonomic unit (OUT) and Shannon indexes (**Figure 3-6a,b**). A higher Shannon index value at the initial stage indicated existence of plenty of species with more even abundances (Yu et al., 2006), while it gradually decreased over middle and end stages, showing the less favorable condition for majority of the species. Consequently, total number of species (i.e., OUT) in the community decreased from 480 species at the beginning to 364 and 147 species, respectively at the middle and end of experiments (the values are average of the unamended, nitrate-amended, and aerated flasks). These changes suggest that metabolism of the microbial community' proportion that was irrelevant to DX biodegradation was inhibited. In the meantime, the microbial community was enriched with the bacteria that were involved in DX biodegradation.

In unamended flasks (**Figure 3-5a**), proportion of four orders in the microbial community showed persistent increase during the three stages of sampling: *Pseudonocardiales* (1.15% to 4.72% to 26.69%), *Rhizobiales* (1.19% to 3.59% to 14.24%), *Bdellovibrionales* (1.46% to 8.72% to 20.79%), and *Chitinophagales* (3.26% to 4.01% to 5.95%). Therefore, it is most likely that microorganisms from these orders were responsible for biodegradation of DX. Co-occurrence of orders *Pseudonocardiales* and *Rhizobiales* has shown a positive relationship to DX biodegradation in another study (Miao et al., 2019). Genus *Pseudonocardia* (26.69%) belonging to the order *Pseudonocardiales* was identified, which is a well-known genus for DX biodegradation. Family of *Xanthobacteraceae* (10.44%) from the order *Rhizobiales* was also identified at the end of the biodegradation stage, which has been previously reported for its DX biodegradation ability (Chen et al., 2021a). Another noticeable identified family was *Chitinophagaceae* (6.42%) from the order *Chitinophagales*, which has previously shown DX biodegradation ability (Chen et

al., 2021a). The fact that majority of the remaining bacteria to the final stage of experiments had been associated with DX biodegradation in the past studies demonstrates that the population was well adapted to DX as the main carbon source despite existence of other carbon sources in the early stages of experiments.

In nitrate-amended and aerated flasks, the order of *Xanthomonadales* dominated the microbial community at the end of the biodegradation stage (respectively 46.83% and 66.03% in nitrate amended and aerated flasks) (**Figure 3-5b,c**). Prevalence of this order in indigenous microbial communities used for DX bioremediation has been reported before by several studies (Nam et al., 2016; Ramalingam and Cupples, 2020; Dang and Cupples, 2021), showing its positive correlation with DX biodegradation. The order of *Xanthomonadales* included four genera/families in the final microbial communities: *Chujaibacter* (26.05% in nitrate-amended and 61.48% in aerated), *Rhodanobacteraceae* (5.07% in nitrate-amended and 4.55% in aerated), *Rhodanobacter* (15.71% in nitrate-amended and negligible in aerated), and *Dyella* (negligible in both flasks). Abundance of *Chujaibacter*, *Rhodanobacteraceae* and *Rhodanobacter* in 1,4-dioxane-degrading microbial communities and/or their DX biodegradation ability have been previously reported by other studies (Pugazhendi et al., 2015; Dang and Cupples, 2021; Goff and Hug, 2022). The combination of *Pseudonocardiales* and *Rhizobiales* also existed in nitrate-amended (respectively 8.13% and 12.28%) and aerated flasks (1.63% and 6.18%), although in lower percentages compared to the unamended flasks. Another noticeable order of bacteria that existed both in nitrate-amended and aerated flasks was *Nitrospirales* with a single genus *Nitrospira* (**Figure 3-5b,c**), an aerobic and nitrate reducing genus (Harms et al., 2003). Ammonia monooxygenase (AMO) enzyme that is produced by this bacteria has previously shown the ability of DX biodegradation inducement (Guan et al., 2018). Moreover, it was identified among the dominating genera in an activated sludge community that was previously used for treatment of a DX-contaminated wastewater (Shin et al., 2010). Majority of the identified bacteria in nitrate-amended flasks such as *Pseudonocardia*, *Rhizobiales*, *Rhodanobacteraceae*, *Rhodanobacter*, and

*Nitrospira* are aerobic species that are also capable of nitrate reduction (Mahendra and Alvarez-Cohen, 2005; Pang and Liu, 2007; Van Den Heuvel et al., 2010; Daims and Wagner, 2018), which justifies the fast consumption of nitrate as the end electron-acceptor in these flasks (**Figure 3-3a**).

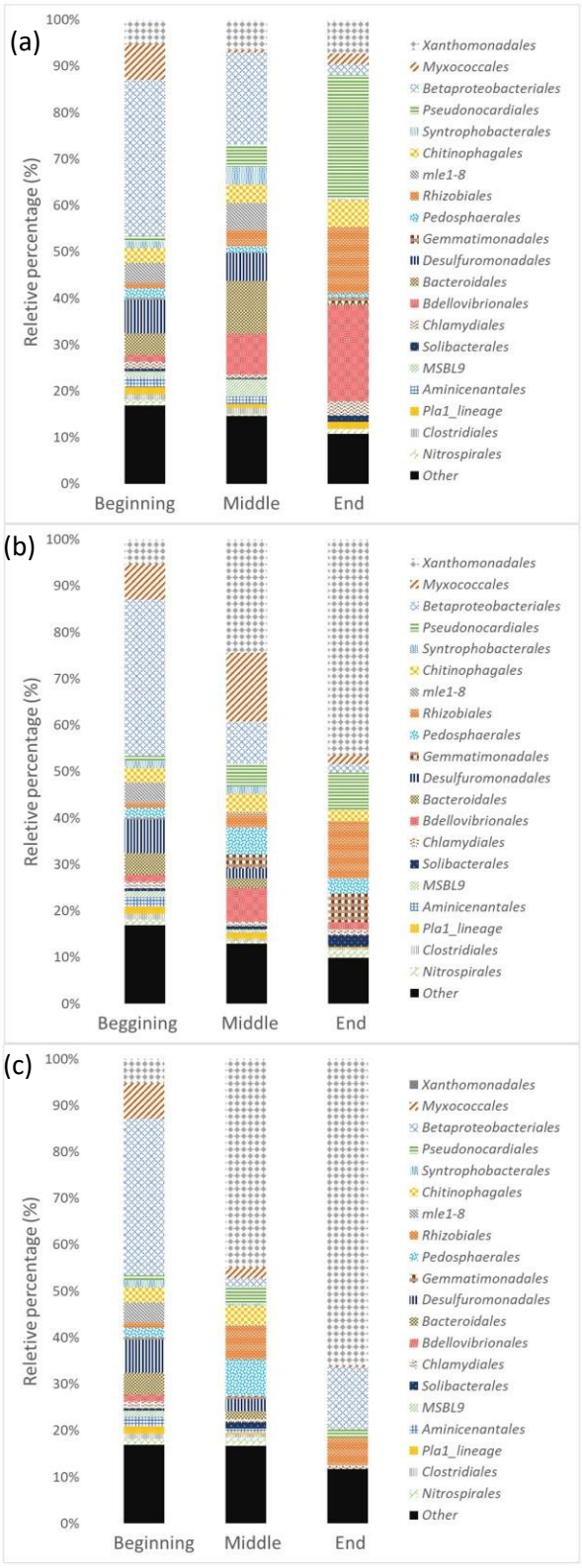


Figure 3-5 Transition of microbial composition in order level for (a) unamended, (b) nitrate-amended and (c) aerated flasks. The colorful version is better for demonstration.

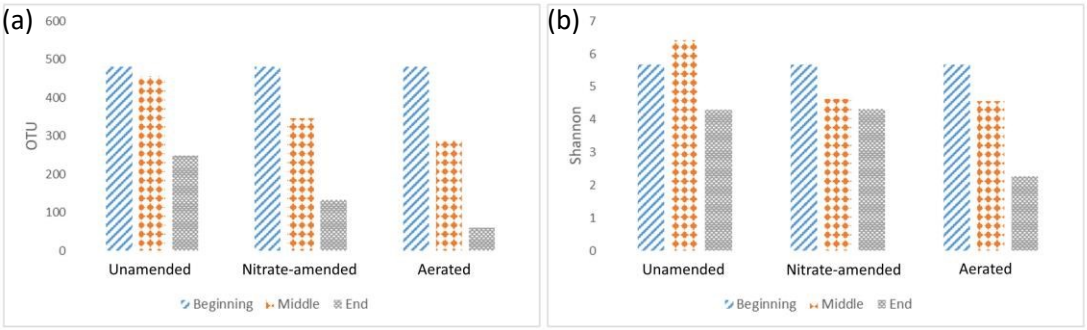


Figure 3-6 Changes in (a) OTU and (b) Shannon index of microbial community in unamended, nitrate-amended and aerated conditions. The colorful version is better for demonstration.

### 3.6.4 Potential metabolites of DX biodegradation

Samples at day 43 from flasks F1-F16 (ambient condition) were analyzed for potential metabolites of DX biodegradation. **Figure 3-7** shows the chromatogram for flask F6 (unamended) as the representative flask for metabolite identification. The peaks at retention times 11.704 and 14.599 minutes were common in the most chromatograms, and were respectively observed in 12 (F1, F2, F3, F4, F5, F6, F7, F9, F10, F12, F13, F14) and 16 (F1-F16) flasks out of 16 flasks that were analyzed. The peak at 14.599 min was identified as phosphoric acid tris(trimethylsilyl ester) by NIST library (mass spectrum not shown) which is formed from sylilation of the monosodium phosphate, a constituent of the MS medium. The peak at 11.704 min was identified as oxalic acid, 2TMS derivative (**Figure 3-7**) by the NIST library. Furthermore, the retention times of the authentic standard showed a similar retention time (11.730 min for silylated oxalic acid), which verified the identification of oxalic acid.

Oxalic acid has been reported as a DX biodegradation metabolite by aerobic species such as *Acinetobacter baumannii* DD1 and *Pseudonocardia dioxanivorans* CB1190 (Mahendra et al., 2007; Huang et al., 2014). It is produced from ethylene glycol (another reported intermediate, (Kim et al., 2009; Huang et al., 2014)) through the TCA cycle (Zhang et al., 2017). Since the most of dominant species in the microbial community were aerobic species, it is most probable that oxalic acid is also produced as a metabolite of DX

biodegradation by aerobic species in the microbial community. This metabolite was identified in all unamended, nitrate-amended and aerated conditions. The fact that this compound was found in trace concentrations indicates that DX biodegradation metabolites did not accumulate in the biodegradation flasks (i.e., were degraded to carbon dioxide).

1,1-dimethoxypropane (another observed peak as potential metabolite) has not been reported as a DX biodegradation metabolite previously. It was speculated that this compound can be potentially a metabolite arising from biodegradation of other carbon sources that existed in the initial sludge samples. An example of this would be transesterification of volatile fatty acids that existed in the initial sludge sample used for the experiments. Furthermore, D-labelled experiment was performed in order to verify if 1,1-dimethoxypropane in fact is DX biodegradation metabolite. However, no evidence of existence of this compound was found in the D-labelled experiments. Therefore, it was concluded that introducing this compound as a DX metabolite would not be a convincing argument.

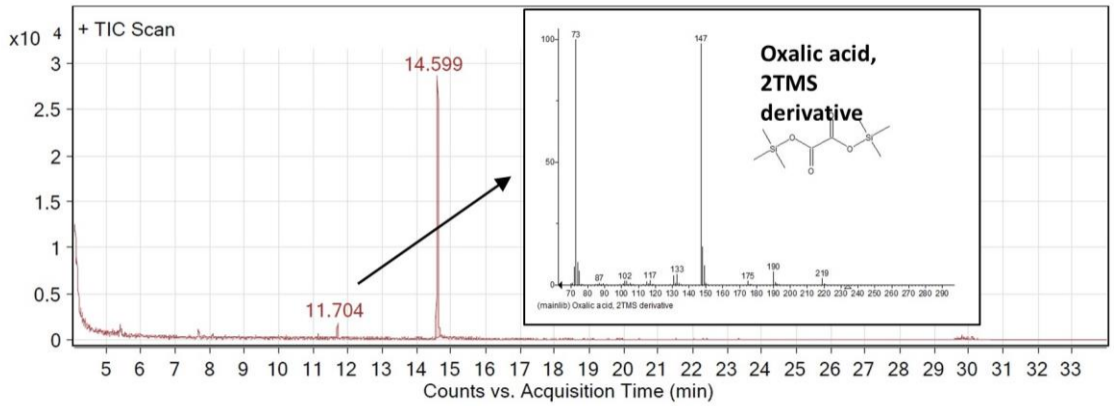


Figure 3-7 Total ion chromatogram (TIC) of DX biodegradation medium after silylation; oxalic acid (peak at 11.704 min) was identified as a metabolite of DX biodegradation and phosphoric acid (peak at 14.599 min) was a compound in the MS medium.

## 3.7 Discussion

DX biodegradation under low DO concentrations, where no external aeration is provided, is of interest to the ongoing research on DX bioremediation in contaminated groundwaters, where DO is depleted by biodegradation of other carbon sources. DX biodegradation was occurred in different electron accepting conditions showing the flexibility of DX degrades in the microbial population. Ramalingam and Cupples (2020) investigated the effect of different electron acceptors (nitrate, sulfate and iron) on DX biodegradation by indigenous microorganisms from uncontaminated agricultural soil and river sediment, and two DX/chlorinated solvents contaminated sites. However, none of the electron acceptors in that study produced a significant improvement in DX biodegradation (**Table 3-2**). Electron acceptors other than nitrate that were used in this study (i.e., sulfate and iron) also did not produce any improvement (**Figure S1-Appendix B**). There is a report of DX biodegradation by iron-reducing microorganisms in anaerobic conditions (Shen et al., 2008), which showed a relatively high biodegradation rate of 0.7 mg/L/d in Fe(III)-EDTA- and HA- amended conditions (**Table 3-2**). This was attributed to the fact that iron reducing bacteria transfer electrons to HA, and the reduced HA abiotically transfers the electrons to Fe(III)-EDTA, thus working as a catalyst in electron shuttling. However, the same inducement by Fe(III)-EDTA was not observed in the study conducted by Ramalingam and Cupples (2020) and our study, possibly because of differences in the sources of microorganisms used for DX biodegradation (**Table 3-2**). Amendment of flasks with nitrate as an electron acceptor in our study significantly increased the mean DX biodegradation rate ($P=0.0008$). Use of nitrate in bioremediation studies to induce the nitrate-reducing microorganisms has been previously reported for organic contaminants such as no. 2 diesel fuel and nonylphenol (Boopathy, 2004; Wang et al., 2015). Comparison of the nitrate consumption (**Figure 3-3b**) and DX removal (**Figure 3-2**) patterns in our experiments suggested an indirect way of enhancement. COD decreased faster in the initial stage of nitrate-amended flasks compared to unamended flasks (**Figure 3-3a**), which also supported this hypothesis that amendment with nitrate eliminated the competitive inhibition of other carbon sources leading to an increased DX biodegradation rate.

DX can be degraded aerobically by many bacteria metabolically or co-metabolically. Mahendra and Alvarez-Cohen (2006) reported the ability of 13 aerobic bacteria such as *Pseudonocardia dioxanivorans* CB1190 (CB1190), *Pseudonocardia benzenivorans* B5 and *Methylosinus trichosporium* OB3b to degrade DX, relying on it as the only carbon source or having other growth substrates such as toluene, methane, propane or tetrahydrofuran. The mean DX biodegradation rate by those isolated species were mostly in the range of 0.1-0.4 mg/hr/mg biomass. Furthermore, bioaugmentation of a DX-contaminated groundwater sample with DX-degrading species including CB1190 or *Rhodococcus ruber* ENV425 resulted in fast and complete biodegradation of DX (345-387 µg/L to < 5 µg/L in 7 days) (Miao et al., 2021). However, non-bioaugmented samples that were biostimulated with oxygen (DO concentration of around 7 mg/L) indicated a slower biodegradation rate (354 to 170 µg/L in 150 days, **Table 3-2**), similar to the results of this study. In our study, aeration of DX biodegradation flasks (F9 and F10, **Table 3-1**) happened at almost the constant rate of 0.36 mg/L/d (**Table 3-2**), which significantly increased the DX biodegradation rate compared to the unamended flasks without external aeration (P=0.0008).

Control of temperature at 30 ˚C improved DX biodegradation in the unamended flasks but not nitrate-amended and aerated flasks (**Table 3-2**), which indicates that DX is mainly degraded by different members of the microbial population in those conditions. This conclusion was supported by the dominant orders of bacteria at final stage of the biodegradation experiments, which were extensively different for unamended flasks versus nitrate-amended or aerated flasks. For example, *Xanthomonadales* was dominant in nitrate-amended and aerated flasks, but not unamended flasks (**Figure 3-5**). Generally, temperature is an important factor in bioremediation (Alvarez and Illman, 2005). Baczynski et al. (2010) showed that biodegradation of organochlorine pesticides were 1.2-1.7 times faster at 30 ˚ compared to 20 ˚C and 12 ˚C in sludge from an anaerobic wastewater treatment plant when no electron acceptor was added to the soil. On the other hand, Jéglot et al. (2021) reported that nitrate-reducing microbiomes were sensitive to temperature only at temperatures lower than 20 ˚C. While >95% of the nitrate content was

depleted within 2-3 days at 30 ˚C and 20 ˚C, it took 7 days at 10 ˚C and only 30-60% depletion was observed after 7 days at 5 ˚C. This supports the results obtained in our study that nitrate-amended flasks were not sensitive to temperature at 20-30 ˚C regarding nitrate consumption (**Figure 3-3b**). On the other hand, several studies have reported that temperature affects the DX biodegradation rate. Inoue et al. (2018) showed that a single aerobic species, *Rhodococcus aetherivorans* JCM 14343, can degrade DX in the range of 5-40 ˚C, while showing the maximum degradation rate in the range of 20-30 ˚C (less than 10% difference in this range and maximum at 25 ˚C). In addition, two more studies have reported the maximum rate of DX biodegradation by aerobic species to be in the temperatures between 20 and 30 ˚C (Parales et al., 1994; Yabuki et al., 2018). Another study on DX biodegradation in arctic areas investigated two aerobic DX-degrading species, CB1190 and *Pseudonocardia antarctica* DVS 5a1, at temperatures of 4 and 14 ˚C for Arctic groundwater remediation (Li et al., 2010). While the DX biodegradation rate by CB1190 decreased dramatically from 0.16 ± 0.04 mg/d/mg protein at 14 ˚C to 0.021 ± 0.007 mg/d/mg protein at 4 ˚C, it remained almost stable for *Pseudonocardia antarctica* DVS 5a1 (0.018 ± 0.004 and 0.015 ± 0.006 mg/d/mg protein respectively at 14 and 4 ˚C).

Presence of TCE as co-contaminant significantly reduced the DX biodegradation rate in both unamended (0.05 mg/L/d) and nitrate-amended (0.09 mg/L/d) flasks compared to the same conditions without addition of TCE (respectively P=0.00029 and P=0.00034). In our study, DX biodegradation is conducted metabolically by the native digestate microbial community as no supporting evidence was found for co-metabolic biodegradation. Thus, TCE's inhibition mechanism was presumably attributed to the enzyme deactivation mechanism (Mahendra et al., 2013). This mechanism is reversible, which means that DX can be degraded efficiently by the TCE-exposed microbial community after TCE has been removed from the medium (Mahendra et al., 2013). This would allow the use of synergistic treatment methods to remove both TCE and DX from contaminated waters (Jasmann et al., 2017; Polasko et al., 2018).

The majority of the bacterial genera/families that were able to survive during the DX biodegradation experiments were aerobic bacteria that could survive under low DO conditions, where no external aeration was provided. Survival and even growth of genera *Pseudonocardia* and *Nitrospira*, and families *Xanthobacteraceae* and *Chujaibacter* in anerobic conditions have been reported in previous studies (Wiegel, 1978; Kim et al., 2015; Polasko et al., 2018; Sayedin et al., 2018). These were the dominating bacteria in the DX biodegradation flasks (unamended and nitrate-amended) at the end of experiments and were identified as the most probable DX-degrading bacteria under low DO concentrations in this study. Four species out of six evaluated species of genus *Pseudonocardia* have shown DX degradation ability (Mahendra et al., 2013). Although it is considered as an aerobic genus, its cooperation with anaerobic microbial communities and survival in anaerobic conditions has been reported before (Polasko et al., 2018; Pica et al., 2021). In fact, *Pseudonocardia* included a higher percentage of the microbial community in unamended condition (26.69%) compared to nitrate-amended (8.13%) and aerated (1.63%) conditions. It is possible because genus *Pseudonocardia* could dominate the microbial community more in the unamended condition compared to the aerated condition, where other aerobic DX-degrading genera exerted a more intense competition over DX consumption. Existence of DX-degrading genus *Pseudonocardia* in the final microbial community indicates the potential of bioaugmentation of low DO groundwaters with well-known DX-degrader species like CB1190, which has been previously applied to the real contaminated groundwaters with relatively higher DO concentrations (3-6 mg/L), and showed promising DX biodegradation results (Miao et al., 2021).

Order of *Xanthomonadales* was the major dominating order in nitrate-amended and aerated flasks. Interestingly, the order of *Xanthomonadales* also existed in the indigenous microbial community of the only other study which identified a microbial community for DX biodegradation under low DO concentrations, where external aeration was not provided (Ramalingam and Cupples, 2020). The large

growth of this order in our microbial communities (**Figure 3-5b,c**) also suggests DX-degrading ability of microorganisms of this order.

Although MS medium was used in all the experiments, its contribution to the microbial community change was minimal. MS medium was used in both acclimatization and biodegradation stages. However, microbial community shifted mostly after starting the biodegradation stage, which indicates MS medium played none or a minor role in the shift. Furthermore, MS medium was used in all the conditions, while microbial community shifted quite differently in the different electron accepting conditions (Figure 4). In addition, there are studies on microbial community shifts in presence of DX as the sole carbon source indicating that addition of nutrients does not contribute significantly to the microbial community shifts (Ramalingam and Cupples, 2020; Miao et al., 2021). Finally, MS medium does not contain any carbon source to support growth of the cells.

In the case of DX biodegradation, intermediates like oxalic acid are not stable compounds (easily degradable). Consequently, measuring DX biodegradation intermediates as surrogate (i.e., biomarker) is impractical. However, oxalic acid was observed as a degradation intermediate in several flasks. Additionally, other biomarkers, such as biomass concentration, dissolved oxygen (DO) consumption, chemical oxygen demand (COD) measurements, and nitrate consumption, were employed, all of which correlated with DX biodegradation.

## 3.8 Conclusions

The microbial community used in this study showed promise in DX biodegradation under both low and high DO concentrations. This diversity would be an important feature of the microbial community to be used for DX bioremediation in field applications because of the wide range of DO in contaminated groundwaters. Availability of nitrate as an electron acceptor and control of temperature at 30 ˚C both

significantly increased DX biodegradation (temperature control at 30 ˚C only increased the unamended flasks), which can be considered in the design of bioremediation processes. TCE as a co-contaminant showed an inhibition effect on DX biodegradation that was likely reversible. Its negative effect can be overcome by employing synergistic methods, which could be an interesting subject for future research on DX biodegradation. Additionally, the transition of the microbial community when exposed to DX as the sole source of carbon showed growth of potential DX-degrading genera, most of which had previously been reported for their DX-degrading abilities. In future research, potential DX-degrading species with the ability of DX biodegradation under low DO concentrations can be isolated to create a better understanding of DX biodegradation kinetics and pathway.

## 3.9 Acknowledgements

The financial support of NSERC-DG is acknowledged. Aryan Samadi is thankful for the NSERC-CREATE ASPIRE and Bruce and Dorothy Rosetti Engineering Research scholarships. Special thanks to Dr. Stanislav Sokolenko for his help on statistical analysis of data and to IMR center at Dalhousie for helping us with bioinformatics analysis.

## 3.10 Supplementary material

Supplementary materials of this manuscript can be found in **Appendix B**

# Chapter 4 Delignified porous wood as biofilm support for 1,4-dioxane-degrading bacterial consortium

This chapter has been published in journal of *Environmental Technology*.

Samadi, A., Kermanshahi pour, A., Beims, R. F., & Xu, C. C. (2023). Delignified porous wood as biofilm support for 1, 4-dioxane-degrading bacterial consortium. *Environmental Technology*, 1-41. https://doi.org/10.1080/09593330.2023.2178330

## 4.1 Highlights

- Delignification improved physical/chemical properties of wood as biofilm carrier.
- Biofilm growth rate was higher on the treated woods than untreated wood.
- Use of treated woods improved 1,4-dioxane biodegradation compared to untreated.
- 1,4-dioxane biodegradation rate by biofilm was lower than planktonic cells.
- Hydrophobicity and rigidity of biofilm increased during the biofilm formation.

## 4.2 Graphical abstract

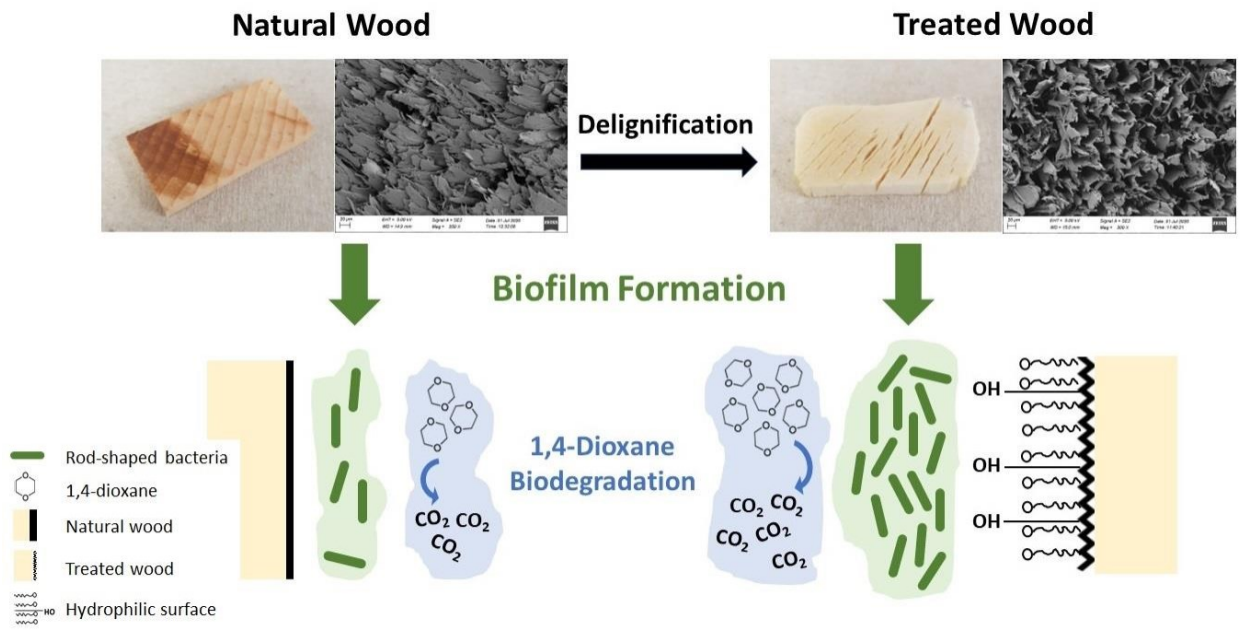


Figure 4-1 Graphical abstract of Chapter 4.

## 4.3 Abstract

Delignified porous wood samples were used as carriers for biofilm formation of a bacterial consortium with the ability to degrade 1,4-dioxane (DX). The delignification treatment of the natural wood resulted in higher porosity, formation of macropores, increase in surface roughness and hydrophilicity of the treated wood pieces. These superior properties of two types of treated carriers (respectively, A and B) compared to the untreated wood resulted in 2.19±0.52- and 2.66±0.23-fold higher growth of biofilm. Moreover, analysis of the fatty acid profiles indicated an increase in proportion of the saturated fatty acids during the biofilm formation, characterizing an enhancement in rigidity and hydrophobicity of the biofilms. DX initial concentration of 100 mg/L was completely degraded (detection limit 0.01 mg/L) in 24 and 32 h using the treated A and B woods, while only 25.84±5.95% was removed after 32 h using the untreated wood. However, fitting the DX biodegradation data to the Monod model showed a lower maximum specific growth rate for biofilm (0.0276±0.0018 1/h) versus planktonic (0.0382±0.0024 1/h), because of gradual accumulation of inactive cells in the biofilm. Findings of this study can contribute to

the knowledge of biofilm formation regarding the physical/chemical properties of biofilm carriers and be helpful to the ongoing research on bioremediation of DX.

***Keywords*****:** Biofilm, Porous wood, Hydrophilicity, Surface roughness, Biodegradation rate, Fatty acids

## 4.4 Introduction

Biofilm is aggregation of microorganisms and secreted extracellular polymer substances (EPS) on a solid surface. Biofilm formation increases cells' resistance to environmental stresses such as pH change, lack of nutrients and electron donors/acceptors, and exposure to toxic chemicals (Rittmann and McCarty, 2001). These advantages especially gain significance in bioremediation systems where microorganisms are exposed to contaminants for long times with frequent variations in environmental conditions (Edwards and Kjellerup, 2013). Biofilm-mediated bioremediation is a promising method to treat the environmental contaminations because of its superb capabilities for biodegradation, adsorption or immobilization of the organic or inorganic pollutants (Sandhya et al., 2022). This method has been successfully applied for remediation of a wide range of contaminants such as polycyclic aromatic hydrocarbons (PAHs), chlorinated ethenes, polychlorinated biphenyls (PCBs), phenol, and pharmaceutical and personal care products in various aquatic environments (Karataş et al., 2014; Mercier et al., 2014; Nakhli et al., 2014; Isaac et al., 2017; Chen et al., 2021b).

Among biofilm-mediated bioremediation studies, the importance of biofilm carriers in bioremediation performance has been extensively emphasized. Some properties of biofilm carriers highly affect the biofilm formation, which includes surface roughness, wettability, pore structure, specific surface area and material type (Zhao et al., 2019; Al-Amshawee et al., 2020). Rougher surfaces with high peaks and valleys provide a better environment for attachment of microorganisms with more resistance to the environmental stresses (Ahmad et al., 2017). Existence of macropores in the biofilm carriers can provide more surface for bacterial adhesion and protect the biofilm formed inside the pores from shock loads and

detachment (Zhang et al., 2010; Al-Amshawee and Yunus, 2021). Modification of biofilm carriers' surface is a practical method which can lead to an enhanced biofilm formation. For examples, surface conditioning of polyethylene biofilm carriers with different coatings such as polyquaternium-10 and PPy@Fe3O4 can increase the surface roughness resulting in higher growth of biomass on the carriers' surface (Hadjiev et al., 2007; Mao et al., 2017; feng Su et al., 2020). Wettability (hydrophobicity/hydrophilicity) of the biofilm carriers is another significant property which affects the interaction of surface with microorganisms and determines the strength of bacterial adhesion (Al-Amshawee et al., 2020). For instance, coating of carriers by substances such as acrylamide, polyacrylamide and N-methyl diethanolamine with hydrophilic functional groups (e.g., —COOH, —CHO, and —OH) improved their performance for biofilm formation (Shen et al., 2007; Chu et al., 2014; Zhang et al., 2018). In addition, modification of the surface characteristics can result in higher ability of pollutant removal through physical adsorption (Davarpanah et al., 2009; Mahmoodi et al., 2010; Ranjbar-Mohammadi et al., 2010; Mahmoodi, 2013).

In general, organic-based carriers have several advantages over inorganic-based carriers which include facilitated microbial adherence, being non-toxic for the microorganisms and causing no environmental contamination (Zhao et al., 2019). Wood has several advantages as biofilm carriers including high surface area, natural material, favorable microbial habitat, presence of various nutrients and micro-niches, cost-effectiveness, lightweight and buoyant and ease of replacement (Sun et al., 2010; Kruszelnicka et al., 2014; Zainab et al., 2020). Woodhas been used as biofilm carriers by several studies (Manju et al., 2009; Asri et al., 2018; Farber et al., 2019a). Delignification is a process to remove lignin and some hemicellulose from the wood block, which results in higher porosity, formation of meso- and macro-pores, increase in specific surface area, and making some hydrophilic groups (e.g., —OH) on the wood surface more available (Frey et al., 2018; Vitas et al., 2019; Beims et al., 2022). Therefore, we hypothesized that using delignified porous wood as biofilm carriers can improve the biofilm formation compared to natural untreated wood, and further increase the bioremediation efficiency of the system.

To test our hypothesis, we selected 1,4-dioxane (DX) as a model contaminant and used a DX-degrading bacterial consortium for biofilm formation. DX is an emerging contaminant which is frequently found in water supplies and has shown carcinogenic effects (Kano et al., 2009; Stepien et al., 2014; Pollitt et al., 2019). Although many recent studies have shown high potential of DX bioremediation as a green and cost-efficient method (Jasmann et al., 2017; Zhang et al., 2017; Polasko et al., 2018; Zhao et al., 2018), only a few studies have focused on biofilm-mediated bioremediation of DX (Isaka et al., 2016; Johnson et al., 2020).

The objectives of this study were: 1) to develop an understanding on the relationship of wood properties (e.g., porosity, surface roughness, wettability, etc.) as biofilm carrier, their corresponding biofilm formation capabilities, and biofilm growth characteristics, and 2) compare the DX biodegradation rates by biofilm grown on two types of treated woods (A and B) by different organic solvents and untreated wood, and further extend the comparison between biofilm and planktonic systems. Using delignified porous wood with enhanced properties as support for biofilm formation is a novel idea, which has not been investigated before.

## 4.5 Materials and methods

### 4.5.1 Chemicals, inoculum and wood samples

DX (99.8%, Sigma-Aldrich) was used to synthetically contaminate the medium. 1,4-dioxane-d8 (DX-d8) (99% and ≥99% Atom D, Sigma-Aldrich) and methyl tert-butyl ether (MTBE) (99.8%, Sigma-Aldrich) were respectively used as internal standard and extraction solvent. The DX-degrading bacterial consortium was originated from a native digestate microbial community (Samadi et al., 2022) and was developed over a period of 13 months in ammonium mineral salts (AMS) medium (Parales et al., 1994) with DX as the only carbon source (kept at 100 mg/L), which was regularly transferred (10% V/V) to the fresh AMS medium every 25 days. The final bacterial consortium used for the biofilm formation experiments consisted of 7

well-known DX-degrading genera including *Afipia*, *Terrimonas*, *Burkholderia*, *Pseudonocardia*, *Sphingomonas*, *Bradyrhizobium* and *Chryseobacterium* (Parales et al., 1994; Mahendra and Alvarez-Cohen, 2006; Sun et al., 2011; Sei et al., 2013; Nam et al., 2016; He et al., 2018; Miao et al., 2020; Chen et al., 2021a; Dang and Cupples, 2021).

Chemicals used in the AMS medium, and all other chemicals were purchased from Sigma-Aldrich or VWR. A piece of lumber of white pine wood was purchased from a local hardware store and were cut into smaller pieces with a table saw (natural or untreated wood). The porous wood samples were prepared by removing lignin from untreated wood pieces using organosolv method with organic solvents assisted by ultrasound (García et al., 2011; Shui et al., 2016; Frey et al., 2018). Two types of delignified wood samples (treated A and treated B) were prepared using different solvents in the delignification process. As the methods of delignification are currently patent-pending, detailed conditions (solvent, temperature, time, etc.) are not disclosed. Lignin content of the untreated and treated wood samples were measured by sulfuric acid hydrolysis method following the procedure described by Shui et al. (2016).

### 4.5.2 Characterization of the biofilm carriers

The wood samples (treated and untreated) were cut into small pieces (0.02-0.03 g each piece) in the shape of rectangular cube to be used as biofilm carriers. Several characterization methods were performed on the samples to investigate the suitability of the wood samples as biofilm carriers. To measure porosity of the samples ($\phi$), bulk density ($\rho$) and specific density ($\rho_s$) were measured (equation 1).

$$(1) \qquad \phi = 1 - \frac{\rho}{\rho_s}$$

Bulk density of the wood samples was determined simply by measuring the dimensions of the wood pieces using a digital caliper and weighing the mass of air dried samples (Plötze and Niemz, 2011). Bulk density of more than 50 pieces of each wood sample (untreated, treated A and treated B) were measured, and

average ± standard deviation (STD) values were obtained. Specific density was measured by volume displacement method using a helium pycnometer (AccuPyc II 1340) (Vitas et al., 2019). The chamber of helium pycnometer was filled with several wood pieces (as much as possible), and specific density was measured 5 times for each wood sample to obtain the average ± STD values.

Diameters of the formed macropores on the surface of treated wood samples were measured (more than 50 pores were measured for each sample) from scanning electron microscopy (SEM) photos of the wood samples using ImageJ software. To determine the hydrophilic/phobic properties of the wood samples and the bacterial biomass, water contact angle test was conducted on the samples using an advanced goniometer (Ramé-Hart Model 500). The apparent contact angle of a sessile drop (1 µL) of distilled water was measured 5 times for each sample (Farber et al., 2019a). To prepare the bacterial biomass for water contact angle test, suspended biomass was collected on a 0.45 µm nylon membrane filter (Whatman) using a vacuum apparatus. The filtered continuous bacterial layers were mounted on glass slides and put in the desiccator for 2 hours before conducting the contact angle test (Van Loosdrecht et al., 1987). For surface roughness measurements, wood samples were sent to Applied Technical Services (Marietta, GA, United States). Surface roughness parameters including roughness Average (Ra), root mean square roughness (Rq) and maximum two-point height difference (Rmax) were measured for different sides and areas of the wood samples using a surface profilometer (ATS-08668).

In order to evaluate stability of the delignified porous wood as biofilm support, X-ray diffraction (XRD) analysis was performed on the wood samples before and after the biofilm formation experiments. Cu source was used for the XRD analysis at 40 kV and 40 mA with scan range of 5-40 degrees at step of 0.01 second time per step. The degree of crystallinity was calculated (equation 2) as an index for degradation of the wood samples (Lionetto et al., 2012).

$$(2) \qquad CrI = \frac{I_{002} - I_{am}}{I_{002}}$$

where CrI is the crystallinity index, $I_{002}$ is the intensity of the 002 crystalline peak at 22˚ and $I_{am}$ is the peak at 18.5˚ in XRD profile of the wood samples representing the intensity of the amorphous area.

### 4.5.3 Biofilm formation stage

As the wood pieces were in contact with acidic chemicals in the delignification process, a pre-biofilm formation step was carried out on the wood pieces. They were put in an abiotic AMS medium for 10 days to eliminate the remining chemicals/lignin on the surface of wood pieces. pH and the released lignin into the medium were measured during this step. Lignin concentration was measured by spectrophotometric Acetyl Bromide Lignin method (Fukushima and Kerley, 2011) at 280 nm wavelength by a UV/Vis spectrophotometer (HACH DR 6000). After 10 days in the abiotic flasks, wood pieces were washed and transferred to the fresh medium for biofilm formation stage.

In this study, we used shaking batch flasks with at least 60% empty headspace for both biofilm formation stage and biodegradation experiments to maintain an aerated condition as efficiency of DX biodegradation greatly depends on dissolved oxygen concentration (Jasmann et al., 2017; Barajas-Rodriguez and Freedman, 2018; da Silva et al., 2020). In addition, preliminary experiments showed a better biofilm formation in the shaking state compared to the static state. Therefore, experiments were conducted in 250 mL conical flasks shaking at 180 RPM containing 100 mL of AMS medium. To avoid shear stress to the biofilm because of collision of the wood pieces to body of the flask, the wood pieces (2 g air dried mass for each flask) were put in a narrow net which was suspended in the medium using a thread. To make sure that the net itself cannot interfere with the biofilm formation process (i.e., no biofilm is formed on the net), an empty net was used as control which showed no evidence of biofilm formation on the net. The set up represented a fixed bed biofilm reactor as the whole pack of wood pieces were moving slowly at center of the flask, and wood pieces had no movement in relative to each other. Flasks (quadruplicate for each wood sample) were inoculated with optical density (OD) of 0.2 of bacterial cells

(approximately $5.8x10^7$ cells/mL) that had been harvested from mid to late exponential phase planktonic flasks. Initial DX concentration of 100 mg/L was added to the medium and monitored regularly (kept at 100 mg/L by additional injections when needed). Lignin concentration in AMS medium was also measured at the end of biofilm formation stage (20 days).

### 4.5.4 Biofilm quantification and qualification

For biofilm quantification during the experiments, several wood pieces (around 10 pieces) were collected at each time. Wood samples from different locations of the pack (i.e., center to surface considering that the pack was in the shape of a sphere) were taken. The collected wood pieces were gently washed with fresh AMS medium to remove the planktonic cells. The wood samples were inserted into a tube containing 10 mL of fresh AMS medium and placed into sonication bath for 20 minutes to detach the biofilm from the wood samples into the medium. The wood samples were separated, washed with distilled water, and placed in the vacuum oven overnight and weighed after. The biomass in the medium (detached biofilm) was quantified by several methods including measurements of volatile suspended solids (VSS), cells direct count (CDC), OD, and whole-cell fatty acid (FA) content. The same measurements were also conducted on abiotic wood samples as control. VSS was measured by the standard method (Federation and Association, 2005) after centrifugation at 10,000 rpm and redissolving the precipitates in distilled water. Cells direct count (CDC) was performed with a light microscope (Hund Wetzlar H600) using a hemocytometer (Bright-Line) for enumeration. A sample of cell medium was diluted as needed, and 100 µL of the diluted medium was mixed with 100 µL Trypan blue solution (Louis and Siegel, 2011). 5 µL of the mixed solution was loaded in the hemocytometer's chamber and observed under x40 magnification objective lens. Photos were taken by a digital camera (MiniVID) connected to the microscope and cells were counted in at least 40 squares. Cell concentration in the initial medium was calculated by applying the proper dilution factor. OD was measured by spectrophotometer (HACH DR 6000) at wavelength of 680 nm (Parales et al., 1994).

Whole-cell FA content of the 10- and 20-days biofilms were measured according to the method described by McGinn et al. (2012) based on methanolic HCl *in-situ* transesterification of FAs to their corresponding fatty acid methyl esters (FAME). Individual FAMEs were separated by GC/FID (Agilent 7890B) using DB-23 capillary column (30 m × 320 µm) and identified by comparing retention times of the peaks with those of FAME 37 standard mixture (Supelco, Sigma-Aldrich) and bacterial acid methyl esters (BAME) mixture (Matreya LLC, Unites States). The GC method was described somewhere else (Sayedin et al., 2020). Internal standard (C19:0, Nonadecanoic acid, Sigma-Aldrich) was added to the samples before transesterification and used for quantification of individual FAMEs using a same response factor. Identification of the FAME peaks in all the samples and standard mixtures were double-checked by GC/MS (Agilent 7890B/5977B) using the same column and GC conditions.

For a better visualization of biofilm formation on the wood samples, SEM images of biofilm on the wood support were obtained following the procedure described by Manju et al. (2009) for sample preparation, with changing the dehydration solvent from acetone to ethanol. Critical point drying, placing on SEM stubs, gold coating, and SEM analysis were conducted in electron microscopy facility at Dalhousie University (Halifax, Canada). To analyze microbial population of the biofilms, bacterial biomass samples after detachment were submitted to Integrated Microbiome Resources at Dalhousie University (Halifax, Canada) for DNA extraction, library preparation, PCR sequencing and bioinformatics analyses. DNA was extracted by QIAGEN PowerWater DNA Kits (Qiagen Incorporation, Canada). PCR was performed by amplifying the full-length 16S rRNA gene amplicon using forward primer 27F(Paliy) = AGRGTTYGATYMTGGCTCAG and reverse primer 1492R = RGYTACCTTGTTACGACTT (Comeau et al., 2011). PacBio Sequel entire region sequencing with 1X depth (max. 10k CCS=HiFi reads/sample) was conducted according to the established protocol (Paliy et al., 2009). The obtained sequences were then analyzed for bioinformatics according to the procedure described on Microbiome Helper website procedure (https://github.com/LangilleLab/microbiome_helper/wiki) (Comeau et al., 2017).

### 4.5.5 DX biodegradation experiments

After 20 days of biofilm formation, the wood samples with attached biofilm on them were gently washed with fresh AMS medium to remove all the planktonic cells. The biofilm on wood samples were then transferred to new 250 mL conical flasks containing 100 mL of abiotic fresh medium shaking at 180 RPM. DX biodegradation experiments were conducted by adding various concentrations of DX (400, 200, 100, 50, and 25 mg/L) to the different flasks and its removal was monitored over time. Biofilm on the wood samples were measured by VSS method before addition of each DX concentration, and after its complete degradation (detection limit of 0.01 mg/L for DX concentration). DX concentration was measured throughout the experiments by solvent extraction (MTBE as the organic solvent) followed by GC/MS analysis. The sample preparation procedure and condition of GC/MS analysis were described elsewhere (Samadi et al., 2022). To compare the DX biodegradation rate by biofilm versus planktonic, DX biodegradation experiments were also conducted in planktonic flasks by adding similar DX concentrations (400, 200, 100, 50, and 25 mg/L). The planktonic flasks were initially inoculated with harvested cells from the stationary phase and with the same biomass concentration that was measured in the biofilm flasks (similar biomass concentrations were prepared based on VSS and verified by CDC). DX removal was monitored over time, and planktonic biomass was measured by VSS method before addition of each DX concentration, and after its complete degradation. To rule out DX removal by biosorption or adsorption means, killed control flasks and abiotic control flasks containing wood samples were also conducted with DX concentrations of 100, 200 and 400 mg/L. DX concentration in the medium was measured periodically (every 8 hours) to monitor for removal.

Bacterial growth yield was calculated in a 20-day period based on biomass growth versus total DX added over time, assuming that yield is constant over different range of concentrations. The assumption was then verified by measuring the biomass growth during the biodegradation experiments at various DX

concentrations. Using the calculated constant yield, and knowing the bacterial biomass concentration, DX utilization rates in first 4 or 8 hours of various DX initial concentrations were converted to biomass specific growth rates (equation 3) (Rittmann and McCarty, 2001).

$$\mu_{syn} = -\frac{Y r_{ut}}{X_a V} \quad (3)$$

$\mu_{syn}$ represents the biomass specific growth rate (1/h), Y the biomass growth yield (mg/mg), $r_{ut}$ the substrate utilization rate (mg/L/h), $X_a$ the biomass concentration (mg/L), and V the volume of medium (L). Then, the DX initial concentrations and calculated biomass specific growth rates at those concentrations were fitted to Monod model (equation 4) through nonlinear regression to minimize the variation among measured and modeled biomass specific growth rates at each DX initial concentration (Rittmann and McCarty, 2001).

$$\mu_{syn} = \mu \frac{S}{K + S} \quad (4)$$

$\mu_{syn}$ represents the biomass's specific growth rate (1/h), $\mu$ the maximum specific rate (1/h), S the substrate concentration (mg/L), and K the half saturation constant (mg/L). The Monod parameters ($\mu$ and K) were calculated for both biofilm and planktonic systems.

### 4.5.6 Biofilm regeneration

Biofilm regeneration experiments were conducted by adding various concentrations of DX (400, 200, and 100 mg/L) to the different flasks with 20-days grown biofilm on treated B wood samples, and DX concentration was monitored over time. After complete removal of DX in each flask, the biofilm on wood was gently transferred to new flask with fresh DX-free AMS medium shaking at 180 rpm. DX concentration was measured in the new flask after 24 hours, and biofilm on wood was transferred to another flask with

fresh AMS medium and various concentrations of DX (400, 200 and 100 mg/L). The DX biodegradation rate was calculated for biofilm before and after the regeneration using Monod model as described above.

In addition to DX biodegradation rate, adenosine triphosphate (ATP) content of biofilm was measured as an index for biomass activity before and after of the biofilm regeneration experiments. The biofilm sample preparation was similar for the preparation for the biofilm VSS measurement as explained above. ATP was measured by luminometric method based on the luciferin-luciferase reaction. Quench-Gone Wastewater kit (QG21W) was used as the ATP assay kit for the reaction and samples were measured using a Photon Master luminometer device (LuminUltra, Canada). The samples were tested for ATP immediately after sampling to obtain the most representative and accurate information. VSS was also measured in those samples and used to correct the biomass content of the samples to compare ATP.

### 4.5.7 Statistical analysis

The results of quadruplicate experiments (DX biodegradation and biofilm quantification data) are reported as average ± STD. The results of different systems (biofilm on different wood samples and biofilm versus planktonic) are compared by T-test using Microsoft Excel software. The results are considered significantly different if the obtained P-values are lower than 0.05 based on the null hypothesis.

## 4.6 Results

### 4.6.1 Characteristics of the biofilm carriers

Organosolv delignification removes lignin, the main component that sticks the wood cells together, but preserves the wood's macroscopic structure (Vitas et al., 2019). After performing the organic acid delignification process, 82.50±2.25% and 96.27±1.74% of the lignin was removed, respectively under treatment conditions of A and B from the natural white pine wood with initial lignin content of 28.40±1.10% (**Table 4-1**). In addition, some of the remaining lignin in the treated wood samples was

released to the medium during the 10-days abiotic period (**Figure S1-Appendix C**). Lignin removal resulted in lower bulk densities of the treated wood samples compared to the natural wood (**Table 4-1**), which increased the porosity from 71.67±3.05% to respectively 79.13±2.7% and 82.77±2.80% for treated A and B wood samples. SEM images of the wood samples (**Figure 4-2A-C**) showed the formation of pores on the treated wood samples, with average diameters of respectively 37.21±7.76 µm and 48.36±6.89 µm for the treated A and B wood samples. The pores were in the range of macropores (2-58 µm) according to the classification by Plötze and Niemz (2011) based on mercury intrusion porosimetry.

Delignification of natural wood removes the lignin from the cellulose block, forming peaks and valleys on the wood's surface. More jagged surface of the treated A and B samples compared to the natural wood can be qualitatively observed from SEM images of the wood samples (**Figure 4-2A-C**). Furthermore, quantification of the surface roughness by measuring the roughness parameters including Rq (**Table 4-1**), Ra and Rmax (**Table S1-Appendix C**) showed an increase in surface roughness of the treated wood samples compared to the natural wood. The water contact angle test showed that delignification of the natural wood (contact angle of 47.88±1.19˚) resulted in creation of more hydrophilic surfaces for the treated wood samples (contact angle of 0˚) (**Figure 4-3**). Possible causes of the increased hydrophilicity include formation of macropores which can adsorb water (Bouguerra et al., 2002), increased availability of the hydroxyl group from cellulose because of delignification (Beims et al., 2022), and rougher surface of the treated samples (Al-Amshawee et al., 2020).

Crystallinity index (CrI) was calculated from XRD profiles of the delignified porous wood samples before and after the biofilm formation experiment (**Figure S2-Appendix C**). Comparison of the CrI for treated A and B wood samples before (respectively 0.44 and 0.48) and after (respectively 0.43 and 0.44) the experiment showed minimal changes (respectively 14.62% and 8.2% for treated A and B wood samples). The small decreases in the CrI could be related to the degradation of the crystalline structure on the surface of the wood samples because of the biofilm formation. However, low percentages of change in

CrI after 20 days of biofilm formation indicated the good stability of the delignified porous wood as biofilm support.

Table 4-1 Results of the wood characterization tests (triplicate samples).

| **Wood sample** | **Lignin content (%)** | **Bulk density ($g/cm^3$)** | **Specific density ($g/cm^3$)** | **Porosity (%)** | **Pore size (μm)** | **Rq[1] (μm)** | **Water contact angle** |
|---|---|---|---|---|---|---|---|
| Untreated | 28.4±1.1 | 0.42±0.030 | 1.5±0.01 | 71.67±3.05 | N/A[2] | 5.34-7.24 | 47.88±1.19˚ |
| Treated A | 5.0±1.6 | 0.34±0.010 | 1.6±0.02 | 79.13±2.70 | 37.21±7.76 | 10.17-12.35 | 0˚ |
| Treated B | 1.1±0.8 | 0.26±0.030 | 1.5±0.01 | 82.77±2.80 | 48.36±6.89 | 12.35-19.78 | 0˚ |

[1]Rq was measured on several areas of the wood samples, and the range of measurements are reported. The measurement uncertainty of the profilometer was 0.13 μm in the roughness range of wood samples.
[2]Pores were not detectable through SEM photos.

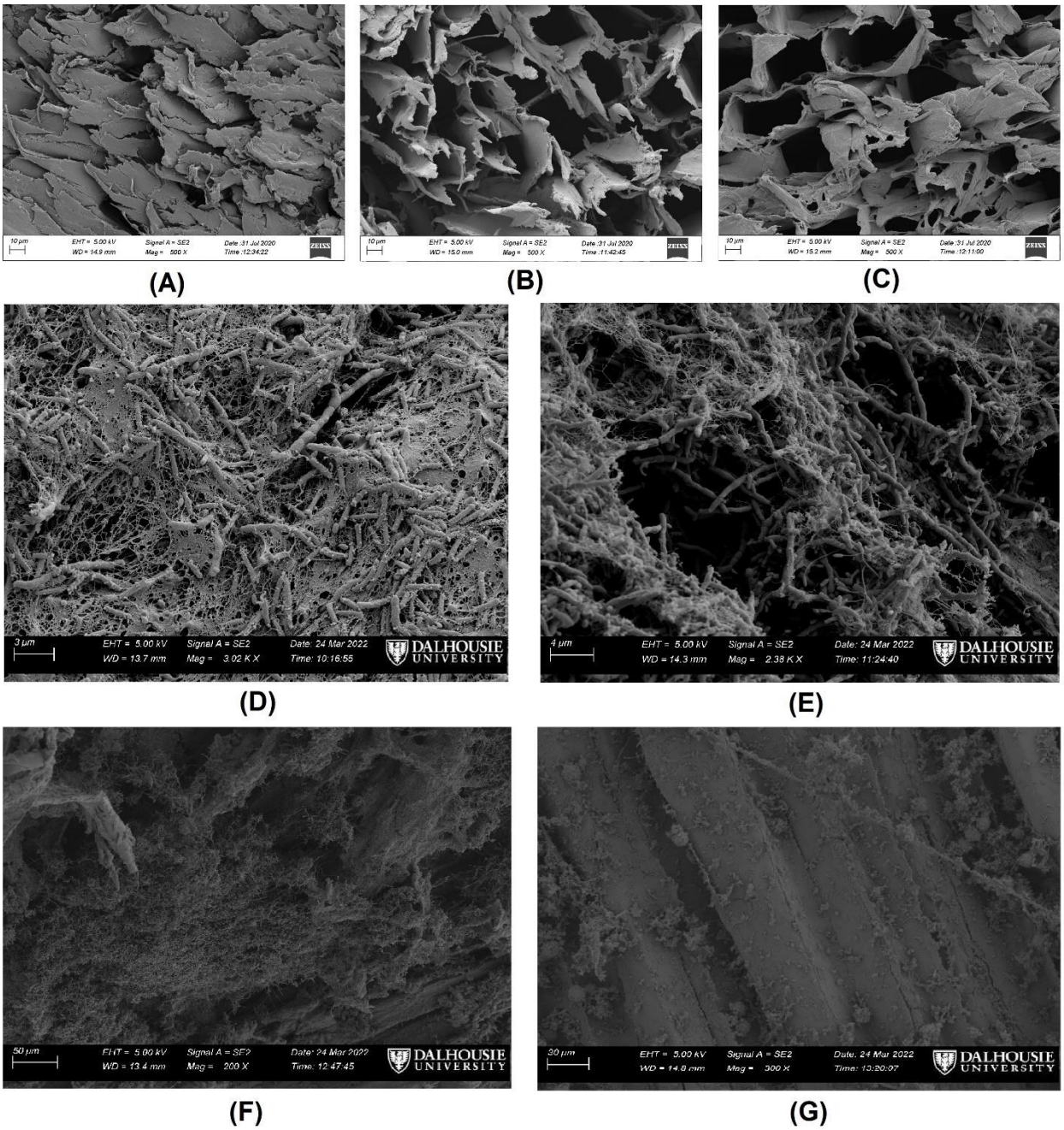


Figure 4-2 SEM images from surface of the wood samples: (A) untreated, (B) treated A and (C) treated B. SEM images from bacterial biofilm formed (D) on the surface and (E) inside the pores of treated B wood sample. SEM images of a wider area of bacterial biofilm formed on the surface of (F) treated A and (G) untreated wood samples.

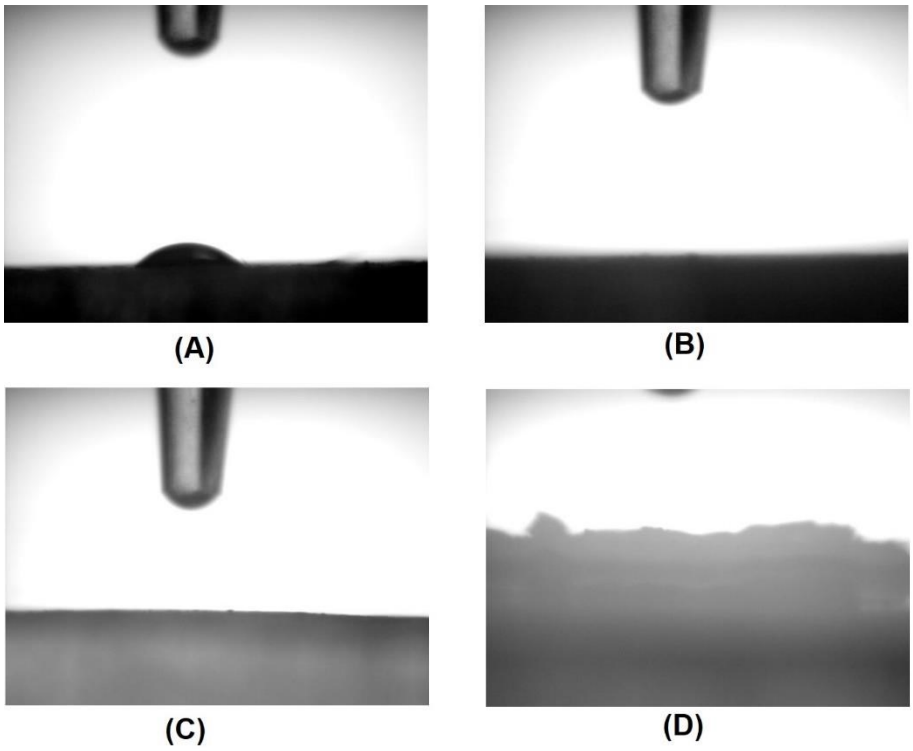


Figure 4-3 Water contact angle test for (A) untreated wood, (B) treated A wood, (C) treated B wood and (D) bacterial biomass.

### 4.6.2 Biofilm formation on the porous wood samples

During the 20 days of biofilm formation, bacterial biofilm was gradually formed on the wood samples as the growth of brownish biomass attached to the wood samples could be visually observed. SEM image of the grown biofilm on treated B wood sample (**Figure 4-2D**) shows the embedded bacterial cells in EPS, which has formed a uniform layer of biofilm on the wood's surface. Biofilm layer continuous to edge of the macropores, as well as inside walls of the macropores, where attachment of the bacterial cells can be observed from the SEM image (**Figure 4-2E**). Quantification of the 20-days old biofilm by all VSS, CDC, OD and total FAME measuring methods indicated a similar pattern of higher biofilm growth on the treated wood samples compared to the untreated wood samples (**Figure 4-4**). This can be qualitatively observed by comparing the SEM images of 20-days old biofilm on treated A wood (**Figure 4-2F**) and untreated wood (**Figure 4-2G**). While an intense and uniform biofilm layer has grown on the treated A wood, only scattered aggregations of biomass has been formed on the untreated wood. Respectively based on VSS, CDC, OD

and total FAME measuring methods, the quantified 20-days old biofilm on treated A wood was 2.04±0.31, 1.83±0.45, 1.81±0.41 and 2.07±0.22 (Avg: 1.93, STD: 0.36) folds higher than the biofilm on untreated wood and the biofilm on treated B wood was 2.59±0.41, 2.24±0.31, 2.19±0.52 and 2.66±0.23 (Avg: 2.42, STD:0.38) folds higher than the biofilm on untreated wood (**Figure 4-4**). These measurements indicated that delignification of the untreated wood samples significantly improved the biofilm formation capacity of the carriers.

Treated woods also outperformed the untreated wood in term of immobilization efficiency. Immobilization efficiency in this manuscript is defined as the ratio of the quantified biofilm to the suspended biomass (Żur et al., 2016). After 10 and 20 days of biofilm formation, the immobilization efficiencies were respectively 1.32 and 2.50 for untreated wood, 4.25 and 6.58 for treated A wood, and 5.15 and 8.13 for treated B wood. The start-up duration (i.e., biofilm formation time) and immobilization efficiency obtained by this study were comparable with the previous studies of biofilm formation on wood samples. Farber et al. (2019a) reported immobilization efficiency of 3.67 and 12.8 for *Pseudomonas putida* on respectively untreated pine tree wood waste and cold nitrogen plasma treated wood waste after 48 hours of biofilm formation in batch flasks using toluene as the carbon source. Moreover, the same wood samples (untreated and plasma treated wood waste) were used as biofilm carriers of a diesel-degrading consortium for bioremediation of diesel (Farber et al., 2019b), which resulted in immobilization efficiencies of 1.70 and 2.65 respectively for untreated and treated wood waste after 7 days of biofilm formation in batch flasks. It is worth mentioning that the difference in the microbial population used could influence the immobilization efficiency reported by different studies. Two more studies also used wood samples, wood powder (Manju et al., 2009) and wood husk (Asri et al., 2018), as biofilm carriers for bioremediation of respectively total ammonia nitrogen and chromium, after start-up duration of respectively 72 and 24 hours in batch flasks. However, immobilization efficiency has not been reported in these two studies.

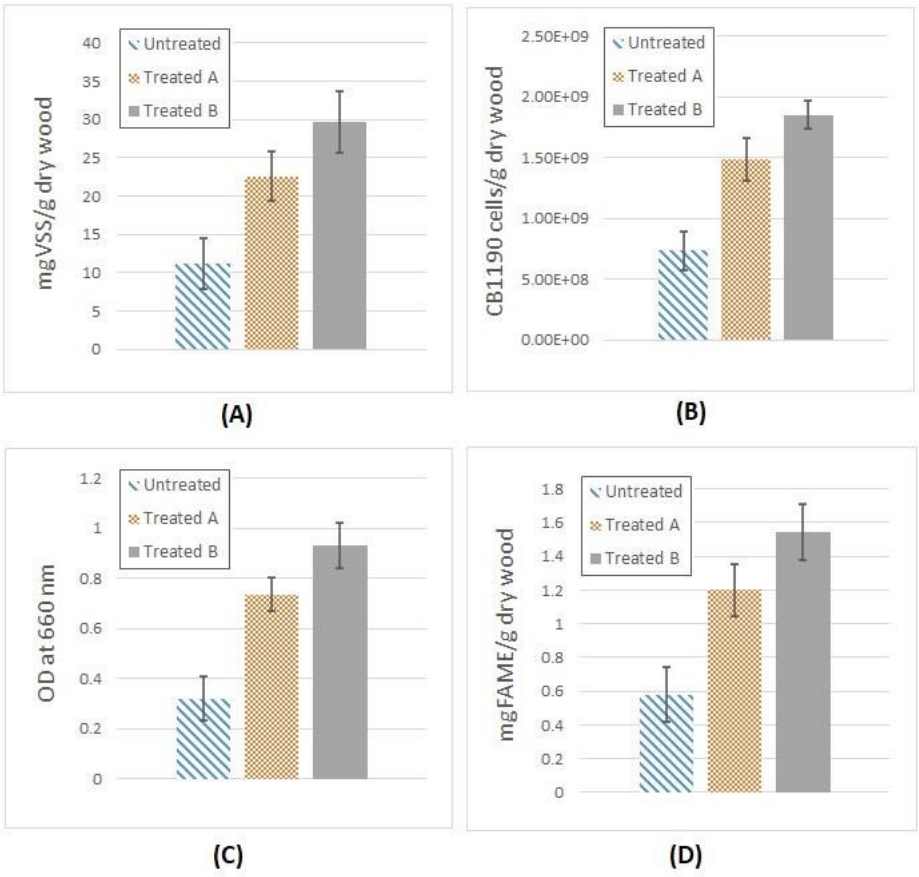


Figure 4-4 Quantification of the 20-days old bacterial biofilm formed on the untreated, treated A and B wood samples by measuring (A) volatile suspended solids, (B) cells direct count, (C) optical density and (D) total fatty acid methyl esters of the biofilm per gram of wood (quadruplicate samples from independent flasks). Values in figures are shown after eliminating the measured values for corresponding abiotic wood samples as control measurements. All control measurements were less than 5% of the shown values.

### 4.6.3 Fatty acid profile of biofilms

To understand the changes in the bacterial biomass during the biofilm formation, fatty acid (FA) profiles were obtained for 10- and 20-days old biofilm formed on untreated and treated wood samples. Twenty-two individual FAs were identified and quantified in the samples and classified to the groups of saturated fatty acids (SFA), unsaturated fatty acids (UFA), hydroxy fatty acids (HFA) and branched fatty acids (BFA) (**Table 4-2**). BFAs, UFAs, and SFAs all represented a great proportion of the FA profiles, while HFAs were only detected in trace amounts. BFAs were the dominating group in all the samples representing 37.70-47.93% of the total FAs. The major individual BFAs were i-16:0 and i-15:0 followed by cis i-16:1 n-9 and a-

17:0 (**Table 4-2**). Prevalence of BFAs is mostly observed in gram-positive bacteria generally serving as the acyl constituents of phospholipids in the cell membranes (Kaneda, 1991). Dominance of i-16:0 and i-15:0 have been respectively observed in FA profiles of genera *Pseudonocardia* (Kämpfer and Kroppenstedt, 2004) and *Terrimonas* (Zhang et al., 2012), which were among the DX-degrading genera of the initial inoculum. UFAs represented 21.34-29.84% of the total FAs dominated by cis18:1n-9, which is the signature FA of genera *Sphingomonas* (Chen et al., 2012) and *Afipia* (Brenner et al., 1991), which also existed in the microbial population. SFAs of carbon chain 12:0 to 18:0 were observed in the FA profiles with higher percentages of SFAs with longer chains (16:0-18:0). The FA profiles of 20-days old biofilm on the wood samples included greater proportion of SFAs (especially longer chain SFAs) compared to the FA profiles of 10-days old biofilm (**Table 4-2**). For example, in the case of biofilm on treated A wood, SFAs' proportion increased from 28.17±3.42% on day 10 to 40.49±4.39% on day 20 ($P<0.05$). The increase in SFAs were concurrent with decreases in both UFAs and BFAs for all three of the carrier types.

Table 4-2 Fatty acid profiles of the 10- and 20-days old bacterial biofilms formed on untreated, treated A, and treated B wood samples (quadruplicate).

| | **Biofilm on untreated** | | **Biofilm on treated A** | | **Biofilm on treated B** | |
|---|---|---|---|---|---|---|
| **Fatty acid** | **10 days** | **20 days** | **10 days** | **20 days** | **10 days** | **20 days** |
| 12:0 | 0.54±0.07 | — | 0.61±0.07 | 0.52±0.04 | 0.72±0.060 | 0.77±0.048 |
| 13:0 | — | — | — | — | 0.44±0.032 | 0.61±0.066 |
| 14:0 | — | — | — | 0.51±0.04 | 0.51±0.044 | 0.48±0.055 |
| i-15:0 | 9.76±1.28 | 8.48±1.23 | 8.94±2.31 | 7.73±1.27 | 9.98±1.11 | 7.13±1.13 |
| ai-15:0 | 3.05±0.68 | 3.41±0.74 | 2.72±0.22 | 2.68±0.24 | 2.66±0.25 | 2.51±0.24 |
| *cis* 15:1 n-6 | 3.76±0.25 | 3.63±0.34 | 2.78±0.18 | 1.95±0.11 | 1.73±0.74 | 1.85±0.28 |
| 15:0 | 6.84±2.85 | 7.37±2.13 | 8.52±2.64 | 9.18±2.33 | 7.95±1.99 | 8.51±2.13 |
| 2-OH-14:0 | 0.58±0.04 | — | 0.42±0.06 | — | — | — |
| 3-OH-14:0 | — | — | 0.47±0.05 | — | 0.45±0.051 | 0.59±0.050 |
| *cis* i-16:1 n-7 | 8.06±0.95 | 7.58±1.46 | 7.81±1.44 | 5.53±1.51 | 8.21±0.81 | 6.31±0.56 |
| i-16:0 | 13.48±2.17 | 12.85±2.35 | 12.34±3.56 | 12.11±2.98 | 12.87±1.18 | 11.95±1.36 |
| *cis* 16:1 n-7 | 5.88±1.12 | 5.95±1.15 | 4.81±0.86 | 2.95±0.58 | 3.73±0.16 | 2.72±0.29 |
| 16:0 | 3.47±0.54 | 4.85±1.09 | 4.82±1.12 | 7.44±2.76 | 4.38±0.55 | 5.47±0.84 |
| *cis* i-17:1 n-8 | 1.64±0.15 | 1.27±0.41 | 1.83±0.36 | 0.77±0.15 | 1.94±0.23 | 1.03±0.18 |

| | | | | | | |
|---|---|---|---|---|---|---|
| i-17:0 | 3.75±0.51 | 3.44±0.72 | 3.29±0.41 | 2.55±0.33 | — | — |
| ai-17:0 | 7.71±0.74 | 7.94±1.04 | 7.52±1.33 | 6.34±1.24 | 6.77±1.61 | 7.19±1.48 |
| *cis* 17:1 n-8 | 3.45±0.38 | 3.17±0.62 | 3.12±0.48 | 2.97±0.23 | 2.36±0.22 | 2.19±0.64 |
| 17:0 | 3.72±0.48 | 6.09±0.84 | 5.61±0.98 | 9.99±1.14 | 7.74±1.72 | 10.94±2.31 |
| 2-OH-16:0 | 0.54±0.14 | 0.61±0.23 | — | — | 0.42±0.21 | 0.48±0.13 |
| i-18:0 | 0.48±0.051 | 0.86±0.094 | — | — | 0.55±0.073 | 0.97±0.092 |
| *cis* 18:1 n-9 | 16.75±2.31 | 15.32±2.05 | 15.87±3.08 | 13.92±2.53 | 16.91±3.41 | 14.58±2.95 |
| 18:0 | 6.53±0.79 | 7.17±1.01 | 8.61±1.59 | 12.85±2.21 | 9.58±2.21 | 13.72±2.72 |
| ∑SFA | 21.1±3.04 | 25.48±2.73 | 28.17±3.42 | 40.49±4.39 | 30.88±3.48 | 39.89±4.24 |
| ∑UFA | 29.84±2.61 | 28.07±2.45 | 26.58±3.24 | 21.79±2.61 | 24.73±3.50 | 21.34±3.05 |
| ∑HFA | 1.12±0.15 | 0.61±0.23 | 0.89±0.08 | — | 0.87±0.22 | 1.07±0.14 |
| ∑BFA | 47.93±2.92 | 45.83±3.39 | 40.45±4.71 | 37.71±3.80 | 43.42±3.06 | 37.7±2.39 |

**Note:** Values are percentages of total fatty acids ± standard deviation. SFA: saturated fatty acids; UFA: unsaturated fatty acids; HFA: Hydroxy fatty acids; BFA: Branched fatty acids.

### 4.6.4 DX biodegradation by the bacterial biofilm on the wood samples

#### 4.6.4.1 Effect of different wood carriers on DX biodegradation and microbial composition

The bacterial biofilm grown on the treated A and B, and untreated wood samples were examined for DX biodegradation capability by spiking 100 mg/L of DX initial concentration into the flasks with fresh AMS medium. DX was completely removed (0.01 mg/L detection limit) in less than 32 h and 24 h in the flasks with grown biofilm on respectively treated A and B wood samples, while only 25.84±5.95% of the DX initial concentration was removed in 32 h in the flasks with grown biofilm on the untreated wood samples (**Figure 4-5**). DX concentration change in the killed control and abiotic flasks containing wood samples was continuously less than 5% in the time of experiments, which indicated that DX removal is completely attributed to biodegradation (**Figure 4-5**). Same result (i.e., no adsorption to the delignified porous wood) was observed for higher DX concentrations of 200 and 400 mg/L. The higher biodegradation rate of DX in the treated B flasks compared to the treated A flasks, and both the treated flasks compared to the untreated flasks were presumably because of the difference in the amount of bacterial biofilm that were grown on those wood samples during the biofilm formation stage (**Figure 4-4**).

To investigate the effect of wood samples on the consortium composition, microbial population of the 20-days old bacterial biofilm was obtained for the biofilms grown on untreated and treated wood samples. Almost all the population was identified to the genus level, while only a few species could be determined. The bar plots of the microbial population in genus level (**Figure 4-6**) showed a similar composition for all the biofilm samples. The population was dominated by the same DX-degrading genera that existed in the initially used bacterial consortium including *Afipia*, *Terrimonas*, *Burkholderia*, *Pseudonocardia*, *Sphingomonas*, *Bradyrhizobium* and *Chryseobacterium*, which indicates the suitability of wood carriers for biofilm formation of various DX-degrading genera. In other words, neither untreated nor treated wood samples inhibited biofilm formation of any of the 7 DX-degrading bacterial genera. However, the biofilm bacterial composition was slightly different from the planktonic bacterial composition (**Figure 4-6**), which can be attributed to the different biofilm-forming abilities of the DX-degrading genera. For example, *Terrimonas* prevalence (21.68%) in the planktonic inoculum decreased in the biofilm composition to 12.27% (average of biofilm on the woods), while *Alipia* proportion increased from 16.35% in planktonic inoculum to 32.05% in the average of biofilms.

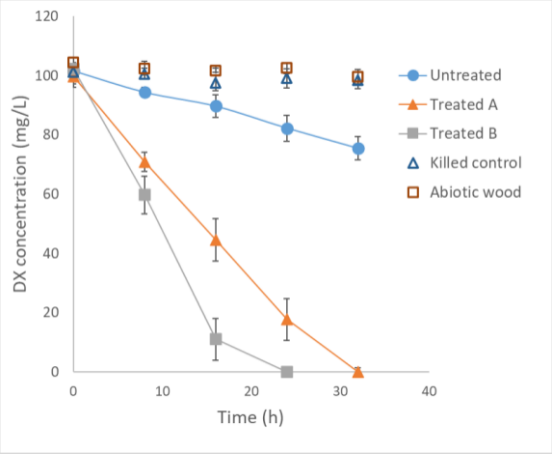


Figure 4-5 DX biodegradation in the biofilm flasks containing untreated, treated A and treated B wood samples as biofilm carriers (quadruplicate samples).

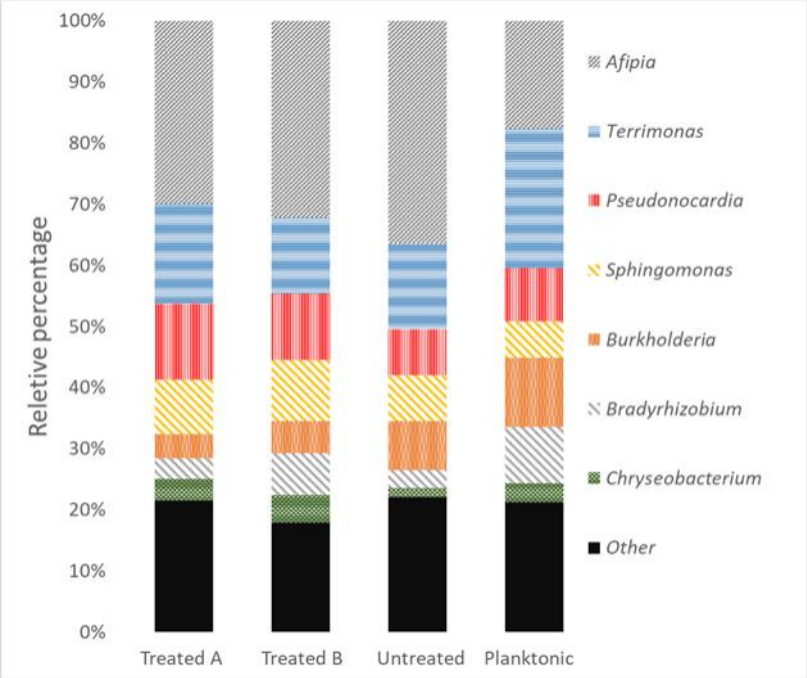


Figure 4-6 Microbial population analysis (genus level) of the 20-days old biofilm on treated A, treated B and untreated wood samples, and the biomass in the planktonic flasks.

### 4.6.4.2 DX biodegradation rate by biofilm and planktonic cultures

Because of showing the highest biodegradation rates, treated B flasks were selected for further kinetic experiments and for comparison of DX biodegradation rate compared to the planktonic flasks. The biofilm on treated B wood samples was measured to be 344±31.52 mgVSS/L in the flasks that were selected for biofilm kinetic experiments. The same biomass concentration of planktonic cells was harvested from the planktonic cells in the stationary phase (measured to be 356±23.52 mgVSS/L, $P>0.05$ with comparison to the biofilm flasks) and used for planktonic kinetic experiments. The cell concentration was also checked by CDC method in both biofilm ($4.83\times10^{7}\pm3.01\times10^{6}$ cells/mL) and planktonic flasks ($5.04\times10^{7}\pm2.58\times10^{6}$ cells/mL), which showed no significant difference ($P>0.05$). Removal of various initial concentrations of DX (25-400 mg/L) in both biofilm and planktonic flasks was monitored, which showed similar patterns (**Figure 4-7A,C**). The yield of biomass growth was calculated to be 0.0890±0.0073 mgVSS/mgDX (**Figure S3-Appendix C**). Low yield of biomass growth by DX utilization is a well known fact (Zenker et al., 2000), and the calculated yield was in alignment with the previously reported yields for biomass growth by DX

utilization (0.025-0.225 mgVSS/mgDX) (Parales et al., 1994; Kelley et al., 2001; Mahendra and Alvarez-Cohen, 2006). The calculated yield was verified to be constant at various DX concentrations (25-400 mg/L) as biomass was measured (data not shown) before addition of each DX concentration and after its complete removal. DX biodegradation data fitted well to the Monod model both for biofilm and planktonic flasks (**Figure 4-7B,D**) and the maximum specific rate ($\mu$) was calculated to be 0.0276±0.0018 1/h and 0.0382±0.0024 1/h respectively for biofilm and planktonic flasks, which showed a higher maximum specific rate in the planktonic flasks ($P<0.05$), while the biodegradation rates were in the same fold. The maximum DX biodegradation rate obtained by the biofilm on treated B wood samples was 106.6±12.3 mgDX/L/h. It is close to the maximum DX biodegradation rate (145.3 mgDX/L/h) achieved by Isaka et al. (2016) using the *Afipia sp.* strain D1 on gel carriers. Applying the Monod model, they estimated the half-saturation constant of 28 mg/L, which was smaller than the half-saturation constant obtained in DX biodegradation by biofilm on treated B wood in this study (82.47±7.21 mg/L, **Figure 4-7B**). On the other hand, two other studies on DX biodegradation by *Mycobacterium austroafricanum* JOB5 biofilm on silica sand (Johnson et al., 2020) and by *Pseudonocardia dioxanivorans* CB1190 biofilm on soil (Zhao et al., 2018) reported DX biodegradation rates of 3 orders of magnitude lower, respectively 0.073 mgDX/L/h and 0.13 mgDX/L/h, than DX biodegradation rate reported in our study. Potential factors affecting the DX biodegradation rate in biofilm-mediated systems are discussed in the next section.

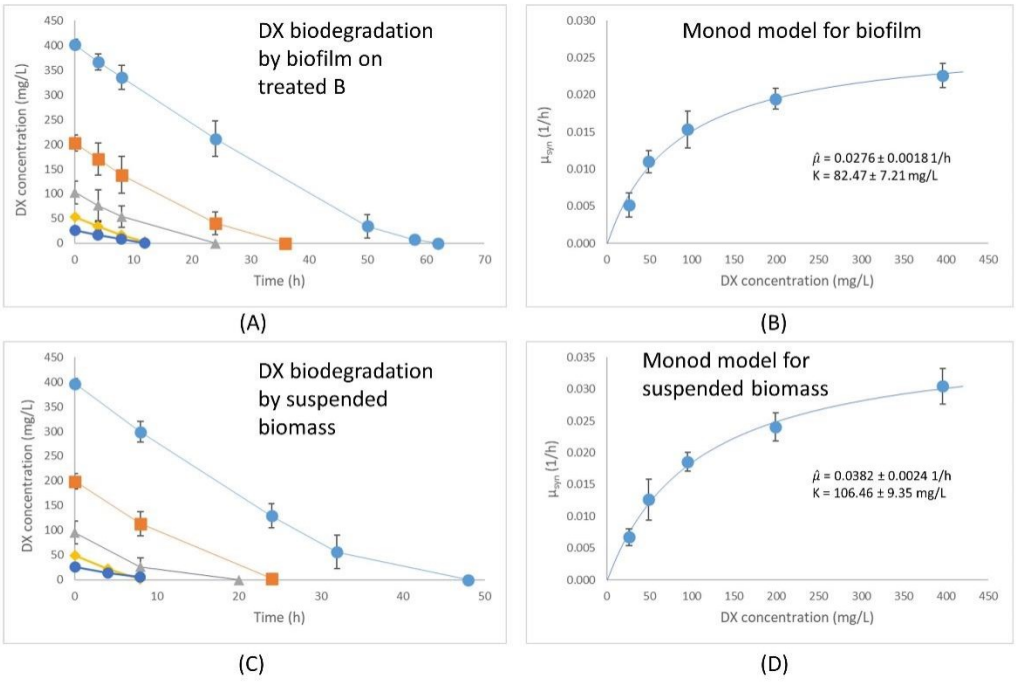


Figure 4-7 (A) DX biodegradation at various concentrations by biofilm on treated B wood samples and (B) Monod plot by biofilm on treated B wood samples; (C) DX biodegradation at various concentrations by planktonic cells and (D) Monod plot by planktonic cells (quadruplicate samples).

#### 4.6.4.3 DX biodegradation rate after biofilm regeneration

The bacterial consortium used by this study contained aerobic DX-degrading microorganisms like *Afipia* and *Pseudonocardia* which remain viable in presence of DX up to concentrations around 700 mg/L (Parales et al., 1994; Isaka et al., 2016). The biofilm regeneration experiments showed that the consortium was able to remain viable in DX concentrations of 400, 200 and 100 mg/L (**Figure S5-Appendix C**). Fitting the DX biodegradation data to the Monod model before and after the biofilm regeneration, showed respectively maximum specific rates of 0.0296±0.0023 and 0.0304±0.0041 1/h (P>0.05). The measured ATP content of biofilm before and after the regeneration, respectively 1552±72 and 1498±65 ngATP/mgVSS, also indicated a similar biomass activity (P>0.05). Furthermore, DX concentration was below the detection limit (0.1 mg/L) in the AMS medium that was used for biofilm regeneration for 24 hours, providing no evidence that DX can be accumulated in the biofilm.

## 4.7 Discussion

### 4.7.1 Improved properties of treated wood samples as biofilm support

As discussed in the section 3.1, comparison of the untreated and treated wood samples showed significant changes in surface roughness and wettability, and formation of macropores on the treated samples (**Table 4-1**), all of which are crucial properties in determining the performance of biofilm carriers (Zhao et al., 2019; Al-Amshawee et al., 2020; Al-Amshawee and Yunus, 2021). Existence of macropores in biofilm carriers increases the surface area and improves the biofilm formation as microorganisms can grow both on the carriers' external surface and inside the macropores (Zhang et al., 2010; Li et al., 2012; Yang et al., 2021). Moreover, the grown biofilm inside the macropores is protected from external shear stress which prevents detachment of biomass (Al-Amshawee and Yunus, 2021). Surface roughness and wettability (hydrophobicity or hydrophilicity) of biofilm carriers are also significant factors (Al-Amshawee et al., 2020). A rough surface with peaks and valleys provides an excellent environment for attachment of microorganisms, meantime protects the microorganisms from shock loads leading to an enhanced growth of biofilm (Paul et al., 2007; Ahmad et al., 2017). Hydrophilic surfaces of the biofilm carriers can overcome the repulsion forces between microorganisms and the carrier's surface resulting in an enhanced attachment (Al-Amshawee et al., 2020). The water contact angle test showed that the bacterial biomass of the employed consortium is completely hydrophilic (**Figure 4-3D**). Surface of bacterial cells includes functional groups such as —COOH, —CHO, and —OH that form hydrogen bonds with the carrier's surface (Renner and Weibel, 2011). Therefore, treated wood samples with super hydrophilic surfaces (**Figure 3-3B,C**) provided an excellent surface for attachment of the bacteria. The same phenomenon was observed by Farber et al. (2019a), where nitrogen-plasma treated wood with hydrophilic surface outperformed untreated wood with hydrophobic surface as biofilm carriers regarding the attachment of hydrophilic biomasses of *Pseudomonas putida* and *Bacillus Cereus*. It was mentioned that nitrogen-plasma treatment led to enrichment of lignin with carboxylic groups increasing the polarity and wettability of the wood surface. The same concept occurs during wood delignification, where chemical composition of wood is

changed during the reaction, and hydroxyl groups from cellulose becomes more available increasing the hydrophilicity of the wood's surface (Beims et al., 2022). Other treatment methods such as coating hydrophilic surfactants on the carriers or blending the carriers with hydrophilic materials have also been used in the literature to increase the hydrophilicity of the carriers in an effort to improve the biofilm attachment (Shen et al., 2007; Mao et al., 2017).

In addition to above-mentioned excellent properties of delignified porous woods as biofilm support, using them provide other advantages. The main concern with natural organic materials as biofilm support is that they provide low mechanical strength and are degraded by the microorganisms (Zhao et al., 2019). However, the XRD test on delignified parous wood samples after biofilm formation showed that they kept almost same mechanical strength, enabling them to be reused. Moreover, no evidence of wood degradation or growth of cellulose-degrading microorganisms were observed. The wood samples also did not adsorb DX, which could impose a chemical toxicity on the microorganisms otherwise. Last but not least, wood is one of the most abundant and sustainable substances on earth with a unique structure, which has attracted the attention of researchers to be used as an advanced material in different applications (Li et al., 2021). The only disadvantage of porous delignified wood is that organic solvents are wasted in the delignification process. However, it has been shown that the acid/base used in this process can be recovered and reused (Wang et al., 2020).

### 4.7.2 Increase in SFAs of biofilm over time

Changes in the FA profile of the biomass can be associated with the variations in physicochemical properties of the surrounding environment (Al-Beloshei et al., 2015). Biofilm formation changes the surrounding environment of bacteria to a more heterogenous matrix (EPS) where nutrients and oxygen are not easily accessible (Bridier et al., 2011). Furthermore, the gradual accumulation of the biomass layers over the surface of carriers intensifies the mentioned changes. Comparison of the quantified

biofilms on day 10 and day 20 showed a substantial increase in the total biofilm amount formed on the wood samples (**Figure S4-Appendix C**). This biomass growth can be positively associated with the increase in the SFAs proportion of the FA profiles. Additionally, SFAs proportion was higher in the biofilm formed on treated woods compared to untreated wood, and on treated B wood compared to treated A wood (**Table 4-2**), which also is consistent with the amount of biofilm that was formed on the carriers (**Figure 4-4**).

Increase in the SFAs proportion of bacterial biomass results in an increased membrane's phase transition temperature and a denser biomass with higher bilayer stability and rigidity (Denich et al., 2003). Specifically, the increase in long chain SFAs would also result in a more hydrophobic biomass (Chao et al., 2010). A more hydrophobic biomass reduces the possibility of biomass detachment from the carrier's surface by the flow effects (Donlan, 2002). On the other hand, as mentioned earlier, high availability of hydrophilic functional groups on the cell surface improves the initial adhesion (Zhao et al., 2019). To explain this contradiction, we speculate that after the initial attachment of the cells, the long chain SFAs of the biomass started to increase during the later stage of biofilm formation, which made the biofilms more rigid, hydrophobic, and resistant to detachment. In addition, increase in SFAs of the biofilm cells has been previously reported under environmental stresses such as acidic condition or nutrient depletion as an adaptive stress response which enables the biofilm cells to survive in harsher environments (Gianotti et al., 2008; Dubois-Brissonnet et al., 2016).

### 4.7.3 Lower DX biodegradation rate by biofilm versus planktonic

Mass transport of substrate in the biofilm layer can be crucial in determining overall biodegradation rate by biofilm as the substrate can reach lower concentrations inside a thick biofilm with high mass transport resistance (Rittmann and McCarty, 2001). Penetration depth of substrate into the biofilm is determined by the rate of diffusion into the biofilm and the rate of substrate utilization in the biofilm. This penetration

depth (a) can be theoretically estimated knowing the substrate diffusion coefficient in biofilm ($D_e$), its concentration at the biofilm interface ($S_p$), and volumetric utilization rate of substrate inside the biofilm ($k_o$) (equation 4) (Stewart, 2003).

$$a = \left(\frac{2D_e S_p}{k_o}\right)^{0.5} \quad (4)$$

Each of these parameters were estimated for the biofilm flasks to calculate the DX penetration depth into the biofilm. DX diffusion coefficient in biofilm ($D_e$) was estimated to be 25% (Stewart, 2003) of its diffusion coefficient in water at 25 ˚C (1.10 x $10^{-5}$ $cm^2/s$ for DX concentrations lower than 880 mg/L, Leaist et al. (2000)), or 2.75 x $10^{-6}$ $cm^2/s$. The DX concentration at biofilm interface ($S_p$) was assumed to be the lowest initial concentration that was used in the biodegradation experiments, or 25 mg/L, and the DX utilization rate in the biofilm was assumed to be the highest calculated utilization rate in the biodegradation experiments or 11.22 mg/L/h. These estimates resulted in DX penetration depth of 2100 µm into the biofilm. Although direct measurement of biofilm thickness was not practical in our study because of the high surface roughness and existence of macropores on the treated wood samples (**Figure 4-2B,C**), the biofilm thickness can be qualitatively observed from SEM images of biofilm (**Figure 4-2E,F**), that should be in the range of 10-50 µm. Therefore, DX could fully penetrate the entire depth of biofilm, and mass transport did not limit the DX biodegradation rate by DX-degrading bacterial cells inside the biofilm.

Although mass transfer did not limit the DX penetration, a lower maximum specific rate was still calculated for DX biodegradation in biofilm flasks compared to the planktonic flasks (**Figure 4-7B,D**). The similar phenomenon was also observed by Mirpuri et al. (1997) that activity of *Pseudomonas putida* 54G cells for toluene biodegradation in planktonic form was around 4 times higher than in biofilm form, when mass transfer was not the limiting factor. They found that accumulation of inactive cells in the biofilm over time caused the lower activity for toluene biodegradation, which presumably could also be the reason of lower DX biodegradation rate in this study too as the biofilm was formed on the wood samples in a 20-day

period. Furthermore, Johnson et al. (2020) reported much lower (factor of $10^{-3}$) DX biodegradation rates in the biofilm of *Mycobacterium austroafricanum* JOB5 formed on silica sand than planktonic cells. They speculated that gross quantification of biofilm by qPCR method cannot differentiate active cells from inactive cells, and results in underestimation of biodegradation rate in biofilm. Although in this study we double checked the total cell numbers by CDC method for the initial biomass concentration in planktonic and biofilm flasks, the measured biomass concentrations based on mgVSS/L were used in the biodegradation calculations, which has the same drawback too. Given that mass transfer was not a limiting factor in DX biodegradation rate by the bacterial biofilm in this study, and the general similarity of the microbial composition of biofilm and planktonic flasks (**Figure 4-6**), we speculate that accumulation of inactive biomass was the main reason of the lower DX biodegradation observed in the biofilm flasks compared to the planktonic flasks, as reported by the previous studies (Mirpuri et al., 1997; Johnson et al., 2020).

There are several general advantages for biofilm systems over planktonic systems that are not related to the contaminant degradation rate. First, biofilms are more resilient to fluctuations in operating conditions and shock loads. Planktonic systems can be highly sensitive to sudden changes in pollutant concentration or flow rates, which may lead to process instability. Second, biofilm systems typically require smaller reactor volumes compared to planktonic systems. This is because the biofilm carriers provide a large surface area for microbial attachment, allowing for higher biomass concentrations in a smaller space. As a result, biofilm systems can be more compact and space efficient. Third, planktonic systems may experience biomass washout during high flow conditions, especially in open systems like activated sludge reactors. In contrast, biofilm systems have a lower risk of washout as the biofilm adheres firmly to the carrier surfaces. Other advantages also include biofilm resiliency to the toxicity, long term stability, and lower energy consumption (Rittmann and McCarty, 2012).

### 4.7.4 DX biodegradation pathway by the bacterial consortium

DX biodegradation pathway by aerobic microorganisms has been well-studied in the literature (Grostern et al., 2012; Zhang et al., 2017). Dioxane monooxygenase (DXMO) is the key enzyme which initiates the biodegradation process. Ethylene glycol and oxalic acid are the major intermediates in most of the proposed pathways (Kim et al., 2009; Huang et al., 2014; Chen et al., 2021a). These compounds are eventually mineralized to carbon dioxide through the tricarboxylic acid (TCA) cycle. This biodegradation pathway has been mainly attributed to *Pseudonocardia* genus (Zhang et al., 2017), that was part of the bacterial consortium used in our study. Similar biodegradation pathway has been reported previously for bacterial consortia that dominated by *Terrimonas*, *Bradyrhizobium*, or *Sphingomonas* genera (Xiong et al., 2020; Chen et al., 2021a; Dang and Cupples, 2021), which also existed in the bacterial consortium used in our study. The other major genera of our bacterial consortium included *Afipia* and *Burkholderia*. Although DX biodegradation pathway by these genera or consortia dominating by them have not been reported directly, both have been identified as monooxygenase producing microorganisms capable of DX biodegradation (Kim et al., 2009; Isaka et al., 2016), which increases the probability of DX biodegradation through the same pathway. Furthermore, no evidence of accumulation of intermediates was observed in the GC/MS analysis performed by us throughout the DX biodegradation experiments, confirming that DX was completely mineralized to carbon dioxide.

## 4.8 Conclusions

Use of treated porous wood as biofilm carriers significantly increased the amount of biofilm that was formed compared to the natural untreated wood because of the changes in physical/chemical properties through the delignification process. Increase in porosity, surface roughness and hydrophilicity, and formation of macropores on the treated woods were identified as the major modifications that played important roles in enhancing the biofilm formation. This enhancement led to substantially higher DX

biodegradation rates by the bacterial biofilm formed on the treated wood samples compared to the untreated samples, although relatively slower than the biodegradation rate by planktonic cells. Biofilm-mediated bioremediation is a robust tool which can increase tolerance of the cells to harsher environmental conditions and exposure to toxic contaminants. The delignified porous wood samples showed excellent properties as biofilm carriers which can be used as the support material for bioremediation of various contaminants.

## 4.9 Acknowledgments

The financial support of NSERC-DG is acknowledged. The author A.S is thankful for the NSERC-CREATE ASPIRE and Bruce and Dorothy Rosetti Engineering Research scholarships in support of his PhD program. The author R.F.B also acknowledges the Coordination for the Improvement of Higher Education Personnel (CAPES) for providing the scholarship for the PhD program (Process Number 88881.174355/2018-01). Special thanks to the SEM facility and IMR center, laboratories of Dr. Jeff Dahn and Dr. Su-Ling Brooks, and protein assembly research team at Dalhousie University for providing equipment and helping us with the measurement or analysis.

## 4.10 Declaration of interests

The authors declare that they have no known competing financial interests or personal relationships that could have appeared to influence the work reported in this paper.

## 4.11 Supplementary material

Supplementary materials of this manuscript can be found in **Appendix C**.

## 4.12 Data availability statement

The data that support the findings of this study are available from the corresponding author, A.K, upon reasonable request.

# Chapter 5 Biodegradation of 1,4-dioxane in a continuous-flow bioelectrochemical reactor by biofilm of *Pseudonocardia dioxanivorans* CB1190 and microbial community on conductive carriers

This chapter will be submitted to a journal to be considered for publication.

## 5.1 Highlights

- Biodegradation of 1,4-dioxane was enhanced at 1.2 V by oxygen production.
- Biodegradation using microbial community was enhanced at 1.0 V.
- Applying 1.0 V changed the microbial community without observable oxygen production.
- ATP of electro-active biomass increased by applying a positive voltage.
- Conductive carriers played a key role in the electrochemical stimulation.

## 5.2 Graphical Abstract

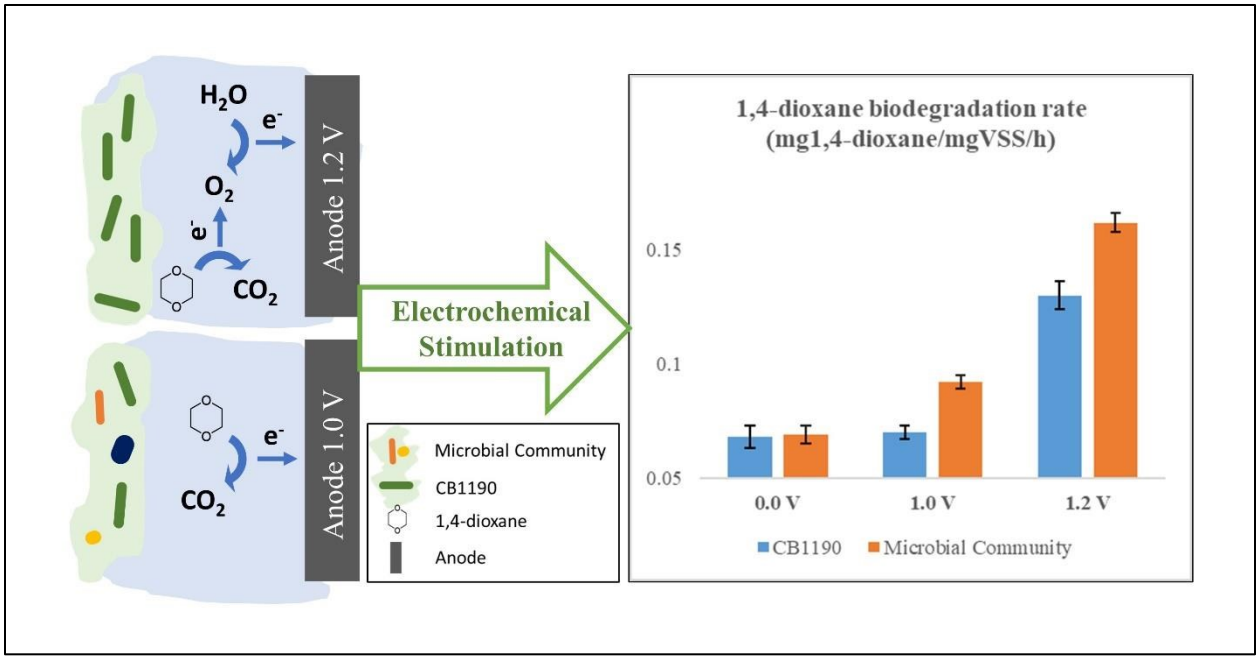


Figure 5-1 Graphical abstract of chapter 5.

## 5.3 Abstract

Bioelectrochemical degradation is an environmentally friendlyand controllable way of providing electron acceptor to the microorganisms. A continuous-flow bioelectrochemical reactor (BER) was developed in this study to investigate of the potential for enhancing the bioelectrochemical degradation of 1,4-dioxane (DX) by *Pseudonocardia dioxanivorans* CB1190 (CB1190) and microbial community biofilm on conductive and non-conductive carriers in low voltages (1.0-1.2 V) and currents (<2 mA ). In the case of CB1190, DX removal efficiency conducting biodegradation at 1.0 V did not result in any observable change in DX removal efficiency and was determined to be (32.63±2.48%) compared to the 0.0 V (31.69±2.33%) but was much higher at 1.2 V (59.08±0.86%). The higher removal at 1.2 V was attributed to an increase in dissolved oxygen (DO) concentration from 3.77±0.33 mg/L at 0.0 V to 5.40±0.11 mg/L at 1.2 V, which resulted from water electrolysis. In the case of microbial community, on the other hand, DX removal efficiency increased at 1.0 V (30.98±1.10%) compared to 0.0 V (23.40±1.02%) that can be attributed to a simultaneous increase in microbial activity from 2389±118.5 ngATP/mgVSS at 0.0 V to 2942±109

ngATP/mgVSS at 1.0 V. Analysis of the changes in microbial composition indicated enrichment of Alistipes and Lutispora at 1.0 V due to the ability of these genera to directly transfer electrons with conductive surface. On the other hand, no change was observed in the microbial community in the case of non-conductive carriers. Results of this study showed that electro-assisted biodegradation of DX at low voltages is possible through two different mechanisms (oxygen production and direct electron transfer with electrode) which makes this technique flexible.

## 5.4 Introduction

Lack of electron acceptors is one of the main challenges in bioremediation of 1,4-dioxane (DX), an emerging contaminant, in the subsurface environments (Jasmann et al., 2017; Zhang et al., 2017; Pollitt et al., 2019). DX usually ends up in groundwaters because of its high solubility, $S_w$=11.35 M or 1000 $g.L^{-1}$, and low octanol-water partition coefficient, log $K_{OW}$=-0.27 (EPA-DSSTox, 2021), and is extremely persistent with half-life of 3-5 years (Pollitt et al., 2019). Dissolved oxygen (DO) concentration is usually not sufficient in groundwaters required by aerobic bacteria for degradation of organic contaminants such as DX (Rivett and Thornton, 2008). Since groundwaters are usually located in empty spaces between rocks, soils, and sediments, they lack a good mixing condition, which results in depletion of electron acceptors (Anneser et al., 2010).

Biostimulation is a way to overcome the problem in the groundwaters by injecting oxygen producing chemicals such as superoxide ($O_2^-$), chlorate ($ClO_3^-$), and perchlorate ($ClO_4^-$), or by provision of the oxygen molecules mechanically. However, it needs periodical supplement of chemicals or continuous transfer of oxygen to the contaminated groundwater, which exert high expenses to the bioremediation process. In addition, control of these processes is hard since they might cause secondary contamination to the groundwater (Li and Yu, 2015). Electrochemical stimulation of the bioremediation (electro-

biodegradation) process is an alternative technique which has several advantages including controllability, environmentally benign nature and high removal efficiency.

The main idea of electro-biodegradation is to install electrodes into contaminated environments (usually groundwaters) and apply electric potentials to the electrodes stimulating the microbial metabolism (Li and Yu, 2015). The stimulation of microorganisms to degrade contaminants occurs in several mechanisms. In the first mechanism, the electrodes work directly as the electron acceptor of the microbial metabolism. This is extremely significant in environments where the availability of electron acceptors such as oxygen, sulfate, and nitrate are minimal. Electron transfer between the cells and the electrode occurs directly, however, it requires use of electro-active microorganisms. Alternatively, provision of electron acceptor can happen through redox mediators (e.g., methyl viologen) in the aqueous medium (Aulenta et al., 2009). Finally, hydrolysis of water caused by the polarized electrodes results in the formation of oxygen molecules which serve as fresh electron acceptors for the aerobic microorganisms (Bellagamba et al., 2017).

Using a high voltage (e.g., 8 V) for the electrical stimulation may result in formation of hydroxyl radicals, which are deadly for the microorganisms, or change the environment condition (pH, temperature, etc.) drastically (Jasmann et al., 2017). In addition, use of higher voltages and currents makes the process costly and energy intensive (Pica et al., 2021). Therefore, using low voltages (in the range of 1-2 V) and currents (in the range of a few mA) that is suitable for stimulation of microorganisms makes the process environmentally friendly and more sustainable (Ailijiang et al., 2016; Abdalrhman et al., 2020). In this case, using conductive carriers such as graphite granules as support material for biomass instead of non-conductive materials can enhance the efficiency of the electrical stimulation by increasing the conductive surface area which makes the electrode-biomass interaction highly efficient (Aulenta et al., 2011; Lu et al., 2014; Verdini et al., 2015).

In this study, we investigated the possibility of electrical stimulation on DX biodegradation by *pseudonocardia dioxanivorans* CB1190 (CB1190), a well-known DX degrader (Parales et al., 1994; Mahendra and Alvarez-Cohen, 2005), and a microbial community that originated from a native digestate microbial community (Samadi et al., 2022) in low voltages (1.0-1.2 V) and currents ( < 2 mA) using the graphite granules as the conductive biofilm carriers. In this work, the impact of voltage in the vicinity of the voltage required for water electrolysis on microbial activity and DX biodegradation rate were explored, and the mechanisms of electrical stimulation for DX biodegradation was investigated. The novelty of this work is that electro-assisted biodegradation of DX in the presence of CB1190 and microbial community has never been investigated in lower voltages than water electrolysis, where microorganisms can be electrochemically stimulated by mechanisms other than oxygen production.

## 5.5 Materials and Methods

### 5.5.1 Chemicals and inoculum preparation

DX (anhydrous 99.8%), DX-d8 (≥99% atom D, used as internal standard) and Methyl tert-butyl ether (anhydrous 99.8%, used as extraction solvent) were purchased from Sigma Aldrich.

Experiments with pure culture were conducted using *Pseudonocardia dioxanivorans* CB1190 (CB1190). It was purchased from ATCC. The vial containing CB1190 was opened according to the vendor's instructions, inoculated to #196 ATCC medium, and incubated at 30°C for 7-14 days. Aseptic techniques and UV-sterilized biosafety cabinet were used to make sure that the inoculum remains pure. Actively grown cells were harvested to inoculate ammonium mineral salts (AMS) medium (Parales et al., 1994) in conical flasks fed with DX as the sole source of carbon. Cells in their stationary phase were used for further experiments. Both genotypic and phenotypic methods were employed throughout the experiments to check CB1190 purity.

Experiments with microbial community was conducted using a DX-acclimated microbial community. The initial inoculum was originated from a native digestate microbial community (Samadi et al., 2022). The community was acclimated to DX during a 18-week period in AMS medium and DX as the sole source of carbon.

### 5.5.2 Biofilm formation

Before biofilm formation, 1-5 mm diameter graphite granules (GG) were soaked in 37% HCl overnight, washed with sterilized distilled water several times and dried in a vacuum oven. The biofilm was formed on GG in the 250 mL conical flasks shaking at 180 RPM that was initially inoculated with 0.2 optical density (OD) at 680 nm of the DX-acclimated CB1190 in AMS medium. To avoid shear stress to the biofilm because of collision of the GG to body of the flask, GGs (10 g) were put in a narrow net which was suspended in the medium using a thread. The potential of biofilm formation on the net was monitored by placing a net, which that did not contain GG and used as control. There was no evidence of biofilm formation on the net, used as control. After 20 days, 3 parallel flasks were sacrificed to measure the biofilm formed on GG.

In the case of experiments with microbial community, non-conductive carrier was also used in additional experiments to compare the performance with GG. Natural pine wood was selected as the non-conductive carrier, which its potential for use as biofilm carrier for DX biodegradation was previously explored (Samadi et al., 2023). The same biofilm formation procedure was followed for the non-conductive carriers. In this study, pine wood and graphite granules (GG) were selected respectively as non-conductive and conductive carriers. The goal was to investigate the role of conductive carriers in spreading the applied potential to the electrode to the whole anode chamber. To fully understand this effect, wood as non-conductive material was used for the control experiments.

Treated wood samples were not used as control material, because the focus here was to compare conductive versus non-conductive carriers. Treated wood would provide superior properties such as high

surface area and porosity for biofilm formation compared to graphite granules, which is not a porous material. Therefore, selecting treated wood as biofilm carriers would add extra layer of complexity to the experiments and would not perform well as “non-conductive control”.

### 5.5.3 Bioelectrochemical reactor setup

Bioelectrochemical reactor (BER) was a H-type electrochemical cell (Adams & Chittenden Scientific Glass, U.S.) with two standard borosilicate media bottles (anode and cathode chambers, each 333 mL) that were separated by a proton exchange membrane (Fuel Cells Etc, U.S.), which was kept between the chambers by wraparound knuckle clamps (**Figure 5-2**). Before the experiments, BER chambers and other components (tubing, valves, feed-stock container, etc.) were filled with 70% ethanol overnight, and washed with sterilized distilled water. The anode chamber was filled with 90 g of GG (or same volume of wood in case of experiments with non-conductive carriers), containing biofilm which was developed in shake flask for 20-day and fresh AMS medium containing 100 mg/L DX.

The empty volume of the anode chamber after loading the GG was 272 mL, and the specific conductive surface aera in the anode chamber was estimated to be 181 $m^2/m^3$. To estimate the empty volume of anode chamber after loading GG, density of GG was measured by volume displacement in a graduate cylinder. Then, volume of 90 g GG was calculated and subtracted from total volume of the anode chamber. To estimate the conductive surface area, it was assumed that the GG are in sphere shape and the average radius was used for calculation of surface area. Total volume of GG was calculated using the measured density.

Graphite rod electrodes (6 mm diameter and 7.5 cm long, BASi, U.S.) were inserted into the anode and cathode chambers respectively as working and counter electrodes. An Ag/AgCl reference electrode (BASi, U.S.) was also inserted in the anode chamber (+0.197 relative to standard hydrogen electrode, SHE). All the electrodes were externally connected to a PalmSens EmStat3+ potentiostat (BASi, U.S.), which was

used to apply a specific voltage to the anode. Throughout the manuscript, all the voltages are reported versus the Ag/AgCl electrode, if not mentioned otherwise.

The reactor was operated in continuous mode, by introducing the influent to the BER using a peristaltic pump (MasterFlex, Canada). Viton tubing was used to minimize adsorption of DX. During the operation of BER, daily samples were taken for physiochemical measurements including DX and DO concentration, pH and oxidation reduction potential (ORP) from the influent and effluent of the anode chamber and the center of cathode chamber.

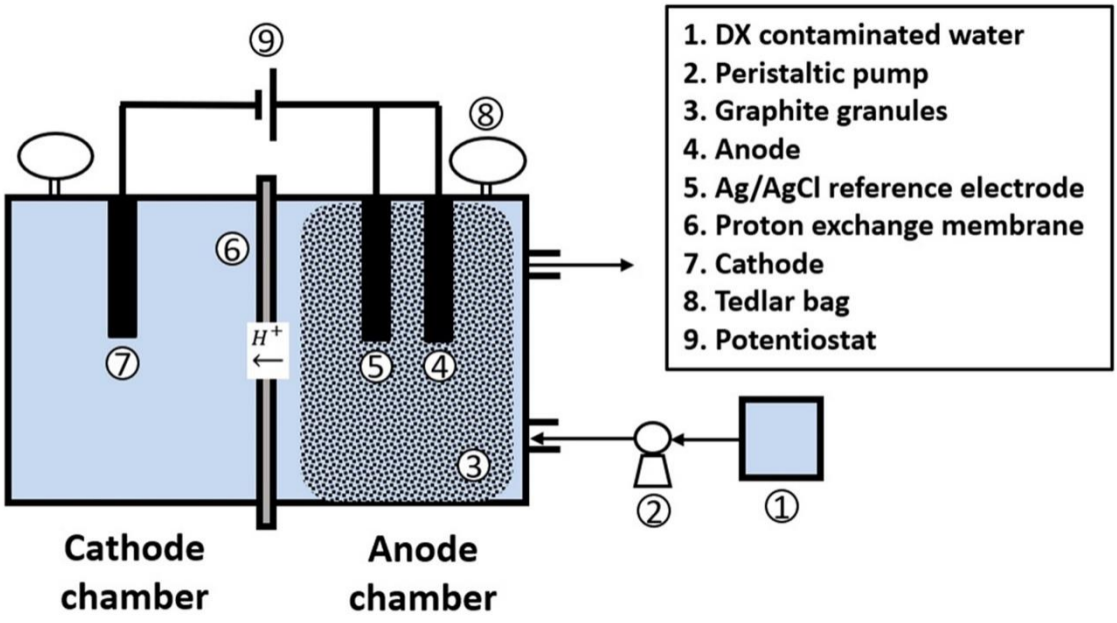


Figure 5-2 Schematic overview of the BER.

### 5.5.4 Bioelectrochemical experiments

A constant flowrate of 0.1 mL/min was set for the influent (AMS medium containing 100 mg/L of DX) using the peristaltic pump. Continuous runs were performed with BER (**Table 5-2**). Different conditions were set to each run regarding the applied voltage to the anode (0.0, 1.0 or 1.2 V). A relatively higher concentration of DX (100 mg/L) compared to the contaminated groundwaters (Adamson et al., 2014) was

spiked to the feedstock in order to ease the differentiation between the removal percentages of different conditions. Each continuous run was performed long enough until stabilization of the monitoring parameters and observing the effect of the selected conditions on DX removal and bacterial activity. Abiotic and killed control runs were also performed (**Table 5-1**) to rule out the possibility of removal of DX by non-biodegradation means (e.g., volatilization, adsorption to the carriers, or biosorption to the biomass). In the case of killed control experiments, 70% ethanol was run in the reactor (after the biodegradation experiments) for 48 hours to make sure the attached biomass is killed. This was check by measuring activity (ATP) of the biomass. Regular samples, daily in the case of physiochemical parameters including DX and DO concentrations, pH and oxidation reduction potential (ORP), and three times in each run in the case of biological parameters including biofilm on GG, suspended biomass and ATP in biofilm were taken during the continuous runs. In the case of change in the pH because of the applied voltage, it was adjusted by using 0.1 N HCL or NaOH to keep it around 7. Liquid samples were taken from the influent and effluent of the anode chamber, as well as center of the cathode chamber. GG samples (around 0.5 g each time) for biological measurements in the biofilm were taken only from the anode chamber. To check population of biofilm, biological samples were also submitted to Integrated Microbiome Resources at Dalhousie University (Halifax, Canada) for DNA extraction, library preparation, PCR sequencing and bioinformatic analysis.

Table 5-1 Sequence of experiments performed with BER.

| Number | Biofilm | Carrier type | Feedstock | Applied voltage (V) | Days of operation (d) |
|---|---|---|---|---|---|
| 1 | Abiotic | Conductive (GG) | AMS + DX (100 mg/L) | 0.0 | 15 |
| 2 | Abiotic | Conductive (GG) | AMS + DX (100 mg/L) | 1.0 | 15 |
| 3 | Killed control | Conductive (GG) | AMS + DX (100 mg/L) | 1.0 | 20 |
| 4 | CB1190 (control biodegradation) | Conductive (GG) | AMS + DX (100 mg/L) | 0.0 | 48 |
| 5 | CB1190 | Conductive (GG) | AMS + DX (100 mg/L) | 1.0 | 30 |
| 6 | CB1190 | Conductive (GG) | AMS + DX (100 mg/L) | 1.2 | 34 |
| 7 | Microbial community (control biodegradation) | Conductive (GG) | AMS + DX (100 mg/L) | 0.0 | 32 |

| | | | | | |
|---|---|---|---|---|---|
| 8 | Microbial community 9 | Conductive (GG) | AMS + DX (100 mg/L) | 1.0 | 18 |
| | Microbial community | Conductive (GG) | AMS + DX (100 mg/L) | 1.2 | 14 |
| 10 | Microbial community (control biodegradation) | Non-conductive (wood) | AMS + DX (100 mg/L) | 0.0 | 10 |
| 11 | Microbial community | Non-conductive (wood) | AMS + DX (100 mg/L) | 1.0 | 17 |
| 12 | Microbial community | Non-conductive (wood) | AMS + DX (100 mg/L) | 1.2 | 20 |

### 5.5.5 Analytical methods

#### 5.5.5.1 Physiochemical measurements

DX concentration was measured throughout the experiments by solvent extraction (MTBE as the organic solvent) followed by GC/MS analysis. The sample preparation procedure and condition of GC/MS analysis has been described elsewhere (Samadi et al., 2022). DO concentration, pH and ORP were respectively measured by Vernier Optical DO probe (ODO-BTA), VWR sympHony™ pH probe, and VWR symHony™ ORP probe, respectively. The applied voltage and current were measured by the PalmSens EmStat3+ potentiostat (BASi, U.S.) connected to a computer with installed PSTrace 5.8 software.

#### 5.5.5.2 Biological measurements

Biomass concentration was measured based on VSS using standard method (Federation and Association, 2005) after centrifugation at 10,000 rpm and redissolving the precipitates in DI water. In the case of measuring sessile biomass, carriers were gently washed with fresh AMS medium to remove the planktonic cells. Then, they were inserted into a tube containing 10 mL of fresh AMS medium and placed into sonication bath for 20 minutes to detach the biofilm from the carriers into the medium. The VSS of medium was measured and carriers were separated, washed with distilled water, and placed in the vacuum oven overnight and weighed after. The carriers' weight was used to compare biomass formed on the carriers at different time points (mg biomass/g carrier). ATP was measured by luminometric method

as described by (Samadi et al., 2023). VSS was measured too in order to report the ATP based on biomass content of the samples (i.e., ngATP/mgVSS).

#### 5.5.5.3 Biofilm qualification

To visually observe the biofilm on GG, scanning electron microscopy (SEM) was performed on GG before biofilm formation and GG after the BER's operation. Since, GG is a conductive material, no sample preparation was needed for the GG before biofilm formation. Therefore, they were added to the stubs with carbon sticky tabs with a bit of silver paint to anchor them and then viewed with the SEM after 24 hours. For the GG with biofilm (after BER's operation), the samples were prepared following the method described by (Manju et al., 2009), except using ethanol instead of acetone as the dehydration solvent. After dehydration, samples were dried in critical point dryer, placed on the stubs with carbon sticky tabs and gold coated. High-quality images were obtained using the SEM device in electron microscopy facility at Dalhousie University (Halifax, Canada).

In addition, microbial population of the biological samples during the BER's operation were analyzed with the bacteria-specific 16S full-length amplicons PacBio (in the case of experiments with CB1190) and bacteria-specific 16S short amplicons MiSeq (in the case of experiments with microbial community) services of Integrated Microbiome Resources at Dalhousie University (Halifax, Canada). Protocols for DNA extraction, library preparation and bioinformatic analysis are described on their website: https://imr.bio/protocols.html.

### 5.5.6 Statistical analysis

Values are reported as average ± standard deviation in this study. The values are compared with the paired t-Test for means of two sets of data using the Microsoft Excel software. Confidence level of 95% (P-value<0.05) was considered for the paired t-Test. Results

### 5.5.7 DX removal by CB1190

#### 5.5.7.1 Physicochemical measurements

DO concentration, pH and ORP were measured daily in the influent and effluent of the anode chamber, as well as in the cathode chamber (**Figures 5-3A, C,** and **E**). DO, pH and ORP were stable in the influent, respectively 8.59±0.37 mg/L, 6.98±0.01, and 361.83±12.39 mV during the 111 days of BER's operation.

During the start-up period (first 10 days), DO concentration in the effluent of anode chamber dropped quickly to less than 4 mg/L because of microbial respiration and the fact that external aeration was not provided to the BER. DO concentration was then stabilized in the range of 3.17-4.32 mg/L during the biodegradation treatment (0.0 V). Applying the voltage of 1.0 V to the anode during the first electro-biodegradation treatment did not increase the DO (**Figure 5-3A**). The range was 3.08-3.75 mg/L during the first electro-biodegradation treatment (1.0 V). Applying the voltage of 1.2 V to the anode, however, resulted in fast increase of DO in a day from 3.39 to 4.53 mg/L. The range of DO during the second electro-biodegradation treatment (2.0 V) was 4.51-5.62 mg/L, indicating a generally higher DO concentration compared to the first electro-biodegradation treatment (P-value<0.05).

The changes in ORP in the effluent of anode chamber were similar to DO concentration. It decreased quickly during the start-up period, was stable during the biodegradation and first electro-biodegradation (1.0 V) periods, and increased in the second electro-biodegradation (1.2 V) period (**Figure 2C**). ORP at 1.2 V after stabilization, 51.9±5.12 mV, was significantly higher than the ORP at 1.0 V, -123±5.29 (P-value<0.05). The increase in the ORP shows the higher tendency of the medium to gain electrons and oxidize the organic chemicals (Jin and Englande Jr, 1997). Therefore, the increase in the ORP at 1.2 V is due to the increase in DO concentration which increases the total oxidizing agents in the medium. Similarly, the initial decrease in ORP and its stability at 0.0 and 1.0 V could be attributed to the similar trends in DO (**Figure 2A**), as there was no other oxidizing agent in the AMS medium.

The mechanism of the increase in DO concentration and ORP at 1.2 V is believed to be the water electrolysis reaction at the anodic chamber. The theoretical potential needed for the water electrolysis reaction is 1.23 V (relative to SHE) at 25 ˚C with pH 7 (Mazloomi and Sulaiman, 2012). However, in practice, a higher potential (overpotential) is usually needed to overcome the existing resistances. Increase of the applied voltage from 1.0 V (1.197 V relative to SHE) to 1.2 V (1.397 V relative to SHE) resulted in more than ten time increase in the current (i.e., from 204.7±13.64 to 1641±72.75 µA). This increase indicated the occurrence of water electrolysis, although in a slow rate.

Occurrence of water electrolysis results in change in the pH of the medium through the following reactions:

$$2H_2O\ (l) \rightarrow O_2\ (g) + 4H^+\ (aq) + 4e^- \quad \text{(Eq. 1)}$$

$$2H^+\ (aq) + 2e^- \rightarrow H_2\ (g) \quad \text{(Eq. 2)}$$

Therefore, pH in the anode chamber, where water is oxidized, and pH in the cathode chamber, where proton is reduced, was respectively decreased and increased during the second electro-biodegradation period (1.2 V) (**Figure 5-3E**). The decrease in the anode chamber and the increase in the cathode chamber were also observed in the first electro-biodegradation run (1.0 V). However, the pH changes at 1.0 V were significantly slower than the pH changes at 1.2 V (P-value<0.05). For example, the pH increase in cathode happened at the rate of 0.028 1/day at 1.2 V, which was more than 1.5-fold of the rate at 1.0 V (0.018 1/day). This could be another evidence that water was electrolyzed at 1.2 V, while not at 1.0 V. Since the pH change occurred at 1.0 V (1.197 relative to SHE) and the applied voltage was very close to the theoretical voltage required for water electrolysis (1.23 V relative to SHE), it can be assumed that the water electrolysis also happened at 1.0 V, but in a very slow rate that did not affect DO concentration or ORP of the medium.

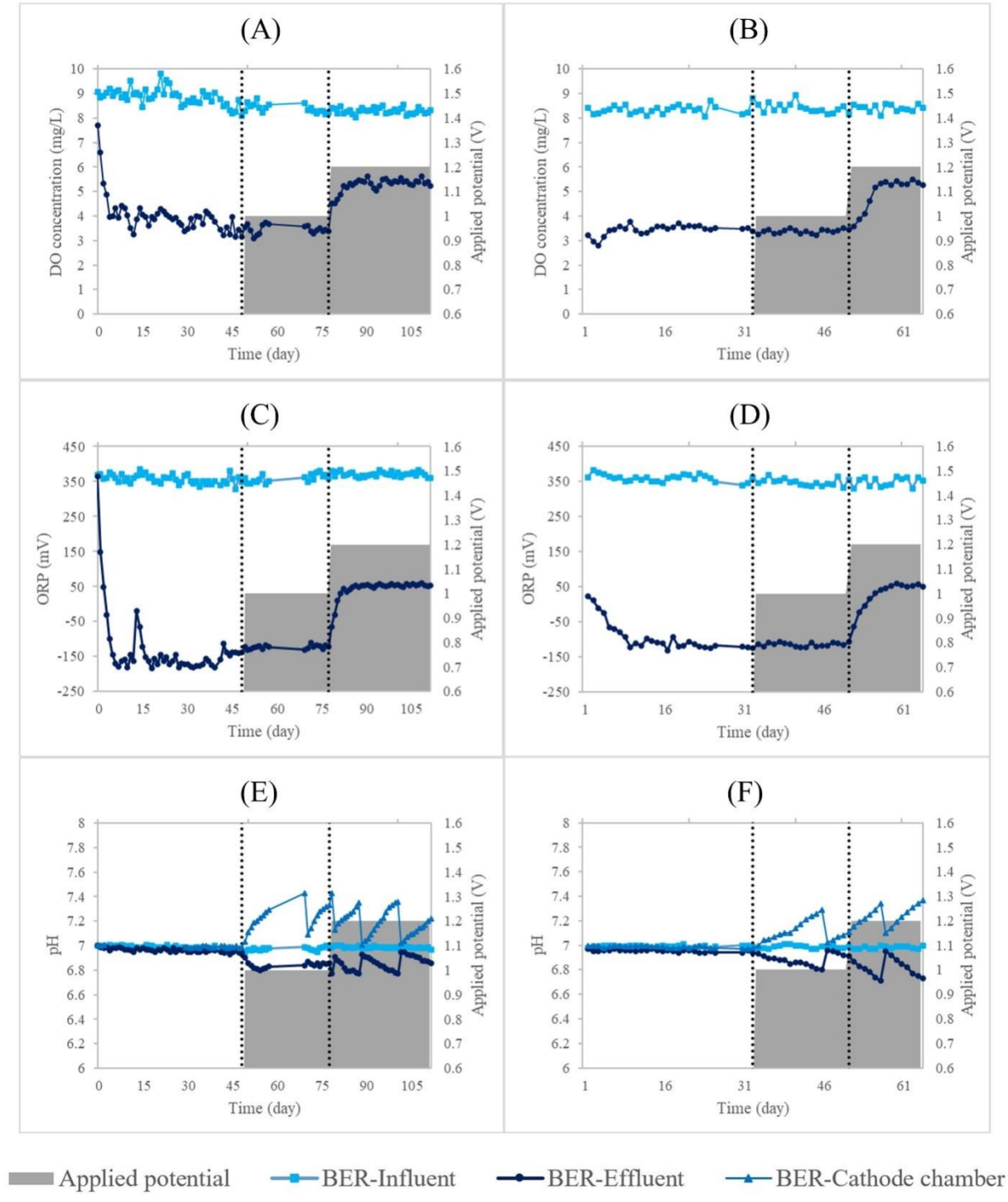


Figure 5-3 Physiochemical measurements during the operation of BER: DO concentration in influent and effluent of anode chamber during operation with (A) CB1190 and (B) microbial community; ORP in influent and effluent of anode chamber during operation with (C) CB1190 and (D) microbial community; pH in influent and effluent of anode chamber and in the cathode chamber during operation with (E) CB1190 and (F) microbial community. Figures show 4 stages of operation: start-up period (S)

and applied voltages of 0.0 V, 1.0 V, and 1.2 V (one replicate measurement at each time). Please note that data was not collected between the days 59 and 69 of the operation with CB1190 and between the days 26 and 29 of the operation with microbial community because the operator got sick. Because of the stability in the data collected after these periods, it was assumed that the system was not affected.

#### 5.5.7.2 Biological measurements

A mass balance on the biomass in the anode chamber based on mgVSS was performed throughout the BER's operation. The biomass formed on a portion of GGs that was put in the anode chamber without any initial biofilm on it. Measuring this biomass on several occasions during the BER's operation (**Figure 5-4A**) and calculating the sum of DX degraded, yield of biomass growth per DX degraded was estimated to be 0.124 mgVSS biomass / mg DX (**Figure S1-Appendix 5**). This yield was assumed to be the average of all the stages of BER's operation as samples was taken at different stages. Knowing the yield and the sum of DX removed during the 110 days operation (541 mg), which was calculated based on the daily removal and the constant flowrate, the total biomass growth was calculated to be 67 mgVSS. Also, the biomass formed on the proton exchange membrane was measured to be 26 mgVSS. Sum of these values resulted in the total biomass formed in the BER (93 mgVSS). In addition, the suspended biomass concentration in the effluent of anode chamber was measured to be 20.14±2.16 mg/L (**Figure 5-4A**), which resulted in total 342.7 mgVSS biomass removal from the system after 110 days. Including the total biomass removed by sampling during the operation (25.9 mgVSS) in the mass balance calculations and considering the initial biomass of 1629 mgVSS loaded to the reactor, the final biomass remaining in the anode chamber was estimated to be 1379 mgVSS. The measured value for the total remaining biomass in the anode chamber after 110 days was 1346 mgVSS, which confirmed the mass balance calculations (2.39% error). Details of mass balance are included in **Table S1-Appendix D**.

In addition to biomass quantity, biomass activity is another important biological parameter that determines the performance of a bioreactor. Only live cells contain ATP as organic molecules to store energy, which is degraded immediately when cells die. Therefore, ATP content of biomass works as an

index of biomass activity, which is affected by the system parameters such as the medium, retention time, applied voltage, pH, DO and DX concentration (Hong, 2004; Ailijiang et al., 2016; Pica et al., 2021). **Figure 5-4B** shows the ATP content of the biomass during the operation of BER. Since flowrate and DX concentration in the influent were kept constant at 0.1 mL/min and 98.55±1.20 mg/L, respectively and the same medium (AMS) was used throughout the operation, it was assumed that DO, pH and the applied voltage were the key parameters in the changes in the ATP content of the biomass. ATP declined during the start-up period (the first 10 days), presumably because of the quick drop of DO in that period (**Figure 5-3A**), which imposed a physiological shock to the aerobic microorganisms. This could unable the microorganisms to create fresh energy, which made them to use the reserved energy, ATP (Hong, 2004). During the biodegradation treatment (0.0 V), ATP content of biomass remained stable (P-value > 0.05 comparing the measured values), which corresponded to the stability of physiochemical properties (pH, DO and ORP) at this stage. Applying a voltage of 1.0 V to the anode resulted in a slightly lower ATP content in the biomass, 1600±99 ngATP/mgVSS at 1.0 V versus 1700±96 ngATP/mgVSS at 0.0 V, but not statistically different (P-Value > 0.05). Therefore, changes in the voltage or pH, which had occurred at 1.0 V (**Figure 5-3C**) did not have a significant impact on the ATP content. On the other hand, increase of the voltage to 1.2 V led to an obvious increasing trend in the ATP content of the biomass (**Figure 5-4B**). The average of last two measurements (days 97 and 110, at 1.2 V) was 2700±130 ngATP/mgVSS, which was 1.63-fold higher than the ATP content at 1.0 V. Since the direct impact of pH or voltage on ATP content were ruled out, it was concluded that DO concentration played the key role in this increase. DO concentration immediately rose after applying the 1.2 V (**Figure 5-3A**), which provided the microorganisms an easily accessible source of electron acceptor. This resulted in a higher metabolic activity in biomass and therefore, an increased content of ATP. The ATP content started to stabilize in the 1.2 V run (**Figure 5-4B**) eventually when DO concentration was also stable (5.40±0.11 mg/L in the last 10 days of the run).

To visually observe the biofilm on GG, SEM images were obtained from surface of GG before biofilm formation (**Figure 5-5A,B**) and after BER's operation (**Figure 5-5C,D**). Images from surface of GG before biofilm formation showed existence of many peaks and valleys, and high roughness of the surface, which creates an ideal environment for microorganisms to attach, and further protects the biofilm from detachment (Zhao et al., 2019; Al-Amshawee et al., 2020). Additionally, the images from surface of GG after BER's operation showed the unified layer of biofilm with high concentration of cells formed on the GG surface. Formation of extracellular polymeric substances (EPS) around the cells (**Figure 5-5D**) indicates that the biofilm was mature and stable at the end of BER's operation. The fact that the measured biomass on GG was stable during different stages of BER's operation (**Figure 5-4A**) also confirms the maturation and stability of biofilm during the whole time of BER's operation.

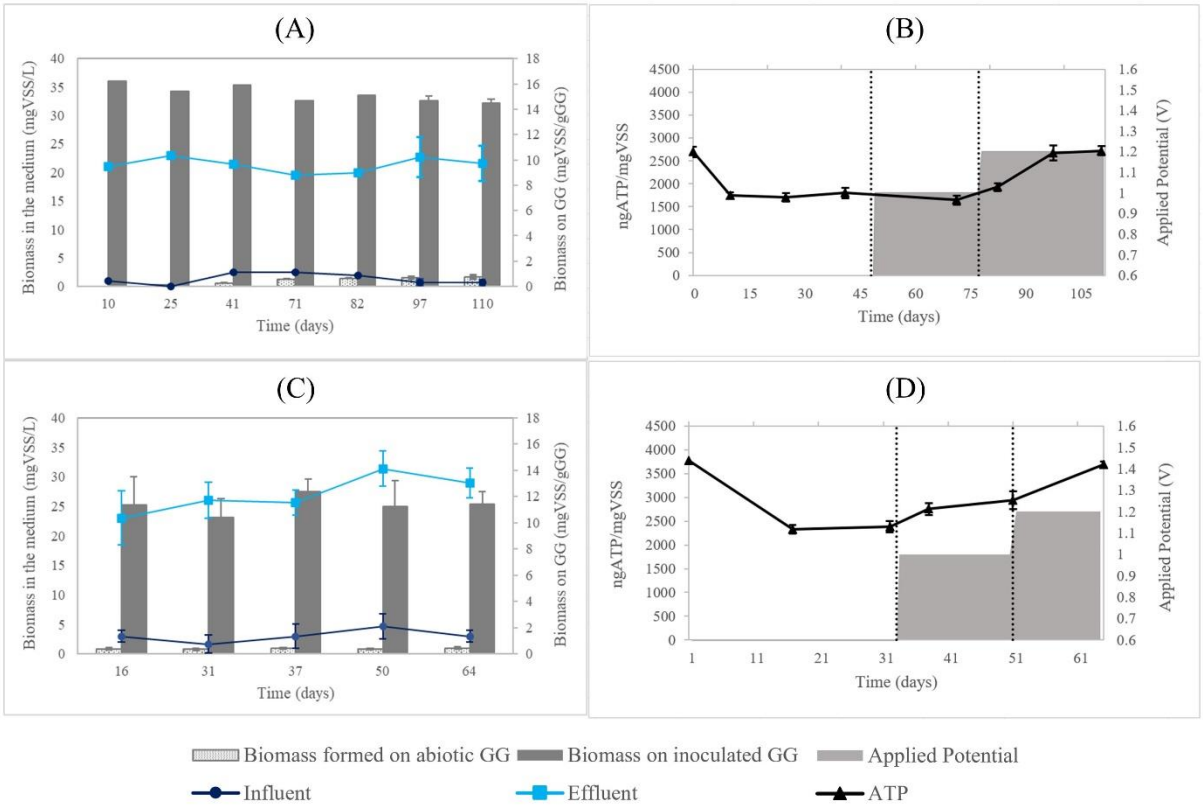


Figure 5-4 Biological measurements during the operation of BER: Biomass measured in the influent and effluent of the medium (mgVSS/L), and biomass measured on the initially inoculated graphite granules (GG) and formed on the initially abiotic GG

(mgVSS/gGG) during operation with (A) CB1190 and (C) microbial community; ATP content of the biomass (ngATP/mgVSS) in the anode chamber of BER during operation with (B) CB1190 and (D) microbial community (triplicate measurement at each time).

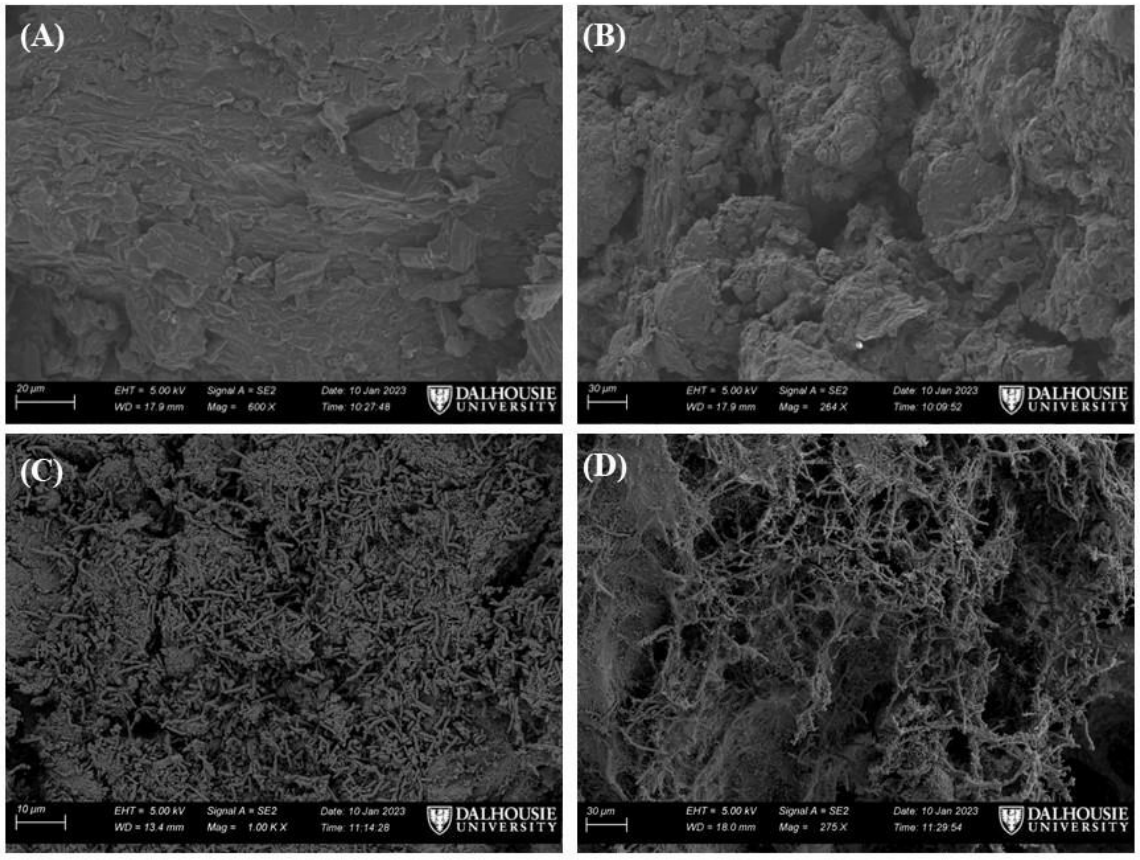


Figure 5-5 SEM images from surface of the GG before biofilm formation (A and B) and after the BER's operation with CB1190 (C and D). Figures A and C have higher magnifications compared to the figures B and D.

### 5.5.7.3 Biodegradation and electro-assisted biodegradation of DX

In the BER's abiotic and killed control operations, the average of DX concentration in the influent and effluent were respectively 99.2±2.34 and 99.4±1.55 mg/L, which rules out the possibility of DX removal in BER's biotic operation by means of evaporation, adsorption to the GG, or biosorption. Therefore, it was assumed that the total removal of DX in the BER's biotic operation was biodegradation by microorganisms. The microbial population analysis showed that the biomass in the anode chamber remained pure (more than 99%) CB1190 during the BER's operation. DX biodegradation mechanism by this species have been

studied before, which is conducted aerobically and mineralize DX to carbon dioxide (Grostern et al., 2012; Zhang et al., 2017).

After the early variations in DX concentration in the effluent of the anode chamber during the start-up period, DX concentration in the effluent was stabilized in the range of 67.6±2.23 mg/L (31.7±2.33% removal) during the biodegradation treatment (0.0 V). Knowing the biomass concentration and the retention time in the anode chamber, the average rate of DX biodegradation was calculated to be 0.07±0.006 mgDX/mgVSS/h. Applying 1.0 V to the anode chamber did not show a tangible impact on the DX concentration in the effluent (**Figure 5-6A**), resulting in the average DX removal percentage of 32.63±2.48% and the biodegradation rate of 0.076±0.005 mgDX/mgVSS/h.

Performing the statistical analysis on the last 10 measurements of the two sample sets (paired t-test for means of two data set), no significant difference was observed between biodegradation (0.0 V) and electro-biodegradation (1.0 V) treatments in terms of DX removal percentage (P-value=0.052) and DX biodegradation rate (P-value=0.34).

In the second electro-biodegradation treatment (1.2 V), the DX concentration in the effluent decreased gradually from 61.53 mg/L on day 78 of the BER's operation (first day of applying 1.2 V) to 40.68 mg/L on day 94 of the BER's operation ($17^{th}$ day of applying 1.2 V). It was then stabilized in the range of 40±0.67 mg/L between the days 95-111 (final day of BER's operation, **Figure 5-6A**). During this period, DX removal percentage and biodegradation rate were respectively 59.08±0.86% and 0.1±0.002 mgDX/mgVSS/h, which were significantly higher than the similar values at 1.0 V. It was assumed that the DO produced by water electrolysis at 1.2 V (**Figure 5-3A**) provided the microorganisms additional source of electron acceptor, increasing the biomass activity (**Figure 5-4B**) and leading to higher biodegradation rate.

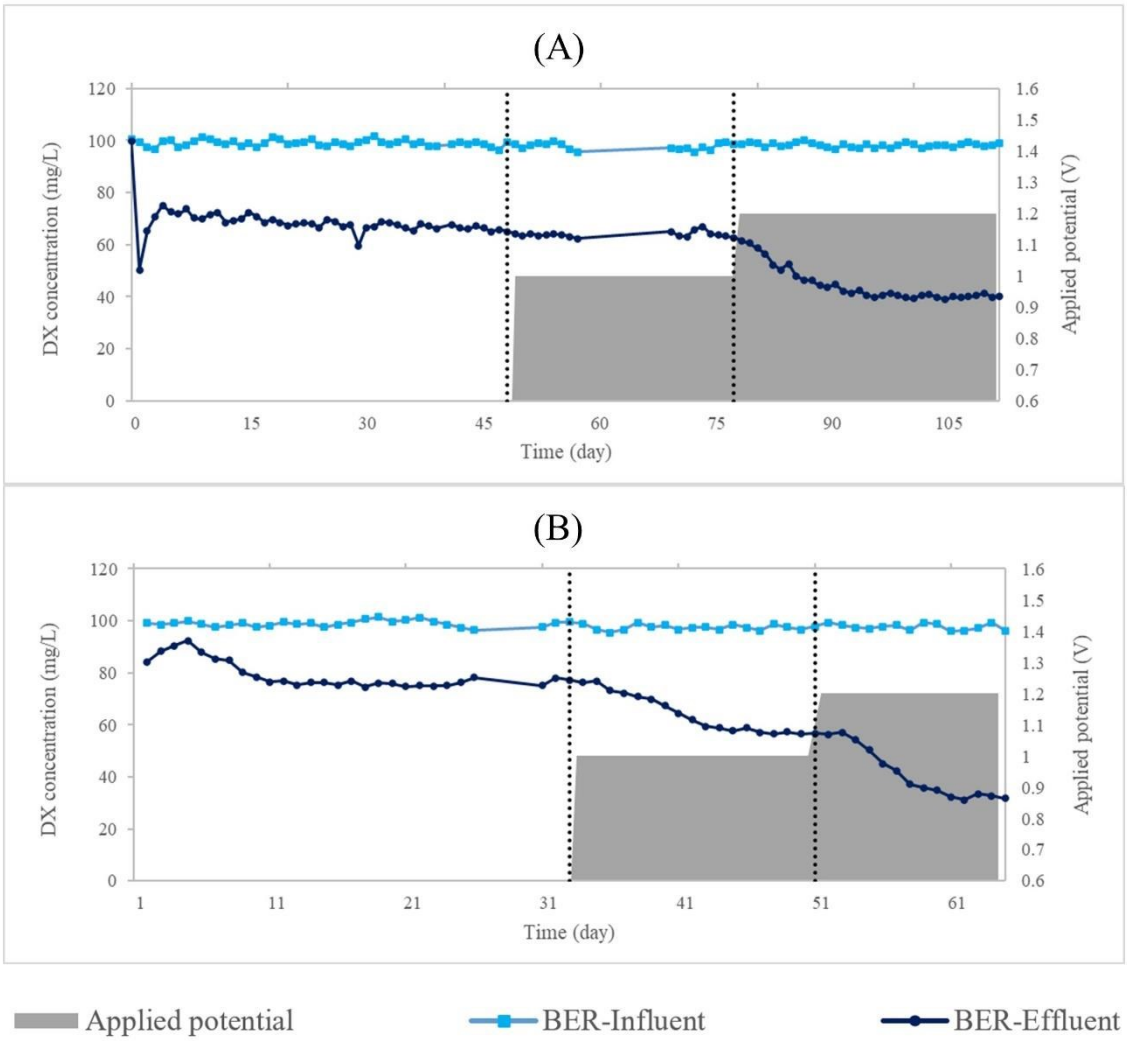


Figure 5-6 DX concentration in the influent and effluent of the anode chamber of BER during its biological operation with (A) CB1190 and (B) microbial community (1 replicate measurement at each time). Please note that data was not collected between the days 59 and 69 of the operation with CB1190 and between the days 26 and 29 of the operation with microbial community because the operator got sick. Because of the stability in the data collected after these periods, it was assumed that the system was not affected.

### 5.5.8 DX removal by microbial community

#### 5.5.8.1 Microbial community acclimatization

Transition of the microbial community during the 18-week period acclimatization is shown in **Figure S2-Appendix D**. The microbial community was stable at the end of this period. The prominent genera of the community at the end of period were *Pseudonocardia*, *Bradyrhizobium, Terrimonas*, *Afipia* and

*Sphingomonas*, which are well-known for their DX-degrading ability (Parales et al., 1994; Isaka et al., 2016; Miao et al., 2020; Chen et al., 2021a; Dang and Cupples, 2021).

#### 5.5.8.2 Physiochemical and biological measurements

The BER experiments with microbial community showed similar patterns to the BER experiments with CB1190 in terms of physiochemical parameters (comparing **Figures 5-3B**, **D** and **F** to **Figures 5-3A**, **C**, and **E**, respectively). DO concentration, ORP and pH in the effluent of the anode chamber were all stable during the 0.0 V treatment (days 15-32) with average values of respectively 3.5±0.080 mg/L, -118±9.65 mV, and 6.95±0.01. DO concentration and ORP stayed stable during the 1.0 V treatment (days 33-50) with average values of 3.44±0.08 mg/L and -115.17±5.34 mV, while pH in anode and cathode chamber respectively decreased and increased with the constant rates of -0.011 and 0.023 1/day. During the 1.2 V treatment (days 51-64), DO and ORP began to increase because of the water electrolysis as discussed for the changes in physiochemical properties of the experiments with CB1190. After stabilization, DO and ORP were respectively 5.4±0.08 mg/L and 53.43±3.41 mV. In addition, during the 1.2 V treatment, pH in anode and cathode chamber, respectively decreased and increased with higher rates (-0.032 and 0.038 1/day) compared to the 1.0 V treatment. Regarding electricity generation, the current was increased from 317±19 μA in the first half of the run under 1V potential (days 33-41) to 349±13 μA in the second half of the run under 1V potential (days 42-50). Similarly, the current was increased from 1565±35 μA in the first half of the run under 1.2V potential (days 51-57) to 1645±13 μA in the second half of the run under 1V potential (days 58-64).

A mass balance on biomass of the BER experiments with microbial community was performed in the similar way to the BER experiments with CB1190. The summary of mass balance is included in **Table S1-Appendix D**. The yield of microbial community's biomass growth per DX degraded was estimated to be 0.091 mgVSS biomass / mg DX (**Figure S2-Appendix D**), which was lower than the estimated yield for

CB1190 (0.124 mgVSS biomass / mg DX). Taking both biomass growth inside the anode chamber of BER and biomass removal by the effluent (**Figure 5-4C**) and sampling into account, the total biomass remained inside the anode chamber after 64 days of operation was estimated to be 1235 mgVSS, which was very close to the measured value of 1247 mgVSS (0.96% error), indicating the accuracy in the mass balance.

The ATP content of the microbial community biofilm was measured at different stages of the BER's operation: start-up and applied voltages of 0.0, 1.0, and 1.2 V (**Figure 5-4D**). Similar to the BER operation with CB1190, ATP content of the microbial community decreased in the start-up period because of the sudden confrontation with low DO concentration. Then, the ATP content remained stable during the 0.0 V treatment (days 15-32). Applying the 1.0 V (days 33-50) to the system resulted in a significant increase in the ATP content, from 2389±118.5 ngATP/mgVSS on day 31 to 2758±126.3 ngATP/mgVSS on day 37, and a gradual increase to 2940±109 ngATP/mgVSS (day 50). Since DO concentration did not change at 1.0 V compared to 0.0 V (**Figure 5-3B**) and the same increase in ATP content was not observed in the BER's operation with CB1190 (**Figure 5-4B**), it was assumed that microbial community played a role in this change, which is further discussed in the section of changes in the microbial community. Applying the 1.2 V (days 51-64) to the BER led to much higher ATP (3689±161.1 ngATP/mgVSS on day 64), which was attributed to the increased DO concentrations (**Figure 5-3B**). This increase of ATP at 1.2 V was also seen in the BER's operation with CB1190.

#### 5.5.8.3 Biodegradation and electro-assisted biodegradation of DX

After the early variations of DX concentration in the effluent of the BER operation with microbial community during the start-up period (**Figure 5-6B**), it eventually reached steady state (0.0 V, days 15-32) with average of 76.0±1.2 mg/L (removal percentage of 23.4±1.02%). The average rate of DX biodegradation was estimated to be 0.069±0.006 mgDX/mgVSS/h during this period using the measured biomass concentration and retention time in the anode chamber in the calculations. Applying 1.0 V to the

anode on day 32 resulted a gradual decrease in the DX concentration in the effluent (**Figure 5-6B**). After reaching steady state, average DX concentration in the effluent was 67.29±0.78 mg/L (removal percentage of 30.98±1.10%) indicating a statistically significant difference compared to the 0.0 V condition ($P<0.05$). Similarly, the calculated average biodegradation rate at 1.0 V, 0.08±0.004 mgDX/mgVSS/h, was significantly higher than the average biodegradation rate at 0.0 V, 0.07±0.006 mgDX/mgVSS/h ($P<0.05$). This increase in DX biodegradation rate could be attributed to the increased ATP content of the biomass of microbial community at 1.0 V (**Figure 5-4D**), while in the BER operation with CB1190, the increase at 1.0 V did not occur neither in ATP content nor in DX biodegradation rate.

Increase of the applied voltage to 1.2 V on day 50 of the operation also resulted in further decrease in the DX concentration in the effluent (**Figure 5-6B**). It dropped quickly during the days 51-60 to around 42.31±0.90 mg/L (average of the days 60-64) resulting in average removal percentage of 57±0.4% and biodegradation rate of 0.160±0.0042 mgDX/mgVSS/h. It was the highest DX biodegradation rate achieved by this study and was 1.25-fold higher than the highest biodegradation rate achieved by the BER operation with CB1190 (0.130±0.0028 mgDX/mgVSS/h). The reason for this increased DX biodegradation rate at 1.2 V was attributed to be the increase observed in DO concentration at 1.2 V (**Figure 5-3B**), similar to in the case of BER's operation with CB1190.

#### 5.5.8.4 Changes in microbial community

Changes in the microbial community was monitored throughout the BER's operation by taking samples at different stages (start up and applied voltages of 0.0, 1.0 and 1.2 V). Bacterial composition of the biomass in the anode chamber on the sampling days are shown in **Figure 5-7A** in genus level. *Pseudonocardia* and *Bradyrhizobium* were the dominant genera in the initially DX-acclimated consortium (**Figure S1-Appendix D**) and maintained their dominance throughout the BER's operation **Figure 5-7A**. Until day 31 (i.e., end of biodegradation treatment or when 1.0 V was applied), no significant change was observed in the microbial

composition, except a decrease in the portion of *Afipia* from 7.34 to 3.10 %. The portion of *Afipia* remained in the range of 1.86-3.10% until the end of experiments. It was assumed that *Afipia* could not tolerate the transfer of biomass on GG from flasks to BER (e.g., change in the DO concentration from above 8 mg/L to less than 4 mg/L) as good as other genera of the consortium.

The heat map of increase or decrease of each bacterium in the community during the BER's operation is shown in **Figure 5-7B**. *Afipia* was the only bacteria with a noticeable decrease throughout the experiment, while *Alistipes* and *Lutispora* started to increase from day 37, or when 1.0 V was applied to the anode, in the microbial community. In other words, the increase in these genera were the most noticeable changes in the microbial composition after starting the electro-assisted biodegradation. The portions of these bacteria were at the highest at the end of 1.0 V stage (day 50), at 4.83 and 8.20 % of the microbial composition, respectively, and slightly decreased to 4.70 and 7.50 %, respectively by applying 1.2 V (sample of day 64). The changes in the portion of other bacteria were negligible.

*Alistipes* is a genus of gram-negative, non-spore-forming, anaerobic bacteria. They are characterized by their rod-shaped cells. As anaerobic bacteria, they thrive in environments with little to no oxygen. *Alistipes* species contribute to the degradation of complex carbohydrates and the fermentation of dietary fibers, producing short-chain fatty acids (SCFAs) as metabolic byproducts (Parker et al., 2020). *Lutispora,* on the other hand, is a less well-known genus of bacteria within the phylum *Bacteroidetes*. Information about this genus is relatively limited, and it is not as extensively studied as some other bacterial groups. *Bacteroidetes* bacteria, in general, are widely distributed in various environments, including soil, sediments, and aquatic systems (Shiratori et al., 2008; El Houari et al., 2023). Both *Alistipes* and *Lutispora* are generally considered mesophiles. Mesophiles are organisms that thrive at moderate temperatures, typically within the range of 20°C to 45°C.

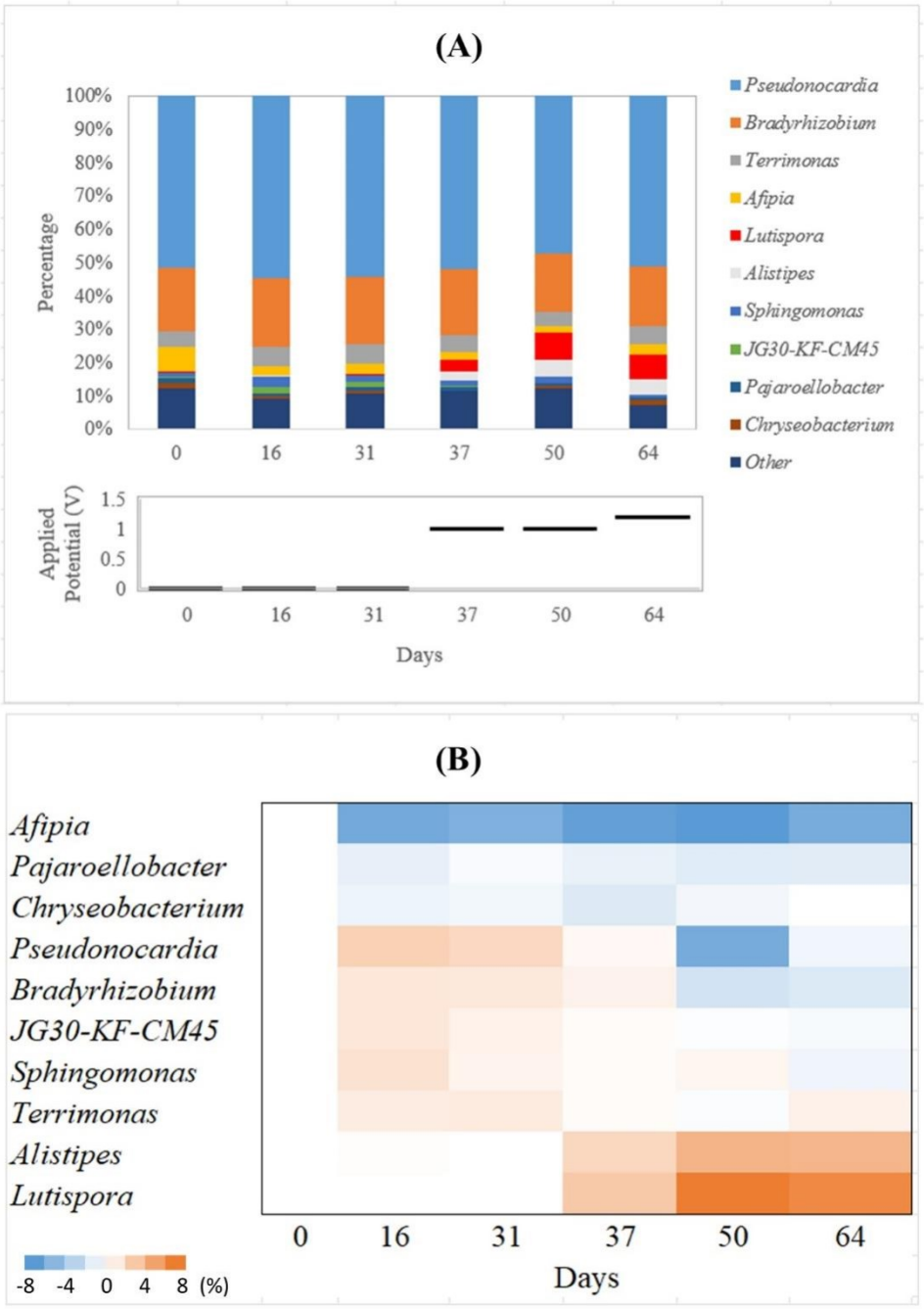


Figure 5-7 (A) Microbial community profiles and (B) heat map of changes in the microbial community (both genus level) of the biofilm on GG in the anode chamber of BER during its biological operation with microbial community.

#### 5.5.8.5 BER's operation with non-conductive carriers

The BER's operation with the same initial microbial community was repeated using the non-conductive materials (natural pine wood) as biofilm support. In this run, DO concentration did not change at different

applied voltages, respectively 3.60±0.23, 3.50±0.31, and 3.60±0.33 mg/L at 0.0, 1.0 and 1.2 V, showing that use of conductive carriers played an important role in dissolved oxygen production (especially at 1.2 V). This resulted in almost a stable DX concentration in the effluent at different voltages, respectively 78.4±3.22, 74.5±4.62, and 70.3±4.3 mg/L at 0.0, 1.0 and 1.2 V (**Figure S3**). The system was also relatively stable in terms of biological parameters. ATP of the biomass was respectively 1600±76, 1529±51, and 1500±99 ngATP/mgVSS at 0.0, 1.0 and 1.2 V. In addition, analysis of microbial population did not show any significant change in bacterial genera (**Figure S4**).

## 5.6 Discussion

### 5.6.1 Electrochemical enhancement through oxygen production

Electrochemical stimulation of DX biodegradation by CB1190 has been studied before by Jasmann et al. (2017) in higher voltages (3-8 V) compared to the voltages that were used in the current study. They developed a continuous reactor (3.5 L) packed with CB1190 bioaugmented on silica and electrochemically stimulated with Ti/$IrO_2$–$Ta_2O_5$ electrodes for removal of DX. The study showed that the DX removal rate at 3 V, 169 mg DX per hour per $m^2$ of electrode surface area, was higher around 3-fold compared to the non-applied voltage condition, 67.7 mg/h/$m^2$. The elevated DO concentration was reported as cause of the improvement in the biodegradation rate, which was supportedby visual observation of oxygen production and the increase in ORP, from -0.2 V to 0.2 V, after applying the voltage. However, DO concentration was not measured directly. At the potential of 8.0 V, lower removal rate, 101 mg/h/$m^2$, was reported as the pH dropped drastically around 4-5 in vicinity of the electrodes. Furthermore, an upgraded version of their reactor reached to 774 mg/h/$m^2$ biodegradation rate at 5.0 V (Pica et al., 2021), which was five times higher than the maximum rate achieved by the earlier version (169 mg/h/$m^2$). However, the high current applied to the system (60-80 mA/cm) not only increased the required energy for operation of the reactor (80 kWh.$m^{-3}$), but also resulted in a higher cytotoxicity to the microorganisms.

The same concept was practiced in this study but in much lower voltages and currents. In this study, the maximum current of 1640.76 µA (i.e., 0.77 mA/cm$^2$) was applied to the anode at 1.2 V, which stimulated the biomass activity and increased DX biodegradation rate. The current was exponentially increased to 5426.67 µA, when the applied voltage was set at 1.5 V for 7 days in the proof-of-concept experiments, which resulted in a drastic increase of DO and decrease of pH in the anode chamber. Use of GG as biomass support plays a key role in electrochemical stimulation at low voltages because all the reactor's space will be engaged in the electro-biodegradation process, instead of only a small portion of it (Cui et al., 2014; Verdini et al., 2015). Therefore, we assumed that the increase in the DO concentration occurred uniformly in the microenvironments around the GG, where the highest biomass concentration also existed in the reactor. As a result, electrochemical stimulation of DX biodegradation by CB1190 in a low applied voltage (1.2 V) and current (1.6 mA) became possible. Another supporting evidence was that at 1.2 V applied voltage when non-conductive carriers were used, DX removal did not significantly increase (**Figure S3**). This phenomenon was attributed to the lower oxygen production rate in the case of experiments with non-conductive carriers compared to the experiments with conductive carriers (respectively DO concentrations of 3.79±0.09 and 5.35±0.08 mg/L in the effluent). The lower oxygen production occurred due the less conductive surface area (Oh and Logan, 2006).

### 5.6.2 Electrochemical enhancement through direct electron transfer

Another method of electrochemical enhancement was also practiced by this study in lower voltages than needed for water electrolysis (i.e., 1.0 V), where DO concentration did not increase, and only electro-active microorganisms were stimulated. In this mechanism, electro-active microorganisms directly transfer electrons to an anodic surface with applied positive voltage when they degrade the electron donor (in our case DX) (Nancharaiah and Venugopalan, 2019). Several studies have used this concept to stimulate the electro-active microorganisms in order to achieve higher biodegradation rates of organic

contaminants (Aulenta et al., 2011; Ailijiang et al., 2016; Abdalrhman et al., 2020). For example, Ailijiang et al. (2016) showed that applying a low current (0.03 mA / $cm^2$ of electrode) could increase the biodegradation percentage of phenol from 38% to 97% in a continuous system. Monitoring the responses of the microbial community, they found that two electro-active genera, *Zoogloea* and *Desulfovibrio*, were noticeably enriched after applying the voltage.

In this study, we found that applying a 1.0 V to the anode produced a current of 333 µA (i.e., 0.16 mA / $cm^2$ of electrode) and increased the DX removal percentage from 23.4±0.02% to 30.98±0.1%. Since ATP content and DX biodegradation rate had increased at 1.0 V in the BER's operation with microbial community and not with pure culture (CB1190), it was hypothesized that these changes could be related to the increases in the portions of *Alistipes* and *Lutispora*. In other words, the 1.0 V applied to the anodic chamber filled with conducive GGs was not enough to change the DO concentration and increase the activity of other bacteria present in microbial community or CB1190 in the pure culture run, but stimulated the growth of *Alistipes* and *Lutispora* resulting in enhanced DX biodegradation.

Furthermore, the results of experiments with non-conductive carriers showed that when a 1.0 V applied to the anode, no change was observed neither in DX concentration in the effluent (**Figure S3-Appendix D**) nor in the microbial composition (**Figure S4-Appendix D**). Therefore, it was concluded that applying a low voltage such as 1.0 V (lower than water electrolysis potential) that does not change the DO concentration in the medium only affects the system regarding DX biodegradation if conductive carriers are used (such as GG) and if DX-degrading electro-active bacteria (such as *Alistipes* and *Lutispora*) exist in the microbial community.

Two DX-degrading electro-active bacteria, *Alistipes* and *Lutispora*, were identified to be enriched in 1.0 V and attributed to the increase in the DX removal percentage. *Alistipes* is a genus from the family *Rikenellaceae*, which includes several other genera as well. One of these genera, *Rikenella*, has been

previously shown dominance in a microbial fuel cell that was developed for removal of DX (Aryal et al., 2019). Moreover, *Lutispora* is from the class *Clostridia* of the microorganisms, which has been previously shown dominance in electro-active biofilms by several studies (Li et al., 2022; Ma et al., 2022; Rivalland et al., 2022).

The two identified electro-active microorganisms in this study, *Alistipes* and *Lutispora* are both anaerobic (Shiratori et al., 2008; Parker et al., 2020). The enrichment of these genera occurred at 1V potential in the anode chamber, where the average DO concentration was 3.44±0.08 mg/L. Although DO concentration at this level is typically associated with aerobic conditions (Wilén and Balmer, 1999), it remains significantly below the saturation level (8-16 mg/L) that is favored by aerobic microorganisms. Additionally, it is possible to create microenvironments within the reactor with lower dissolved oxygen (DO) levels. As a result, *Alistipes* and *Lutispora* may become enriched within the microbial community under these conditions. However, despite this enrichment, aerobic cultures still remained dominant within the community, as shown in Figure 6A.

### 5.6.3 DX biodegradation pathway

DX was degraded by CB1190 in the case of pure culture operation and mostly aerobic microorganisms in the case of microbial community operation (CB1190, *Bradyrhizobium*, *Terrimonas*, etc.). The literature extensively covers the biodegradation pathway of DX by aerobic microorganisms (Grostern et al., 2012; Zhang et al., 2017). The crucial enzyme responsible for initiating the biodegradation process is dioxane monooxygenase (DXMO). In most proposed pathways, ethylene glycol and oxalic acid are prominent intermediate compounds (Kim et al., 2009; Huang et al., 2014; Chen et al., 2021a). Ultimately, these compounds are converted to carbon dioxide through the tricarboxylic acid (TCA) cycle. The *Pseudonocardia* genus has been primarily associated with this biodegradation pathway (Zhang et al., 2017). Previous studies have reported a similar biodegradation pathway in bacterial consortia dominated

by *Terrimonas* or *Bradyrhizobium* (Chen et al., 2021a; Dang and Cupples, 2021; Xiong et al., 2022). Although this study did not extensively investigate the DX biodegradation pathway, our GC/MS analysis conducted throughout the DX biodegradation experiments revealed no evidence of intermediate accumulation. This confirms the complete mineralization of DX to carbon dioxide.

## 5.7 Conclusions

Electrochemical stimulation of the microorganisms at low voltages (1.0-1.2 V) and currents (<2 mA) significantly increased the biomass activity and DX removal efficiency in the anode chamber of BER. Two different mechanisms were involved in the electrochemical stimulation: 1) Production of oxygen at 1.2 V which served as electron acceptor of aerobic DX-degrading microorganisms such as CB1190, and 2) Direct transfer of electrons from electro-active microorganisms such as *Alistipes* and *Lutispora* to the anodic surface with a 1.0 V positive voltage. Elector-assisted biodegradation is a clean and controllable way of providing electron acceptors to the microorganisms. The results of this study showed that applying this system can overcome the challenge of lack of electron acceptors in DX-contaminated water resources through two different mechanisms at low voltages, which provides a flexible and energy-efficient solution.

## 5.8 Acknowledgments

The financial support of NSERC-DG is acknowledged. The author A.S is thankful for the NSERC-CREATE ASPIRE and Bruce and Dorothy Rosetti Engineering Research scholarships in support of his PhD program. Special thanks to the SEM facility and IMR center at Dalhousie University for providing equipment and helping us with the analysis.

## 5.9 Declaration of interests

The authors declare that they have no known competing financial interests or personal relationships that could have appeared to influence the work reported in this paper.

## 5.10 Supplementary material

Supplementary materials of this manuscript can be found in **Appendix D**.

# Chapter 6 Conclusions

The objective of this study was to investigate the efficiency of new applications of of bioremediation of DX in an effort to fill the knowledge gaps in the literature about DX biodegradation in low dissolved oxygen concentrations, effect of carrier's properties on growth of DX-degrading biofilm, and mechanisms of electrochemical stimulation of DX biodegradation. In order to answer the related research questions to each gap, experiments were designed systematically and performed in lab-scale batch or continuous reactors using pure culture or microbial community as the inoculation source.

The results of experiments in low dissolved oxygen concentrations (between 1-3 mg/L) showed that DX biodegradation occurred in a very slow rate (removal of 25 mg/L in 119 days) when oxygen was not provided by external means. In this condition, the overall diversity and richness of the microbial community decreased over time, but certain genera such as *Pseudonocardiaceae*, *Xanthobacteraceae* and *Chitinophagaceae* could enrich using DX as the carbon source. Provision of external electron acceptors such as oxygen and nitrate lowered the time needed for removal of 25 mg/L of DX (respectively to 77 and 91 days) and strengthened the portion of the microbial population that could use these electron acceptors. Moreover, control of temperature at 30 ˚C and addition of trichloroethylene (TCE) as co-contaminant showed respectively positive and negative effects on DX biodegradation rate. In conclusion, the microbial community was found to be flexible regarding DX biodegradation in different electron-accepting conditions which could play a key role in the success of in situ bioremediation or natural attenuation of DX in water resources.

The experiments on delignified porous wood as biofilm carriers showed an improvement in biofilm formation in terms of growth rate and hydrophobicity compared to natural untreated wood as biofilm carriers. The improvement was attributed to the superior physiochemical properties of the treated wood compared to untreated wood such as higher porosity, formation of macropores, and increase in surface

roughness and hydrophilicity. Furthermore, XRD test showed a good stability of the treated wood after the biofilm formation experiments. DX biodegradation rate increased significantly when treated woods were used as carriers compared to untreated woods, but a lower maximum specific growth rate was calculated (based on Monod model) for biofilm (0.0276±0.0018 1/h) versus planktonic (0.0382±0.0024 1/h). Analysis of the possible causes indicated that DX mass transfer into the biofilm layer does not limit the biodegradation rate, while gradual accumulation of inactive cells in the biofilm layer could be the reason for slower biodegradation. Characterization of the biofilm showed an increase in the content of saturated fatty acids during the biofilm formation which resulted in a higher hydrophobicity and rigidity. In addition, biofilm regeneration experiments indicated that even exposure to high concentration of DX up to 500 mg/L did not adversely affect the viability of the biofilm. The findings of biofilm experiments can contribute to the knowledge of biofilm formation regarding the physiochemical properties of biofilm carriers and be helpful to the ongoing research on bioremediation of DX.

Last but not least, the experiments on electrochemical stimulation of DX biodegradation in the continuous-flow bioelectrochemical reactor (BER) showed that two different mechanisms could be involved in stimulation at low applied voltages in the range of 1.0-1.2 V. DX biodegradation rate did not increase at 1.0 V compared to 0.0 V when pure culture (*Pseudonocardia dioxanivorans* CB1190) was used in BER's operation, while it increased significantly at 1.2 V compared to 0.0 V or 1.0 V. The reason was identified to be the production of oxygen that occurred with a much higher rate at 1.2 V (thousand times higher) compared to 1.0 V because of water electrolysis reaction. The produced oxygen could be used by the aerobic microorganisms as a source of electron acceptor in the medium. On the other hand, the DX biodegradation rate did increase at 1.0 V compared to 0.0 V when the BER was operated using the microbial community. This increase was concurrent with an increase in the biomass activity measured through ATP test. Analysis of the changes in microbial composition indicated enrichment of *Alistipes* and *Lutispora* at 1.0 V due to the ability of these genera to directly transfer electrons with conductive surface.

This observation was confirmed by comparing the changes in microbial community in BER's operation with conductive versus non-conductive carriers. Therefore, the results showed that electrochemical stimulation of DX biodegradation is possible at low voltages and occurs with two possible mechanisms. This provides a promising approach to solve the problem of lack of electron acceptors in case of DX bioremediation because electrochemical stimulation is considered as a clean, effective and controllable method of providing electron acceptors.

## 6.1 Recommendations

Based on the results and discussions of the research chapters, the following recommendations are provided:

1. Enhanced Biodegradation Strategies: The study in chapter 3 shows that complete DX biodegradation is achievable under low DO concentrations. To expedite the biodegradation process, especially in cases where rapid treatment is required, it is recommended to consider the following strategies: Nitrate Amendment: The results indicate that the addition of nitrate can significantly enhance DX biodegradation, leading to complete degradation in a shorter timeframe (91 days). Therefore, when feasible and environmentally acceptable, nitrate amendment could be implemented in contaminated sites to promote more rapid DX biodegradation.

2. Maintaining DX-Degrading Bacteria: The study in chapter 3 shows that specific bacterial families known for their ability to degrade DX, such as *Pseudonocardiaceae*, *Xanthobacteraceae*, and *Chitinophagaceae*, were able to persist and grow in different electron-accepting conditions. To ensure sustained and efficient DX biodegradation, it is essential to maintain and promote the growth of these DX-degrading bacteria within the microbial community. Strategies that encourage the proliferation of these specific bacterial families, such as providing suitable growth conditions and nutrients, could be employed.

3. Natural Attenuation Potential: The study in chapter 3 indicates that the native digestate microbial community has the potential to biodegrade DX under low DO conditions without external aeration. This finding highlights the potential for natural attenuation processes in certain environments. When considering remediation strategies for DX-contaminated sites, natural attenuation could be a viable option, especially in cases where it is not feasible to provide external aeration or other interventions.

4. Using Delignified Wood as Biofilm Carrier: The study in chapter 4 shows that delignification treatment of natural wood significantly improved the porosity, formation of macropores, surface roughness, and hydrophilicity of the wood pieces, resulting in higher biofilm growth. Further research could focus on optimizing the delignification process to achieve even better carrier properties for biofilm formation. This could include exploring different delignification methods, treatment durations, and conditions to fine-tune the physical and chemical characteristics of the wood carriers.

5. Address Inactive Cells Accumulation: The study in chapter 4 found a lower maximum specific growth rate for biofilm versus planktonic cells, attributed to the gradual accumulation of inactive cells in the biofilm. Addressing this issue could help improve the overall biodegradation rate of DX in the biofilm. Strategies to reduce the accumulation of inactive cells, such as optimizing nutrient availability and flow conditions, could be explored.

6. Comparative Studies: The study in chapter 4 suggests that conducting comparative studies between different carrier materials, including the delignified carriers and other commonly used biofilm carriers, to determine their relative advantages and limitations. Understanding how different carrier materials impact biofilm growth, stability, and biodegradation efficiency could help identify the most suitable carrier options for specific bioremediation scenarios.

7. Optimize Voltage and Current Conditions: The study in chapter 5 demonstrates that different voltage and current conditions have varying effects on the bioelectrochemical degradation of DX by *Pseudonocardia dioxanivorans* CB1190 and the microbial community biofilm. It is recommended to conduct further experiments to optimize the voltage and current settings to achieve the highest DX removal efficiency. Fine-tuning the electrochemical conditions may lead to even better results in terms of DX degradation and microbial activity.

8. Explore Synergistic Effects: The study in chapter 5 shows that electro-assisted biodegradation of DX at low voltages (1.0-1.2 V) is possible through two different mechanisms: oxygen production resulting from water electrolysis at 1.2 V and direct electron transfer with the electrode at 1.0 V, leading to different removal efficiencies. It would be beneficial to investigate potential synergistic effects of using both mechanisms simultaneously. This could involve implementing a dynamic voltage control strategy that alternates between the two voltage levels to harness the benefits of both oxygen production and direct electron transfer.

9. Enhance Microbial Community Understanding: The study in chapter 5 highlights changes in microbial composition, including the enrichment of specific genera like *Alistipes* and *Lutispora* at 1.0 V due to their ability to directly transfer electrons with conductive surfaces. Further research into the functional roles of these genera and their interactions within the microbial community could provide deeper insights into the mechanisms driving the bioelectrochemical degradation process. Understanding these interactions could aid in optimizing the BER and potentially identifying ways to further enhance DX removal efficiency.

## References


2018. 1,4-dioxane in Drinking Water Document for Public Consultation, Health Canada. https://www.canada.ca/en/health-canada/programs/consultation-1-4-dioxane-drinking-water/document.html#a52.

2019. Emerging Contaminants and Federal Facility Contaminants of Concern, United States Environmental Protection Agency (USEPA). https://www.epa.gov/fedfac/emerging-contaminants-and-federal-facility-contaminants-concern.

Abdalrhman, A.S., Zhang, Y., Arslan, M., El-Din, M.G., 2020. Low-current electro-oxidation enhanced the biodegradation of the recalcitrant naphthenic acids in oil sands process water. Journal of Hazardous Materials 398, 122807.

Adamson, D.T., Mahendra, S., Walker Jr, K.L., Rauch, S.R., Sengupta, S., Newell, C.J., 2014. A multisite survey to identify the scale of the 1, 4-dioxane problem at contaminated groundwater sites. Environmental Science & Technology Letters 1, 254-258.

Adamson, D.T., Piña, E.A., Cartwright, A.E., Rauch, S.R., Anderson, R.H., Mohr, T., Connor, J.A., 2017. 1, 4-Dioxane drinking water occurrence data from the third unregulated contaminant monitoring rule. Science of the Total Environment 596, 236-245. https://doi.org/10.1016/j.scitotenv.2017.04.085.

Ahmad, M., Liu, S., Mahmood, N., Mahmood, A., Ali, M., Zheng, M., Ni, J., 2017. Effects of porous carrier size on biofilm development, microbial distribution and nitrogen removal in microaerobic bioreactors. Bioresource technology 234, 360-369. https://doi.org/10.1016/j.biortech.2017.03.076.

Ailijiang, N., Chang, J., Liang, P., Li, P., Wu, Q., Zhang, X., Huang, X., 2016. Electrical stimulation on biodegradation of phenol and responses of microbial communities in conductive carriers supported biofilms of the bioelectrochemical reactor. Bioresource technology 201, 1-7. https://doi.org/10.1016/j.biortech.2015.11.026.

Al-Amshawee, S., Yunus, M.Y.B.M., 2021. Geometry of biofilm carriers: A systematic review deciding the best shape and pore size. Groundwater for Sustainable Development 12, 100520. https://doi.org/10.1016/j.gsd.2020.100520.

Al-Amshawee, S., Yunus, M.Y.B.M., Lynam, J.G., Lee, W.H., Dai, F., Dakhil, I.H., 2020. Roughness and wettability of biofilm carriers: a systematic review. Environmental Technology & Innovation, 101233. https://doi.org/10.1016/j.eti.2020.101233.

Al-Beloshei, N.E., Al-Awadhi, H., Al-Khalaf, R.A., Afzal, M., 2015. A comparative study of fatty acid profile and formation of biofilm in Geobacillus gargensis exposed to variable abiotic stress. Canadian journal of microbiology 61, 48-59. https://doi.org/10.1139/cjm-2014-0615.

Allen, D.T., Shonnard, D.R., 2001. Green engineering: environmentally conscious design of chemical processes. Pearson Education.

Alvarez, P.J., Illman, W.A., 2005. Bioremediation and natural attenuation: process fundamentals and mathematical models. John Wiley & Sons.

Anneser, B., Pilloni, G., Bayer, A., Lueders, T., Griebler, C., Einsiedl, F., Richters, L., 2010. High resolution analysis of contaminated aquifer sediments and groundwater—what can be learned in terms of natural attenuation? Geomicrobiology Journal 27, 130-142.

Artyushkova, K., Cornejo, J.A., Ista, L.K., Babanova, S., Santoro, C., Atanassov, P., Schuler, A.J., 2015. Relationship between surface chemistry, biofilm structure, and electron transfer in Shewanella anodes. Biointerphases 10, 019013.

Aryal, R., Xia, C., Liu, J., 2019. 1, 4-Dioxane-contaminated groundwater remediation in the anode chamber of a microbial fuel cell. Water Environment Research 91, 1537-1545.

Asri, M., El Ghachtouli, N., Elabed, S., Koraichi, S.I., Elabed, A., Silva, B., Tavares, T., 2018. Wicherhamomyces anomalus biofilm supported on wood husk for chromium wastewater treatment. Journal of hazardous materials 359, 554-562. https://doi.org/10.1016/j.jhazmat.2018.05.050.

Aulenta, F., Canosa, A., Roma, L.D., Reale, P., Panero, S., Rossetti, S., Majone, M., 2009. Influence of mediator immobilization on the electrochemically assisted microbial dechlorination of trichloroethene (TCE) and cis-dichloroethene (cis-DCE). Journal of Chemical Technology & Biotechnology: International Research in Process, Environmental & Clean Technology 84, 864-870.

Aulenta, F., Catervi, A., Majone, M., Panero, S., Reale, P., Rossetti, S., 2007. Electron transfer from a solid-state electrode assisted by methyl viologen sustains efficient microbial reductive dechlorination of TCE. Environmental science & technology 41, 2554-2559.

Aulenta, F., Tocca, L., Verdini, R., Reale, P., Majone, M., 2011. Dechlorination of trichloroethene in a continuous-flow bioelectrochemical reactor: effect of cathode potential on rate, selectivity, and electron transfer mechanisms. Environmental science & technology 45, 8444-8451.

Babauta, J., Renslow, R., Lewandowski, Z., Beyenal, H., 2012. Electrochemically active biofilms: facts and fiction. A review. Biofouling 28, 789-812.

Baczynski, T.P., Pleissner, D., Grotenhuis, T., 2010. Anaerobic biodegradation of organochlorine pesticides in contaminated soil–significance of temperature and availability. Chemosphere 78, 22-28. https://doi.org/10.1016/j.chemosphere.2009.09.058.

Baird, R.B., Eaton, A.D., Rice, E.W., Bridgewater, L., 2017. Standard methods for the examination of water and wastewater. American Public Health Association Washington, DC.

Barajas-Rodriguez, F.J., Freedman, D.L., 2018. Aerobic biodegradation kinetics for 1, 4-dioxane under metabolic and cometabolic conditions. Journal of hazardous materials 350, 180-188. https://doi.org/10.1016/j.jhazmat.2018.02.030.

Beims, R.F., Arredondo, R., Carrero, D.J.S., Yuan, Z., Li, H., Shui, H., Zhang, Y., Leitch, M., Xu, C.C., 2022. Functionalized wood as bio-based advanced materials: Properties, applications, and challenges. Renewable and Sustainable Energy Reviews 157, 112074. https://doi.org/10.1016/j.rser.2022.112074.

Bellagamba, M., Viggi, C.C., Ademollo, N., Rossetti, S., Aulenta, F., 2017. Electrolysis-driven bioremediation of crude oil-contaminated marine sediments. New biotechnology 38, 84-90.

Bilal, M., Iqbal, H.M., 2019. An insight into toxicity and human-health-related adverse consequences of cosmeceuticals—a review. Science of the total environment 670, 555-568.

Boopathy, R., 2004. Anaerobic biodegradation of no. 2 diesel fuel in soil: a soil column study. Bioresource Technology 94, 143-151. https://doi.org/10.1016/j.biortech.2003.12.006.

Bouguerra, A., Amiri, O., Aït-Mokhtar, A., Diop, M., 2002. Water sorptivity and pore structure of wood–cementitious composites. Magazine of Concrete Research 54, 103-112. https://doi.org/10.1680/macr.2002.54.2.103.

Boving, T., Eberle, D., Ball, R., 2014. Activated Persulfate Treatment of 1, 4-Dioxane in the Presence of Chlorinated Solvent Co-contaminants. AGU Fall Meeting Abstracts.

Brenner, D., Hollis, D., Moss, C.W., English, C., Hall, G., Vincent, J., Radosevic, J., Birkness, K., Bibb, W., Quinn, F., 1991. Proposal of Afipia gen. nov., with Afipia felis sp. nov.(formerly the cat scratch disease bacillus), Afipia clevelandensis sp. nov.(formerly the Cleveland Clinic Foundation strain), Afipia broomeae sp. nov., and three unnamed genospecies. Journal of Clinical Microbiology 29, 2450-2460. https://doi.org/10.1128/jcm.29.11.2450-2460.1991.

Bridier, A., Briandet, R., Thomas, V., Dubois-Brissonnet, F., 2011. Resistance of bacterial biofilms to disinfectants: a review. Biofouling 27, 1017-1032. https://doi.org/10.1080/08927014.2011.626899.

Chao, J., Wolfaardt, G.M., Arts, M.T., 2010. Characterization of Pseudomonas aeruginosa fatty acid profiles in biofilms and batch planktonic cultures. Canadian journal of microbiology 56, 1028-1039. https://doi.org/10.1139/W10-093.

Chen, H., Jogler, M., Rohde, M., Klenk, H.-P., Busse, H.-J., Tindall, B.J., Spröer, C., Overmann, J., 2012. Reclassification and emended description of Caulobacter leidyi as Sphingomonas leidyi comb.

nov., and emendation of the genus Sphingomonas. International journal of systematic and evolutionary microbiology 62, 2835-2843. https://doi.org/10.1099/ijs.0.039636-0.

Chen, R., Miao, Y., Liu, Y., Zhang, L., Zhong, M., Adams, J.M., Dong, Y., Mahendra, S., 2021a. Identification of novel 1, 4-dioxane degraders and related genes from activated sludge by taxonomic and functional gene sequence analysis. Journal of Hazardous Materials 412, 125157. https://doi.org/10.1016/j.jhazmat.2021.125157.

Chen, S., Xie, J., Wen, Z., 2021b. Removal of pharmaceutical and personal care products (PPCPs) from waterbody using a revolving algal biofilm (RAB) reactor. Journal of Hazardous Materials 406, 124284. https://doi.org/10.1016/j.jhazmat.2020.124284.

Chu, L., Wang, J., Quan, F., Xing, X.-H., Tang, L., Zhang, C., 2014. Modification of polyurethane foam carriers and application in a moving bed biofilm reactor. Process Biochemistry 49, 1979-1982. https://doi.org/10.1016/j.procbio.2014.07.018.

Comeau, A.M., Douglas, G.M., Langille, M.G., 2017. Microbiome helper: a custom and streamlined workflow for microbiome research. MSystems 2, e00127-00116. https://doi.org/10.1128/mSystems.00127-16 •.

Comeau, A.M., Li, W.K., Tremblay, J.-É., Carmack, E.C., Lovejoy, C., 2011. Arctic Ocean microbial community structure before and after the 2007 record sea ice minimum. PloS one 6, e27492. https://doi.org/10.1371/journal.pone.0027492.

Costerton, J.W., Lewandowski, Z., Caldwell, D.E., Korber, D.R., Lappin-Scott, H.M., 1995. Microbial biofilms. Annual review of microbiology 49, 711-745.

Cui, D., Guo, Y.-Q., Lee, H.-S., Cheng, H.-Y., Liang, B., Kong, F.-Y., Wang, Y.-Z., Huang, L.-P., Xu, M.-Y., Wang, A.-J., 2014. Efficient azo dye removal in bioelectrochemical system and post-aerobic bioreactor: optimization and characterization. Chemical Engineering Journal 243, 355-363.

da Silva, M.L.B., He, Y., Mathieu, J., Alvarez, P.J., 2020. Enhanced long-term attenuation of 1, 4-dioxane in bioaugmented flow-through aquifer columns. Biodegradation 31, 201-211. https://doi.org/10.1007/s10532-020-09903-0.

Daims, H., Wagner, M., 2018. Nitrospira. Trends in Microbiology 26, 462-463.

Dang, H., Cupples, A.M., 2021. Identification of the phylotypes involved in cis-dichloroethene and 1, 4-dioxane biodegradation in soil microcosms. Science of The Total Environment 794, 148690. https://doi.org/10.1016/j.scitotenv.2021.148690.

Das, D., 2018. Microbial Fuel Cell. Springer.

Davarpanah, S., Mahmoodi, N.M., Arami, M., Bahrami, H., Mazaheri, F., 2009. Environmentally friendly surface modification of silk fiber: Chitosan grafting and dyeing. Applied Surface Science 255, 4171-4176.

Denich, T., Beaudette, L., Lee, H., Trevors, J., 2003. Effect of selected environmental and physico-chemical factors on bacterial cytoplasmic membranes. Journal of microbiological methods 52, 149-182. https://doi.org/10.1016/S0167-7012(02)00155-0.

Donlan, R.M., 2002. Biofilms: microbial life on surfaces. Emerging infectious diseases 8, 881. 10.3201/eid0809.020063.

Dubois-Brissonnet, F., Trotier, E., Briandet, R., 2016. The biofilm lifestyle involves an increase in bacterial membrane saturated fatty acids. Frontiers in microbiology 7, 1673. https://doi.org/10.3389/fmicb.2016.01673.

Edwards, S.J., Kjellerup, B.V., 2013. Applications of biofilms in bioremediation and biotransformation of persistent organic pollutants, pharmaceuticals/personal care products, and heavy metals. Applied microbiology and biotechnology 97, 9909-9921. https://doi.org/10.1007/s00253-013-5216-z.

El Houari, A., Carpenter, M., Chaplin, D., Golyshin, P., McDonald, J.E., 2023. Lutispora saccharofermentans sp. nov., a mesophilic, non-spore-forming bacterium isolated from a lab-scale methanogenic landfill bioreactor digesting anaerobic sludge, and emendation of the genus Lutispora to include species which are non-spore-forming and mesophilic. International Journal of Systematic and Evolutionary Microbiology 73, 005683.

EPA-DSSTox, 2021. 1,4-Dioxane. https://comptox.epa.gov/dashboard/DTXSID4020533.

EPA, 2006. Treatment Technologies for 1,4-Dioxane: Fundamentals and Field Applications.

EPA, 2017. Technical Fact Sheet - 1,4-dioxane.

EPA, 2019. U.S Environmental Protection Agency - Contaminants of Emerging Concern including Pharmaceuticals and Personal Care Products. https://www.epa.gov/wqc/contaminants-emerging-concern-including-pharmaceuticals-and-personal-care-products.

EPA, 2020a. Emerging Contaminants and Federal Facility Contaminants of Concern. https://www.epa.gov/fedfac/emerging-contaminants-and-federal-facility-contaminants-concern.

EPA, 2020b. Final Risk Evaluation for 1,4-Dioxane.

EPA, 2023. 1,4-Dioxane Draft Revised Unreasonable Risk Determination.

Farber, R., Dabush-Busheri, I., Chaniel, G., Rozenfeld, S., Bormashenko, E., Multanen, V., Cahan, R., 2019a. Biofilm grown on wood waste pretreated with cold low-pressure nitrogen plasma: Utilization for toluene remediation. International Biodeterioration & Biodegradation 139, 62-69. https://doi.org/10.1016/j.ibiod.2019.03.003.

Farber, R., Rosenberg, A., Rozenfeld, S., Banet, G., Cahan, R., 2019b. Bioremediation of artificial diesel-contaminated soil using bacterial consortium immobilized to plasma-pretreated wood waste. Microorganisms 7, 497.

Federation, W.E., Association, A., 2005. Standard methods for the examination of water and wastewater. American Public Health Association (APHA): Washington, DC, USA 21.

feng Su, J., han Bai, Y., lin Huang, T., Wei, L., yu Gao, C., Wen, Q., 2020. Multifunctional modified polyvinyl alcohol: A powerful biomaterial for enhancing bioreactor performance in nitrate, Mn (II) and Cd (II) removal. Water Research 168, 115152. https://doi.org/10.1016/j.watres.2019.115152.

Fockink, D.H., Morais, A.R., Ramos, L.P., Łukasik, R.M., 2018. Insight into the high-pressure CO2 pre-treatment of sugarcane bagasse for a delivery of upgradable sugars. Energy 151, 536-544. https://doi.org/10.1016/j.energy.2018.03.085.

Frey, M., Widner, D., Segmehl, J.S., Casdorff, K., Keplinger, T., Burgert, I., 2018. Delignified and densified cellulose bulk materials with excellent tensile properties for sustainable engineering. ACS Applied Materials & Interfaces 10, 5030-5037. https://doi.org/10.1021/acsami.7b18646.

Fukushima, R.S., Kerley, M.S., 2011. Use of lignin extracted from different plant sources as standards in the spectrophotometric acetyl bromide lignin method. Journal of Agricultural and Food Chemistry 59, 3505-3509. https://doi.org/10.1021/jf104826n.

García, A., Alriols, M.G., Llano-Ponte, R., Labidi, J., 2011. Ultrasound-assisted fractionation of the lignocellulosic material. Bioresource Technology 102, 6326-6330. https://doi.org/10.1016/j.biortech.2011.02.045.

Gaur, N., Narasimhulu, K., PydiSetty, Y., 2018. Recent advances in the bio-remediation of persistent organic pollutants and its effect on environment. Journal of cleaner production 198, 1602-1631.

Gi, M., Fujioka, M., Kakehashi, A., Okuno, T., Masumura, K., Nohmi, T., Matsumoto, M., Omori, M., Wanibuchi, H., Fukushima, S., 2018. In vivo positive mutagenicity of 1, 4-dioxane and quantitative analysis of its mutagenicity and carcinogenicity in rats. Archives of toxicology 92, 3207-3221.

Gianotti, A., Serrazanetti, D., Kamdem, S.S., Guerzoni, M.E., 2008. Involvement of cell fatty acid composition and lipid metabolism in adhesion mechanism of Listeria monocytogenes.

International journal of food microbiology 123, 9-17. https://doi.org/10.1016/j.ijfoodmicro.2007.11.039.

Gill, R., Harbottle, M.J., Smith, J., Thornton, S., 2014. Electrokinetic-enhanced bioremediation of organic contaminants: a review of processes and environmental applications. Chemosphere 107, 31-42.

Goff, K.L., Hug, L.A., 2022. Environmental Potential for Microbial 1, 4-Dioxane Degradation Is Sparse despite Mobile Elements Playing a Role in Trait Distribution. Applied and Environmental Microbiology 88, e02091-02021. https://doi.org/10.1128/aem.02091-21.

Gorby, Y.A., Yanina, S., McLean, J.S., Rosso, K.M., Moyles, D., Dohnalkova, A., Beveridge, T.J., Chang, I.S., Kim, B.H., Kim, K.S., 2006. Electrically conductive bacterial nanowires produced by Shewanella oneidensis strain MR-1 and other microorganisms. Proceedings of the National Academy of Sciences 103, 11358-11363.

Grostern, A., Sales, C.M., Zhuang, W.-Q., Erbilgin, O., Alvarez-Cohen, L., 2012. Glyoxylate metabolism is a key feature of the metabolic degradation of 1, 4-dioxane by Pseudonocardia dioxanivorans strain CB1190. Applied and environmental microbiology 78, 3298-3308.

Guan, X., Liu, F., Wang, J., Li, C., Zheng, X., 2018. Mechanism of 1, 4-dioxane microbial degradation revealed by 16S rRNA and metatranscriptomic analyses. Water Science and Technology 77, 123-133. https://doi.org/10.2166/wst.2017.498.

Hadjiev, D., Dimitrov, D., Martinov, M., Sire, O., 2007. Enhancement of the biofilm formation on polymeric supports by surface conditioning. Enzyme and microbial technology 40, 840-848. https://doi.org/10.1016/j.enzmictec.2006.06.022.

Hand, S., Wang, B., Chu, K.-H., 2015. Biodegradation of 1, 4-dioxane: effects of enzyme inducers and trichloroethylene. Science of the Total Environment 520, 154-159.

Harms, G., Layton, A.C., Dionisi, H.M., Gregory, I.R., Garrett, V.M., Hawkins, S.A., Robinson, K.G., Sayler, G.S., 2003. Real-time PCR quantification of nitrifying bacteria in a municipal wastewater treatment plant. Environmental science & technology 37, 343-351. https://doi.org/10.1021/es0257164.

He, J., Sung, Y., Krajmalnik-Brown, R., Ritalahti, K.M., Löffler, F.E., 2005. Isolation and characterization of Dehalococcoides sp. strain FL2, a trichloroethene (TCE)-and 1, 2-dichloroethene-respiring anaerobe. Environmental Microbiology 7, 1442-1450.

He, Y., Mathieu, J., da Silva, M.L., Li, M., Alvarez, P.J., 2018. 1, 4-Dioxane-degrading consortia can be enriched from uncontaminated soils: prevalence of Mycobacterium and soluble di-iron monooxygenase genes. Microbial Biotechnology 11, 189-198. https://doi.org/10.1111/1751-7915.12850.

Hong, C., 2004. ATP content and biomass activity in sequential anaerobic/aerobic reactors. Journal of Zhejiang University-SCIENCE A 5, 727-732.

Huang, H., Shen, D., Li, N., Shan, D., Shentu, J., Zhou, Y., 2014. Biodegradation of 1, 4-dioxane by a novel strain and its biodegradation pathway. Water, Air, & Soil Pollution 225, 1-11.

Inoue, D., Tsunoda, T., Yamamoto, N., Ike, M., Sei, K., 2018. 1, 4-Dioxane degradation characteristics of Rhodococcus aetherivorans JCM 14343. Biodegradation 29, 301-310. https://doi.org/10.1007/s10532-018-9832-2.

Isaac, P., Alessandrello, M.J., Macedo, A.J., Estévez, M.C., Ferrero, M.A., 2017. Pre-exposition to polycyclic aromatic hydrocarbons (PAHs) enhance biofilm formation and hydrocarbon removal by native multi-species consortium. Journal of environmental chemical engineering 5, 1372-1378. https://doi.org/10.1016/j.jece.2017.02.031.

Isaka, K., Udagawa, M., Sei, K., Ike, M., 2016. Pilot test of biological removal of 1, 4-dioxane from a chemical factory wastewater by gel carrier entrapping Afipia sp. strain D1. Journal of hazardous materials 304, 251-258. https://doi.org/10.1016/j.jhazmat.2015.10.066.

Jasmann, J.R., Gedalanga, P.B., Borch, T., Mahendra, S., Blotevogel, J., 2017. Synergistic treatment of mixed 1, 4-dioxane and chlorinated solvent contaminations by coupling electrochemical oxidation with aerobic biodegradation. Environmental science & technology 51, 12619-12629. https://doi.org/10.1021/acs.est.7b03134.

Jefferson, K.K., 2004. What drives bacteria to produce a biofilm? FEMS microbiology letters 236, 163-173.

Jéglot, A., Sørensen, S.R., Schnorr, K.M., Plauborg, F., Elsgaard, L., 2021. Temperature Sensitivity and Composition of Nitrate-Reducing Microbiomes from a Full-Scale Woodchip Bioreactor Treating Agricultural Drainage Water. Microorganisms 9, 1331. https://doi.org/10.3390/microorganisms9061331.

Jin, G., Englande Jr, A.J., 1997. Effects of electron donor, dissolved oxygen, and oxidation–reduction potential biodegradation of carbon tetrachloride by Escherichia coli K-12. Water environment research 69, 1100-1105.

Johnson, N.W., Gedalanga, P.B., Zhao, L., Gu, B., Mahendra, S., 2020. Cometabolic biotransformation of 1, 4-dioxane in mixtures with hexavalent chromium using attached and planktonic bacteria. Science of the Total Environment 706, 135734. https://doi.org/10.1016/j.scitotenv.2019.135734.

Kämpfer, P., Kroppenstedt, R.M., 2004. Pseudonocardia benzenivorans sp. nov. International Journal of Systematic and Evolutionary Microbiology 54, 749-751. https://doi.org/10.1099/ijs.0.02825-0.

Kaneda, T., 1991. Iso-and anteiso-fatty acids in bacteria: biosynthesis, function, and taxonomic significance. Microbiological reviews 55, 288-302. https://doi.org/10.1128/mr.55.2.288-302.1991.

Kano, H., Umeda, Y., Kasai, T., Sasaki, T., Matsumoto, M., Yamazaki, K., Nagano, K., Arito, H., Fukushima, S., 2009. Carcinogenicity studies of 1, 4-dioxane administered in drinking-water to rats and mice for 2 years. Food and chemical toxicology 47, 2776-2784. https://doi.org/10.1016/j.fct.2009.08.012.

Karataş, S., Hasar, H., Taşkan, E., Özkaya, B., Şahinkaya, E., 2014. Bio-reduction of tetrachloroethen using a H2-based membrane biofilm reactor and community fingerprinting. Water research 58, 21-28. https://doi.org/10.1016/j.watres.2014.03.053.

Karges, U., Becker, J., Püttmann, W., 2018. 1, 4-Dioxane pollution at contaminated groundwater sites in western Germany and its distribution within a TCE plume. Science of the Total Environment 619, 712-720.

Kelley, S.L., Aitchison, E.W., Deshpande, M., Schnoor, J.L., Alvarez, P.J., 2001. Biodegradation of 1, 4-dioxane in planted and unplanted soil: effect of bioaugmentation with Amycolata sp. CB1190. Water Research 35, 3791-3800. https://doi.org/10.1016/S0043-1354(01)00129-4.

Kermanshahi Pour, A., Mamer, O.A., Cooper, D.G., Maric, M., Nicell, J.A., 2009. Metabolites from the biodegradation of 1, 6-hexanediol dibenzoate, a potential green plasticizer, by Rhodococcus rhodochrous. Journal of Mass Spectrometry 44, 662-671. https://doi.org/10.1002/jms.1541.

Kim, S.-J., Ahn, J.-H., Weon, H.-Y., Hong, S.-B., Seok, S.-J., Kim, J.-S., Kwon, S.-W., 2015. Chujaibacter soli gen. nov., sp. nov., isolated from soil. Journal of Microbiology 53, 592-597. https://doi.org/10.1007/s12275-015-5136-y.

Kim, Y.-M., Jeon, J.-R., Murugesan, K., Kim, E.-J., Chang, Y.-S., 2009. Biodegradation of 1, 4-dioxane and transformation of related cyclic compounds by a newly isolated Mycobacterium sp. PH-06. Biodegradation 20, 511.

Kruszelnicka, I., Michałkiewicz, M., Zajchowski, S., Kloziński, A., Tomaszewska, J., 2014. The use of wood-polymer composites in a Moving Bed Biofilm Reactor Technology. Polimery 59, 423-426.

Kumar, A., Hsu, L.H.-H., Kavanagh, P., Barrière, F., Lens, P.N., Lapinsonnière, L., Schröder, U., Jiang, X., Leech, D., 2017. The ins and outs of microorganism–electrode electron transfer reactions. Nature Reviews Chemistry 1, 1-13.

Law, A.M., Aitken, M.D., 2003. Bacterial chemotaxis to naphthalene desorbing from a nonaqueous liquid. Applied and Environmental Microbiology 69, 5968-5973.

Leaist, D.G., MacEwan, K., Stefan, A., Zamari, M., 2000. Binary mutual diffusion coefficients of aqueous cyclic ethers at 25 C. Tetrahydrofuran, 1, 3-dioxolane, 1, 4-dioxane, 1, 3-dioxane, tetrahydropyran, and trioxane. Journal of Chemical & Engineering Data 45, 815-818. https://doi.org/10.1021/je000079n.

Lee, J.-H., Park, J.-J., Byun, I.-G., Park, T.-J., Lee, T.-H., 2014. Anaerobic digestion of organic wastewater from chemical fiber manufacturing plant: lab and pilot-scale experiments. Journal of Industrial and Engineering Chemistry 20, 1732-1736.

Li, G., Park, S., Rittmann, B.E., 2012. Developing an efficient TiO2-coated biofilm carrier for intimate coupling of photocatalysis and biodegradation. water research 46, 6489-6496. https://doi.org/10.1016/j.watres.2012.09.029.

Li, J., Chen, C., Zhu, J.Y., Ragauskas, A.J., Hu, L., 2021. In situ wood delignification toward sustainable applications. Accounts of Materials Research 2, 606-620.

Li, J., Zhang, Y., Sun, K., Liu, W., Yan, H., Meng, J., 2022. Optimization of a cathodic electro-fermentation process for enhancing co-production of butanol and hydrogen via acetone-butanol-ethanol fermentation of Clostridium beijerinckii. Energy Conversion and Management 251, 114987.

Li, M., Fiorenza, S., Chatham, J.R., Mahendra, S., Alvarez, P.J., 2010. 1, 4-Dioxane biodegradation at low temperatures in Arctic groundwater samples. water research 44, 2894-2900. https://doi.org/10.1016/j.watres.2010.02.007.

Li, W.-W., Yu, H.-Q., 2015. Electro-assisted groundwater bioremediation: Fundamentals, challenges and future perspectives. Bioresource technology 196, 677-684.

Lionetto, F., Del Sole, R., Cannoletta, D., Vasapollo, G., Maffezzoli, A., 2012. Monitoring wood degradation during weathering by cellulose crystallinity. Materials 5, 1910-1922.

Lohner, S.T., Katzoreck, D., Tiehm, A., 2008. Electromigration of microbial electron acceptors and nutrients:(II) Transport in groundwater. Journal of Environmental Science and Health Part A 43, 922-925.

Louis, K.S., Siegel, A.C., 2011. Cell viability analysis using trypan blue: manual and automated methods. Mammalian cell viability. Springer, pp. 7-12.

Lu, L., Yazdi, H., Jin, S., Zuo, Y., Fallgren, P.H., Ren, Z.J., 2014. Enhanced bioremediation of hydrocarbon-contaminated soil using pilot-scale bioelectrochemical systems. Journal of hazardous materials 274, 8-15.

Lund, H., Hammerich, O., 2001. Organic electrochemistry. Marcel Dekker New York.

Ma, J., Wang, Z., Li, L., Shi, Z., Ke, S., He, Q., 2022. Granular activated carbon stimulated caproate production through chain elongation in fluidized cathode electro-fermentation systems. Journal of Cleaner Production 365, 132757.

Mahendra, S., Alvarez-Cohen, L., 2005. Pseudonocardia dioxanivorans sp. nov., a novel actinomycete that grows on 1, 4-dioxane. International Journal of Systematic and Evolutionary Microbiology 55, 593-598. https://doi.org/10.1099/ijs.0.63085-0.

Mahendra, S., Alvarez-Cohen, L., 2006. Kinetics of 1, 4-dioxane biodegradation by monooxygenase-expressing bacteria. Environmental science & technology 40, 5435-5442. https://doi.org/10.1021/es060714v.

Mahendra, S., Grostern, A., Alvarez-Cohen, L., 2013. The impact of chlorinated solvent co-contaminants on the biodegradation kinetics of 1, 4-dioxane. Chemosphere 91, 88-92.

Mahendra, S., Petzold, C.J., Baidoo, E.E., Keasling, J.D., Alvarez-Cohen, L., 2007. Identification of the intermediates of in vivo oxidation of 1, 4-dioxane by monooxygenase-containing bacteria. Environmental Science & Technology 41, 7330-7336. https://doi.org/10.1021/es0705745.

Mahmoodi, N.M., 2013. Synthesis of amine-functionalized magnetic ferrite nanoparticle and its dye removal ability. Journal of Environmental Engineering 139, 1382-1390.

Mahmoodi, N.M., Arami, M., Bahrami, H., Khorramfar, S., 2010. Novel biosorbent (Canola hull): Surface characterization and dye removal ability at different cationic dye concentrations. Desalination 264, 134-142.

Makkar, R.S., Rockne, K.J., 2003. Comparison of synthetic surfactants and biosurfactants in enhancing biodegradation of polycyclic aromatic hydrocarbons. Environmental Toxicology and Chemistry: An International Journal 22, 2280-2292.

Mangwani, N., Shukla, S.K., Kumari, S., Das, S., Rao, T.S., 2016. Effect of biofilm parameters and extracellular polymeric substance composition on polycyclic aromatic hydrocarbon degradation. RSC advances 6, 57540-57551.

Manju, N., Deepesh, V., Achuthan, C., Rosamma, P., Singh, I.B., 2009. Immobilization of nitrifying bacterial consortia on wood particles for bioaugmenting nitrification in shrimp culture systems. Aquaculture 294, 65-75. https://doi.org/10.1016/j.aquaculture.2009.05.008.

Mao, Y., Quan, X., Zhao, H., Zhang, Y., Chen, S., Liu, T., Quan, W., 2017. Accelerated startup of moving bed biofilm process with novel electrophilic suspended biofilm carriers. Chemical Engineering Journal 315, 364-372. https://doi.org/10.1016/j.cej.2017.01.041.

Marshall, K.C., 2006. Planktonic versus sessile life of prokaryotes. The prokaryotes 2, 3-15.

Mazloomi, S., Sulaiman, N., 2012. Influencing factors of water electrolysis electrical efficiency. Renewable and Sustainable Energy Reviews 16, 4257-4263.

McGinn, P.J., Dickinson, K.E., Park, K.C., Whitney, C.G., MacQuarrie, S.P., Black, F.J., Frigon, J.-C., Guiot, S.R., O'Leary, S.J., 2012. Assessment of the bioenergy and bioremediation potentials of the microalga Scenedesmus sp. AMDD cultivated in municipal wastewater effluent in batch and continuous mode. Algal Research 1, 155-165. https://doi.org/10.1016/j.algal.2012.05.001.

Mercier, A., Joulian, C., Michel, C., Auger, P., Coulon, S., Amalric, L., Morlay, C., Battaglia-Brunet, F., 2014. Evaluation of three activated carbons for combined adsorption and biodegradation of PCBs in aquatic sediment. Water research 59, 304-315. https://doi.org/10.1016/j.watres.2014.04.021.

Miao, Y., Heintz, M.B., Bell, C.H., Johnson, N.W., Polasko, A.L., Favero, D., Mahendra, S., 2021. Profiling microbial community structures and functions in bioremediation strategies for treating 1, 4-dioxane-contaminated groundwater. Journal of Hazardous Materials 408, 124457. https://doi.org/10.1016/j.jhazmat.2020.124457.

Miao, Y., Johnson, N.W., Gedalanga, P.B., Adamson, D., Newell, C., Mahendra, S., 2019. Response and recovery of microbial communities subjected to oxidative and biological treatments of 1, 4-dioxane and co-contaminants. Water Research 149, 74-85. https://doi.org/10.1016/j.watres.2018.10.070.

Miao, Y., Johnson, N.W., Phan, T., Heck, K., Gedalanga, P.B., Zheng, X., Adamson, D., Newell, C., Wong, M.S., Mahendra, S., 2020. Monitoring, assessment, and prediction of microbial shifts in coupled catalysis and biodegradation of 1, 4-dioxane and co-contaminants. Water Research 173, 115540. https://doi.org/10.1016/j.watres.2020.115540.

Mirpuri, R., Jones, W., Bryers, J.D., 1997. Toluene degradation kinetics for planktonic and biofilm-grown cells of Pseudomonas putida 54G. Biotechnology and Bioengineering 53, 535-546. https://doi.org/10.1002/(SICI)1097-0290(19970320)53:6<535::AID-BIT1>3.0.CO;2-N.

Mohr, T.K., DiGuiseppi, W.H., Hatton, J.W., Anderson, J.K., 2020. Environmental investigation and remediation: 1, 4-dioxane and other solvent stabilizers. CRC Press.

Munch, D.J., Hautman, D.P., 1995. EPA METHOD 551.1.

Myers, M.A., Johnson, N.W., Marin, E.Z., Pornwongthong, P., Liu, Y., Gedalanga, P.B., Mahendra, S., 2018. Abiotic and bioaugmented granular activated carbon for the treatment of 1, 4-dioxane-contaminated water. Environmental Pollution 240, 916-924.

Nadal, M., Marquès, M., Mari, M., Domingo, J.L., 2015. Climate change and environmental concentrations of POPs: A review. Environmental research 143, 177-185.

Nakhli, S.A.A., Ahmadizadeh, K., Fereshtehnejad, M., Rostami, M.H., Safari, M., Borghei, S.M., 2014. Biological removal of phenol from saline wastewater using a moving bed biofilm reactor containing acclimated mixed consortia. SpringerPlus 3, 1-10. https://doi.org/10.1186/2193-1801-3-112.

Nam, J.-H., Ventura, J.-R.S., Yeom, I.T., Lee, Y., Jahng, D., 2016. Structural and kinetic characteristics of 1, 4-dioxane-degrading bacterial consortia containing the phylum TM7. Journal of Microbiology and Biotechnology 26, 1951-1964. https://doi.org/10.4014/jmb.1601.01095.

Nancharaiah, Y., Venugopalan, V.P., 2019. Microbial Biofilms in Bioremediation and Wastewater Treatment. CRC Press.

Oh, S.-E., Logan, B.E., 2006. Proton exchange membrane and electrode surface areas as factors that affect power generation in microbial fuel cells. Applied microbiology and biotechnology 70, 162-169.

Oldenhuis, R., Vink, R., Janssen, D.B., Witholt, B., 1989. Degradation of chlorinated aliphatic hydrocarbons by Methylosinus trichosporium OB3b expressing soluble methane monooxygenase. Appl. Environ. Microbiol. 55, 2819-2826.

Paliy, O., Kenche, H., Abernathy, F., Michail, S., 2009. High-throughput quantitative analysis of the human intestinal microbiota with a phylogenetic microarray. Applied and environmental microbiology 75, 3572-3579. https://doi.org/10.1128/AEM.02764-08.

Pang, C.M., Liu, W.-T., 2007. Community structure analysis of reverse osmosis membrane biofilms and the significance of Rhizobiales bacteria in biofouling. Environmental science & technology 41, 4728-4734. https://doi.org/10.1021/es0701614.

Parales, R., Adamus, J., White, N., May, H., 1994. Degradation of 1, 4-dioxane by an actinomycete in pure culture. Appl. Environ. Microbiol. 60, 4527-4530. https://doi.org/10.1128/aem.60.12.4527-4530.1994.

Park, Y.-M., Pyo, H., Park, S.-J., Park, S.-K., 2005. Development of the analytical method for 1, 4-dioxane in water by liquid–liquid extraction. Analytica Chimica Acta 548, 109-115.

Parker, B.J., Wearsch, P.A., Veloo, A.C., Rodriguez-Palacios, A., 2020. The genus Alistipes: gut bacteria with emerging implications to inflammation, cancer, and mental health. Frontiers in immunology 11, 906.

Paul, E., Wolff, D.B., Ochoa, J.C., Ribeiro da Costa, R.H., 2007. Recycled and virgin plastic carriers in hybrid reactors for wastewater treatment. Water environment research 79, 765-774. https://doi.org/10.2175/106143006X123139.

Pica, N.E., Miao, Y., Johnson, N.W., Ramos, P., Mahendra, S., Blotevogel, J., 2021. Bioelectrochemical Treatment of 1, 4-Dioxane in the Presence of Chlorinated Solvents: Design, Process, and Sustainability Considerations. ACS Sustainable Chemistry & Engineering 9, 3172-3182.

Plötze, M., Niemz, P., 2011. Porosity and pore size distribution of different wood types as determined by mercury intrusion porosimetry. European Journal of Wood and Wood Products 69, 649-657. https://doi.org/10.1007/s00107-010-0504-0.

Polasko, A.L., Zulli, A., Gedalanga, P.B., Pornwongthong, P., Mahendra, S., 2018. A mixed microbial community for the biodegradation of chlorinated ethenes and 1, 4-dioxane. Environmental Science & Technology Letters 6, 49-54. https://doi.org/10.1021/acs.estlett.8b00591.

Pollitt, K.J.G., Kim, J.-H., Peccia, J., Elimelech, M., Zhang, Y., Charkoftaki, G., Hodges, B., Zucker, I., Huang, H., Deizel, N.C., 2019. 1, 4-Dioxane as an emerging water contaminant–State of the science and evaluation of research needs. Science of The Total Environment. https://doi.org/10.1016/j.scitotenv.2019.06.443.

Pugazhendi, A., Rajesh Banu, J., Dhavamani, J., Yeom, I.T., 2015. Biodegradation of 1, 4-dioxane by Rhodanobacter AYS5 and the role of additional substrates. Annals of microbiology 65, 2201-2208. https://doi.org/10.1007/s13213-015-1060-y.

Raj, C.C., Ramkumar, N., Chidambaram, S., 1997. Biodegradation of acetic, benzoic, isophthalic, toluic and terephthalic acids using a mixed culture: effluents of PTA production. Process safety and environmental protection 75, 245-256.

Ramalingam, V., Cupples, A.M., 2020. Anaerobic 1, 4-dioxane biodegradation and microbial community analysis in microcosms inoculated with soils or sediments and different electron acceptors. Applied Microbiology and Biotechnology, 1-16.

Ranjbar-Mohammadi, M., Arami, M., Bahrami, H., Mazaheri, F., Mahmoodi, N.M., 2010. Grafting of chitosan as a biopolymer onto wool fabric using anhydride bridge and its antibacterial property. Colloids and Surfaces B: Biointerfaces 76, 397-403.

Reguera, G., Nevin, K.P., Nicoll, J.S., Covalla, S.F., Woodard, T.L., Lovley, D.R., 2006. Biofilm and nanowire production leads to increased current in Geobacter sulfurreducens fuel cells. Applied and environmental microbiology 72, 7345-7348.

Renner, L.D., Weibel, D.B., 2011. Physicochemical regulation of biofilm formation. MRS bulletin 36, 347-355. https://doi.org/10.1557/mrs.2011.65.

Ringeisen, B.R., Henderson, E., Wu, P.K., Pietron, J., Ray, R., Little, B., Biffinger, J.C., Jones-Meehan, J.M., 2006. High power density from a miniature microbial fuel cell using Shewanella oneidensis DSP10. Environmental science & technology 40, 2629-2634.

Rittmann, B.E., McCarty, P.L., 2001. Environmental biotechnology: principles and applications. McGraw-Hill Education.

Rittmann, B.E., McCarty, P.L., 2012. Environmental biotechnology: principles and applications. Tata McGraw-Hill Education.

Rivalland, C., Radouani, F., Gonzalez-Rizzo, S., Robert, F., Salvin, P., 2022. Enrichment of Clostridia enhances Geobacter population and electron harvesting in a complex electroactive biofilm. Bioelectrochemistry 143, 107954.

Rivett, M.O., Thornton, S.F., 2008. Monitored natural attenuation of organic contaminants in groundwater: principles and application. Proceedings of the Institution of Civil Engineers-Water Management. Thomas Telford Ltd, pp. 381-392.

Rodrigo, J., Boltes, K., Esteve-Nuñez, A., 2014. Microbial-electrochemical bioremediation and detoxification of dibenzothiophene-polluted soil. Chemosphere 101, 61-65.

Rozendal, R.A., Hamelers, H.V., Rabaey, K., Keller, J., Buisman, C.J., 2008. Towards practical implementation of bioelectrochemical wastewater treatment. Trends in biotechnology 26, 450-459.

Sakuragi, Y., Kolter, R., 2007. Quorum-sensing regulation of the biofilm matrix genes (pel) of Pseudomonas aeruginosa. Journal of bacteriology 189, 5383-5386.

Samadi, A., Budge, S.M., Huang, Y., Jamieson, R., 2022. Biodegradation of 1, 4-dioxane by a native digestate microbial community. SSRN. http://dx.doi.org/10.2139/ssrn.4045861.

Samadi, A., Kermanshahi pour, A., Beims, R.F., Xu, C.C., 2023. Delignified porous wood as biofilm support for 1, 4-dioxane-degrading bacterial consortium. Environmental Technology, 1-41.

Sandhya, M., Huang, Y., Li, J., Wu, X., Zhou, Z., Lei, Q., Bhatt, P., Chen, S., 2022. Biofilm-mediated bioremediation is a powerful tool for the removal of environmental pollutants. Chemosphere, 133609. https://doi.org/10.1016/j.chemosphere.2022.133609.

Sayedin, F., Kermanshahi-pour, A., He, Q.S., 2019. Evaluating the potential of a novel anaerobic baffled reactor for anaerobic digestion of thin stillage: Effect of organic loading rate, hydraulic retention time and recycle ratio. Renewable Energy 135, 975-983.

Sayedin, F., Kermanshahi-pour, A., He, Q.S., Tibbetts, S.M., Lalonde, C.G., Brar, S.K., 2020. Microalgae cultivation in thin stillage anaerobic digestate for nutrient recovery and bioproduct production. Algal Research 47, 101867. https://doi.org/10.1016/j.algal.2020.101867.

Sayedin, F., Kermanshahi-pour, A., He, S.Q., 2018. Anaerobic digestion of thin stillage of corn ethanol plant in a novel anaerobic baffled reactor. Waste Management 78, 541-552.

Sei, K., Miyagaki, K., Kakinoki, T., Fukugasako, K., Inoue, D., Ike, M., 2013. Isolation and characterization of bacterial strains that have high ability to degrade 1, 4-dioxane as a sole carbon and energy source. Biodegradation 24, 665-674. https://doi.org/10.1007/s10532-012-9614-1.

Shen, W., Chen, H., Pan, S., 2008. Anaerobic biodegradation of 1, 4-dioxane by sludge enriched with iron-reducing microorganisms. Bioresource technology 99, 2483-2487.

Shen, Y.-J., Wu, G.-X., Fan, Y.-B., Zhong, H., Wu, L.-L., Zhang, S.-L., Zhao, X.-H., Zhang, W.-J., 2007. Performances of biological aerated filter employing hollow fiber membrane segments of surface-improved poly (sulfone) as biofilm carriers. Journal of Environmental Sciences 19, 811-817. https://doi.org/10.1016/S1001-0742(07)60136-3.

Shin, D., Sung, D.Y., Moon, H.S., Nam, K., 2010. Microbial succession in response to 1, 4-dioxane exposure in activated sludge reactors: effect of inoculum source and extra carbon addition. Journal of Environmental Science and Health Part A 45, 674-681. https://doi.org/10.1080/10934521003648859.

Shiratori, H., Ohiwa, H., Ikeno, H., Ayame, S., Kataoka, N., Miya, A., Beppu, T., Ueda, K., 2008. Lutispora thermophila gen. nov., sp. nov., a thermophilic, spore-forming bacterium isolated from a thermophilic methanogenic bioreactor digesting municipal solid wastes. International journal of systematic and evolutionary microbiology 58, 964-969.

Shui, T., Feng, S., Yuan, Z., Kuboki, T., Xu, C.C., 2016. Highly efficient organosolv fractionation of cornstalk into cellulose and lignin in organic acids. Bioresource technology 218, 953-961. https://doi.org/10.1016/j.biortech.2016.07.054.

Shukla, S.K., Mangwani, N., Rao, T.S., Das, S., 2014. Biofilm-mediated bioremediation of polycyclic aromatic hydrocarbons. Microbial biodegradation and bioremediation. Elsevier, pp. 203-232.

Skoog, D.A., Holler, F.J., Crouch, S.R., 2017. Principles of instrumental analysis. Cengage learning.

Springael, D., Peys, K., Ryngaert, A., Roy, S.V., Hooyberghs, L., Ravatn, R., Heyndrickx, M., Meer, J.R.v.d., Vandecasteele, C., Mergeay, M., 2002. Community shifts in a seeded 3-chlorobenzoate degrading membrane biofilm reactor: indications for involvement of in situ horizontal transfer of the clc-element from inoculum to contaminant bacteria. Environmental microbiology 4, 70-80.

Stepien, D.K., Diehl, P., Helm, J., Thoms, A., Püttmann, W., 2014. Fate of 1, 4-dioxane in the aquatic environment: from sewage to drinking water. Water research 48, 406-419. https://doi.org/10.1016/j.watres.2013.09.057.

Stewart, P.S., 2003. Diffusion in biofilms. Journal of bacteriology 185, 1485-1491. https://doi.org/10.1128/JB.185.5.1485-1491.2003.

Sun, B., Ko, K., Ramsay, J.A., 2011. Biodegradation of 1, 4-dioxane by a Flavobacterium. Biodegradation 22, 651-659. https://doi.org/10.1007/s10532-010-9438-9.

Sun, Y.-L., Zhang, G.-C., Yan, Z., Li, X.-J., Wang, K.-J., 2010. Removing nitrate-nitrogen from wastewater using rotten wood as carbon source. Huan Jing ke Xue= Huanjing Kexue 31, 1494-1498.

Tyagi, M., da Fonseca, M.M.R., de Carvalho, C.C., 2011. Bioaugmentation and biostimulation strategies to improve the effectiveness of bioremediation processes. Biodegradation 22, 231-241.

Van Den Heuvel, R., Van Der Biezen, E., Jetten, M., Hefting, M., Kartal, B., 2010. Denitrification at pH 4 by a soil-derived Rhodanobacter-dominated community. Environmental Microbiology 12, 3264-3271. https://doi.org/10.1111/j.1462-2920.2010.02301.x.

Van Loosdrecht, M., Lyklema, J., Norde, W., Schraa, G., Zehnder, A., 1987. The role of bacterial cell wall hydrophobicity in adhesion. Applied and environmental microbiology 53, 1893-1897. https://doi.org/10.1128/aem.53.8.1893-1897.1987.

Vatankhah, H., Szczuka, A., Mitch, W.A., Almaraz, N., Brannum, J., Bellona, C., 2019. Evaluation of enhanced ozone–biologically active filtration treatment for the removal of 1, 4-dioxane and disinfection byproduct precursors from wastewater effluent. Environmental science & technology 53, 2720-2730.

Verdini, R., Aulenta, F., de Tora, F., Lai, A., Majone, M., 2015. Relative contribution of set cathode potential and external mass transport on TCE dechlorination in a continuous-flow bioelectrochemical reactor. Chemosphere 136, 72-78.

Vitas, S., Segmehl, J.S., Burgert, I., Cabane, E., 2019. Porosity and pore size distribution of native and delignified beech wood determined by mercury intrusion porosimetry. Materials 12, 416. https://doi.org/10.3390/ma12030416.

Wang, J., Fishwild, S.J., Begel, M., Zhu, J., 2020. Properties of densified poplar wood through partial delignification with alkali and acid pretreatment. Journal of Materials Science 55, 14664-14676.

Wang, Z., Yang, Y., Dai, Y., Xie, S., 2015. Anaerobic biodegradation of nonylphenol in river sediment under nitrate-or sulfate-reducing conditions and associated bacterial community. Journal of Hazardous Materials 286, 306-314. https://doi.org/10.1016/j.jhazmat.2014.12.057.

Wiegel, J.K.W., 1978. Xanthobacter. Bergey's Manual of Systematics of Archaea and Bacteria, pp. 1-22.

Wilén, B.-M., Balmer, P., 1999. The effect of dissolved oxygen concentration on the structure, size and size distribution of activated sludge flocs. Water research 33, 391-400.

Wolfaardt, G., Lawrence, J., Robarts, R., Caldwell, D., 1995. Bioaccumulation of the herbicide diclofop in extracellular polymers and its utilization by a biofilm community during starvation. Applied and environmental microbiology 61, 152-158.

Xiong, Y., Mason, O.U., Lowe, A., Zhang, Z., Zhou, C., Chen, G., Villalonga, M.J., Tang, Y., 2020. Investigating promising substrates for promoting 1, 4-dioxane biodegradation: effects of ethane and tetrahydrofuran on microbial consortia. Biodegradation 31, 171-182.

Xiong, Y., Wang, B., Zhou, C., Chen, H., Chen, G., Tang, Y., 2022. Determination of growth kinetics of microorganisms linked with 1, 4-dioxane degradation in a consortium based on two improved methods. Frontiers of Environmental Science & Engineering 16, 1-11. https://doi.org/10.1007/s11783-022-1567-y.

Yabuki, Y., Yoshida, G., Daifuku, T., Ono, J., Banno, A., 2018. Biological treatment of 1, 4-dioxane in wastewater from landfill by indigenous microbes attached to flowing carriers. Journal of Water and Environment Technology 16, 245-255. https://doi.org/10.2965/jwet.18-032.

Yang, S., Peng, Y., Zhang, S., Han, X., Li, J., Zhang, L., 2021. Carrier type induces anammox biofilm structure and the nitrogen removal pathway: Demonstration in a full-scale partial nitritation/anammox process. Bioresource Technology 334, 125249. https://doi.org/10.1016/j.biortech.2021.125249.

Yu, H., Wan, H., Feng, C., Yi, X., Liu, X., Ren, Y., Wei, C., 2017. Microbial polychlorinated biphenyl dechlorination in sediments by electrical stimulation: The effect of adding acetate and nonionic surfactant. Science of The Total Environment 580, 1371-1380.

Yu, Y., Breitbart, M., McNairnie, P., Rohwer, F., 2006. FastGroupII: a web-based bioinformatics platform for analyses of large 16S rDNA libraries. BMC Bioinformatics 7, 1-9. https://doi.org/10.1186/1471-2105-7-57.

Zainab, A., Meraj, S., Liaquat, R., 2020. Study on natural organic materials as biofilm carriers for the optimization of anaerobic digestion. Waste and biomass valorization 11, 2521-2531.

Zenker, M.J., Borden, R.C., Barlaz, M.A., 2000. Mineralization of 1, 4-dioxane in the presence of a structural analog. Biodegradation 11, 239-246. https://doi.org/10.1023/A:1011156924700.

Zhang, J., Gu, T., Zhou, Y., He, J., Zheng, L.-Q., Li, W.-J., Huang, X., Li, S.-P., 2012. Terrimonas rubra sp. nov., isolated from a polluted farmland soil and emended description of the genus Terrimonas. International journal of systematic and evolutionary microbiology 62, 2593-2597. https://doi.org/10.1099/ijs.0.036079-0.

Zhang, S., Gedalanga, P.B., Mahendra, S., 2016. Biodegradation kinetics of 1, 4-dioxane in chlorinated solvent mixtures. Environmental science & technology 50, 9599-9607. https://doi.org/10.1021/acs.est.6b02797.

Zhang, S., Gedalanga, P.B., Mahendra, S., 2017. Advances in bioremediation of 1, 4-dioxane-contaminated waters. Journal of environmental management 204, 765-774. https://doi.org/10.1016/j.jenvman.2017.05.033.

Zhang, X., Zhou, X., Ni, H., Rong, X., Zhang, Q., Xiao, X., Huan, H., Liu, J.F., Wu, Z., 2018. Surface modification of basalt fiber with organic/inorganic composites for biofilm carrier used in wastewater treatment. ACS Sustainable Chemistry & Engineering 6, 2596-2602. https://doi.org/10.1021/acssuschemeng.7b04089.

Zhang, Y., Liu, H., Shi, W., Pu, X., Zhang, H., Rittmann, B.E., 2010. Photobiodegradation of phenol with ultraviolet irradiation of new ceramic biofilm carriers. Biodegradation 21, 881-887. https://doi.org/10.1007/s10532-010-9348-x.

Zhao, L., Hou, H., Fujii, A., Hosomi, M., Li, F., 2014. Degradation of 1, 4-dioxane in water with heat-and Fe 2+-activated persulfate oxidation. Environmental Science and Pollution Research 21, 7457-7465.

Zhao, L., Lu, X., Polasko, A., Johnson, N.W., Miao, Y., Yang, Z., Mahendra, S., Gu, B., 2018. Co-contaminant effects on 1, 4-dioxane biodegradation in packed soil column flow-through systems. Environmental pollution 243, 573-581. https://doi.org/10.1016/j.envpol.2018.09.018.

Zhao, Y., Liu, D., Huang, W., Yang, Y., Ji, M., Nghiem, L.D., Trinh, Q.T., Tran, N.H., 2019. Insights into biofilm carriers for biological wastewater treatment processes: Current state-of-the-art, challenges, and opportunities. Bioresource technology 288, 121619. https://doi.org/10.1016/j.biortech.2019.121619.

Żur, J., Wojcieszyńska, D., Guzik, U., 2016. Metabolic responses of bacterial cells to immobilization. Molecules 21, 958.

# Appendix A Copyright agreements

Copyright agreement for Chapter 3:

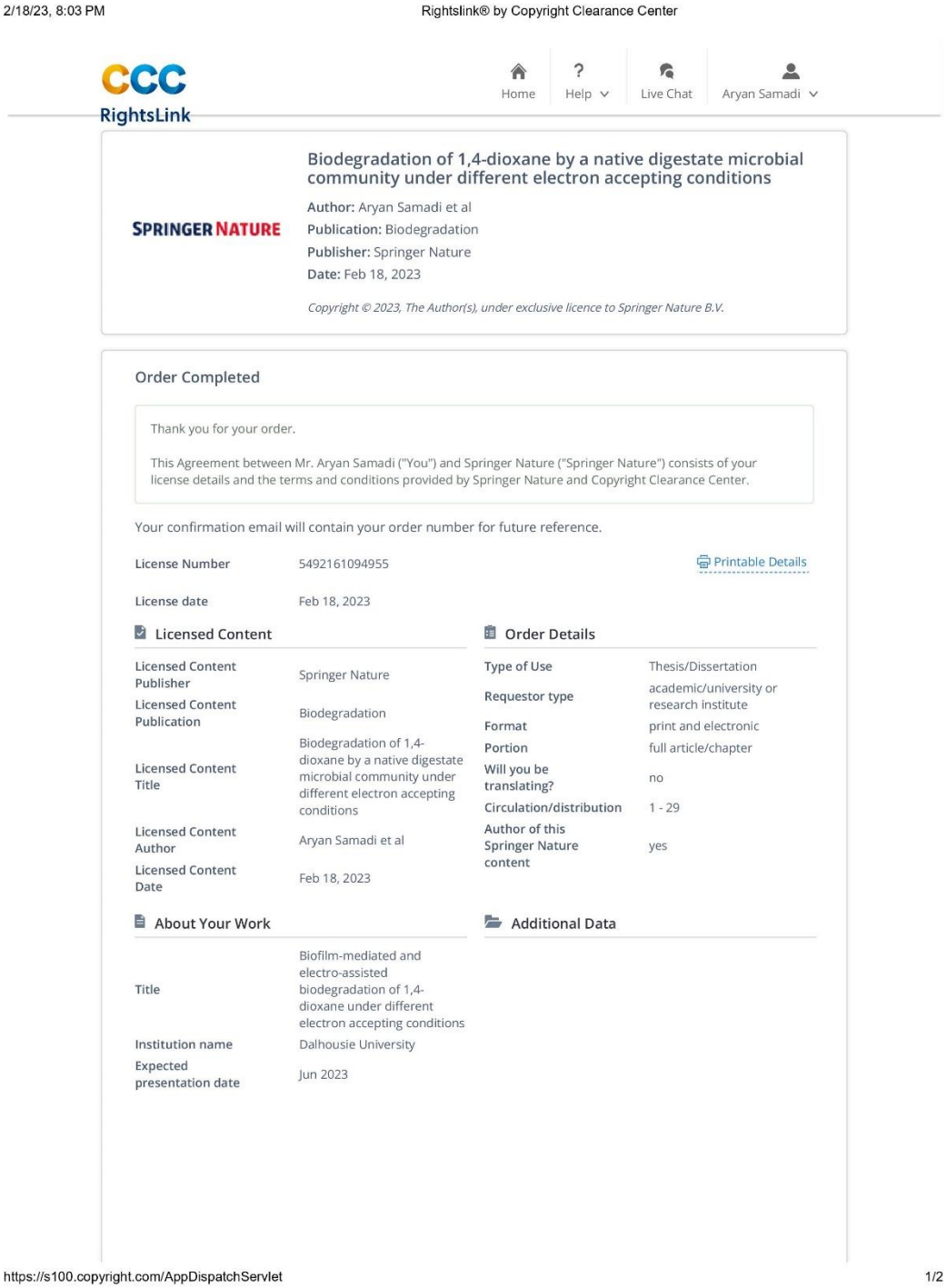

2/18/23, 8:03 PM Rightslink® by Copyright Clearance Center

CCC RightsLink

Home | Help | Live Chat | Aryan Samadi

SPRINGER NATURE

Biodegradation of 1,4-dioxane by a native digestate microbial community under different electron accepting conditions

**Author:** Aryan Samadi et al
**Publication:** Biodegradation
**Publisher:** Springer Nature
**Date:** Feb 18, 2023

*Copyright © 2023, The Author(s), under exclusive licence to Springer Nature B.V.*

Order Completed

Thank you for your order.

This Agreement between Mr. Aryan Samadi ("You") and Springer Nature ("Springer Nature") consists of your license details and the terms and conditions provided by Springer Nature and Copyright Clearance Center.

Your confirmation email will contain your order number for future reference.

Printable Details

| | |
|---|---|
| License Number | 5492161094955 |
| License date | Feb 18, 2023 |

**Licensed Content**

| | |
|---|---|
| Licensed Content Publisher | Springer Nature |
| Licensed Content Publication | Biodegradation |
| Licensed Content Title | Biodegradation of 1,4-dioxane by a native digestate microbial community under different electron accepting conditions |
| Licensed Content Author | Aryan Samadi et al |
| Licensed Content Date | Feb 18, 2023 |

**Order Details**

| | |
|---|---|
| Type of Use | Thesis/Dissertation |
| Requestor type | academic/university or research institute |
| Format | print and electronic |
| Portion | full article/chapter |
| Will you be translating? | no |
| Circulation/distribution | 1 - 29 |
| Author of this Springer Nature content | yes |

**About Your Work**

| | |
|---|---|
| Title | Biofilm-mediated and electro-assisted biodegradation of 1,4-dioxane under different electron accepting conditions |
| Institution name | Dalhousie University |
| Expected presentation date | Jun 2023 |

**Additional Data**

https://s100.copyright.com/AppDispatchServlet 1/2

**Requestor Location**

| | |
|---|---|
| Requestor Location | Mr. Aryan Samadi<br>1510 Lilac St.<br>Unit 43<br>Halifax, NS B3H 3W3<br>Canada<br>Attn: Mr. Aryan Samadi |

**Tax Details**

**$ Price**

| | |
|---|---|
| Total | 0.00 CAD |

Total: 0.00 CAD

CLOSE WINDOW ORDER MORE

Copyright agreement for Chapter 4:



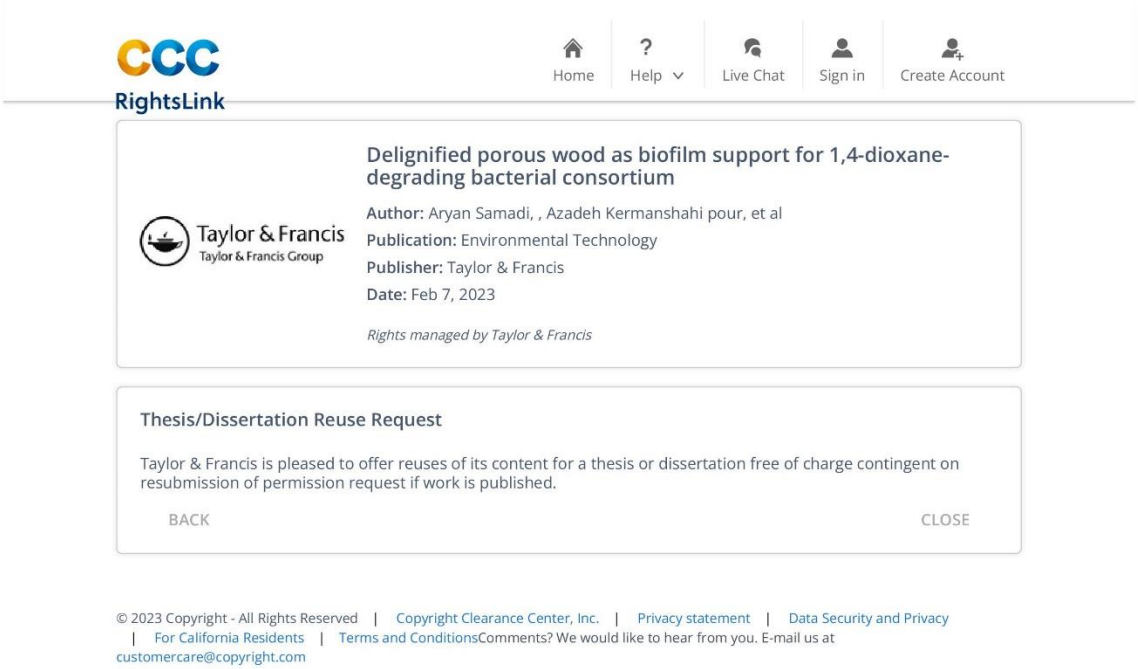

## Appendix B Supplementary information for Chapter 3

**Section S1**

1 liter of MS medium contained 1.5 g of $NH_4Cl$, 0.6 g of $NaH_2PO_4$, 0.1 g of $CaCl_2.2H_2O$, 0.1 g of KCl, 0.002 g $MgCl_2.6H_2O$, 5 mL of vitamin solution, 1 mL of vitamin $B_{12}$ solution, and 1 mL of trace element solution. The vitamin solution contained (per liter) 10 mg of biotin, 50 mg of 4-aminobenzoic acid, 10 mg of pantothenate, 250 mg of pyridoxamine, 100 mg of nicotinic acid and 20 mg of thiamine. The $B_{12}$ solution contained (per liter) 50 mg of vitamin $B_{12}$. The trace element solution contained (per liter) 12.8 g of nitrilotriacetic acid, 2 g of $FeCl_2.4H_2O$, 190 mg of $CoCl_2.6H_2O$, 100 mg of $MnCl_22H_2O$, 70 mg of $ZnCl_2$, 6 mg of $H_3BO_3$, 24 mg of $NiCl_2.6H_2O$, 2 mg of $CuCl_2.2H_2O$, 36 mg of $Na_2MoO_4.2H_2O$ (Shen et al., 2008).

**Section S2**

DX concentration was measured by liquid-liquid extraction (LLE) followed by GC/MS analysis. MTBE was used as the extraction organic solvent because it has shown high and stable recovery percentages for DX even in ppb levels (Park et al., 2005). The extractability achieved in this study was 60-80%. For LLE, 2 mL of 0.45 µm filtered sample from the biodegradation medium was added to a 20 mL glass vial. Then, 4 mL of MTBE containing 40 mg/L of DX-d8 as internal standard was added to the vial. 0.5 g of anhydrous sodium sulfate was also added to improve the recovery. The vial was vortexed for 2 minutes, and sat for 3 minutes until the organic and aqueous phases were separated. 0.5 g of anhydrous sodium sulfate was added again to remove the water from the top layer (organic phase) (Vatankhah et al., 2019). 1 mL of the top layer was collected in a 2 mL auto-injector vial for GC/MS analysis. 1 µL of sample was injected in a split/spitless injector at 280 ˚C and split ratio of 1:20. The carrier gas (Helium) flowrate was set at 0.8 mL/min. HP-5ms (5%-phenyl)-methylpolysiloxane) Agilent column, 25m (L) x 0.25mm (ID) x 25µm (thickness), was used in the GC. The oven temperature was initially set at 40 ˚C and held for 4 minutes, then increased to 100 ˚C with a rate of 5 ˚C/min, then increased to 250 ˚C with the rate of 25 ˚C/min and

kept at that temperature for 1 minute. Full-scan at the range of 50-350 m/z after 2.5 min solvent delay was conducted by MS. Quantification of DX and DX-d8 peaks were conducted by Masshunter Quantitative Analysis software using extracted ion count of 88.0 m/z for DX and 96.1 m/z for DX-d8. To calculate the concentration, standard curves for two ranges of concentrations of 10-100 mg/L ($R^2$=0.9995, detection limit=2.42 mg/L) and 1-10 mg/L ($R^2$ =0.9999, detection limit=0.01 mg/L) were developed. Detection limits were determined from the calibration curves and confirmed by injecting standard samples of those concentrations (Skoog et al., 2017).

TCE concentration was also measured by LLE followed by GC/MS analysis. DCM was used as the organic solvent in LLE which has shown a high recovery for chlorinated solvents (Munch and Hautman, 1995; Jasmann et al., 2017). For LLE, 3 mL of 0.45 µm filtered sample from the biodegradation medium was added to a 20 mL glass vial. Then, 3 mL of DCM was added to the vial. The vial was vortexed for 1 minute, and then sat for 3 minutes until the organic and aqueous phases were separated. 1 mL of the bottom layer (organic solvent) was collected in a 2 mL auto-injector vial for GC/MS analysis. The same GC/MS method employed with DX was used for TCE measurement. To calculate the concentration, a standard curve for the range of concentrations of 5-30 mg/L ($R^2$=0.9947, detection limit=2.83 mg/L) was developed.

Glucose concentration was measured by high-performance liquid chromatography (HPLC) (Fockink et al., 2018). 1 mL of 0.2 µm filtered medium was transferred to 2 mL glass auto-injector vials. 10 µL of sample was injected in the HPLC (Agilent 1260 Infinity II) connected to a Refractive Index Detector (RID, G7162A Agilent). A mobile phase of water at a flow rate of 0.6 mL/min, with column and RID temperature at 65 & 55 ˚C were set for the parameters. A Hiplex H column (300x7.7 mm; hydrogen phase, Agilent) was used for quantification of glucose. A standard curve for the range of concentrations of 40-200 mg/L ($R^2$=0.9980, detection limit=9.73 mg/L) was developed.

Concentrations of selected volatile fatty acids (VFAs), including acetic acid, propanoic acid and butyric acid, were measured in the medium by GC with flame ionization detection (FID) (Sayedin et al., 2018). 4 mL of 0.2 µm filtered samples were collected from the biodegradation medium and were acidified to pH=2 using sulfuric acid. 4 mL of diethyl ether was added to the samples and vortexed for 2 minutes. After standing for 3 minutes to separate the phases, 1 mL of organic phase was transferred to 2 mL glass auto-injector vials. 2 µL of sample was injected in the GC/FID at injector temperature of 180 ˚C and split ratio of 1:10. A DB-23ms Agilent column (50% cyanopropyl-methylsiloxane), 30m x 0.32mm x 10µm, was used in the GC. The oven temperature was initially set at 125 ˚C and held for 1 minute, then increased to 190 ˚C at a rate of 10 ˚C/min and kept at that temperature for 15 minutes. Detector temperature was set at 200 ˚C. A standard curved in the range of 10-100 mg/L was developed for acetic acid ($R^2$=0.995, detection limit=2.26 mg/L), propanoic acid ($R^2$=0.995, detection limit=3.45 mg/L), and butyric acid ($R^2$=0.9955, detection limit=8.23 mg/L).

GC/MS method for metabolite identification: Injector and detector transfer line temperatures were respectively set at 230 ˚C and 250 ˚C. The carrier gas (Helium) flowrate was set at 1 mL/min in constant flow mode. The GC oven temperature was initially set at 70 ˚C, held for 5 minutes, then increased up to 230 ˚C at a rate of 5 ˚C/min, resulting in a total run time of 37 minutes. 1 µL of sample was injected by automatic liquid sampler (7650A Agilent) with a split ratio between 1:10 to 1:40, which was adjusted according to the obtained chromatograms.

**Tables**

**Table S1** Condition of the acclimatization stage flasks.

| Flask | Sludge sample | DX concentration | Electron acceptor | Co-substrate | Temperature | VSS (mg/L)[1] |
|---|---|---|---|---|---|---|
| S1 | Compartment 1 | 25 mg/L | --- | Glucose, 200 mg/L | Ambient | 218 |
| S2 | Compartment 1 | 25 mg/L | Fe (III), 30 mM | --- | Ambient | 372 |
| S3 | Compartment 2 | 25 mg/L | --- | Glucose, 200 mg/L | Ambient | 19,405 |
| S4 | Compartment 2 | 25 mg/L | Fe (III), 30 mM | ---- | Ambient | 9,380 |
| S5 | Compartment 3 | 25 mg/L | --- | Glucose, 200 mg/L | Ambient | 415 |

| | | | | | | |
|---|---|---|---|---|---|---|
| S6 | Compartment 3 | 25 mg/L | --- | ---Glucose, | Ambient | 90 |
| S7 | Compartment 4 | 25 mg/L | --- | 200 mg/L | Ambient | 4,460 |
| S8 | Compartment 4 | 25 mg/L | --- | --- | Ambient | 6,100 |
| S9 | Compartment 1 | 25 mg/L | $NO_3$, 10 mM | --- | Ambient | 114 |
| S10 | Compartment 1 | 25 mg/L | $SO_4$, 10 mM | --- | Ambient | 127 |
| S11 | Compartment 1 | 25 mg/L | $O_2$, >8 mg/L | --- | Ambient | 232 |
| S12 | Compartment 1 | 25 mg/L | $O_2$, >8 mg/L | --- | Ambient | 436 |
| S13 | Abiotic | 25 mg/L | --------- | --- | Ambient | --- |
| S14 | Abiotic | 25 mg/L | $NO_3$, 10 mM | --- | Ambient | --- |
| S15 | Compartment 1 | 25 mg/L | $NO_3$, 10 mM | --- | 30 ˚C | 1,212 |
| S16 | Compartment 1 | 25 mg/L | $O_2$, >8 mg/L | --- | 30 ˚C | 1,430 |
| S17 | Compartment 1 | 25 mg/L | ------ | --- | 30 ˚C | 1,840 |
| S18 | Compartment 1 | 25 mg/L | --- | --- | 30 ˚C | 1,950 |
| S19 | Compartment 2 | 25 mg/L | | --- | 30 ˚C | 7.378 |
| S20 | Compartment 2 | 25 mg/L | | Glucose, 200 mg/L | 30 ˚C | 7.502 |
| S21 | Abiotic | 25 mg/L | | --- | 30 ˚C | --- |

[1] There was a substantial difference in initial VSS concentrations of the sludge samples. However, it did not have noticeable effect on DX biodegradation.

**Table S2** Rate of DX evaporation in different conditions (aerated or non-aerated, ambient (20-25 ˚C) or 30 ˚C) and the percentage of DX loss due to evaporation in the biological flasks (containing sludge) in different conditions.

| Flask condition (abiotic) | DX evaporation rate (mg/L/d) | DX percentage loss due to evaporation (%) in the indicated time | Flask condition (biological) | DX percentage loss due to evaporation (%) in the indicated time |
|---|---|---|---|---|
| Ambient and non-aerated (flasks F17 & F18) | 0.028 | 11.12±1.08 (in 119 days) | Ambient and non-aerated (flasks F1-F8) | 11.57±0.43 (in 119 days) |
| Ambient and aerated (flasks F19 & F20) | 0.044 | 19.31±1.75 (in 119 days) | Ambient and aerated (flasks F9 & F10) | 13.42±0.74 (in 84 days) |
| 30 ˚C and non-aerated (flasks F27-1 & F27-2) | 0.046 | 16.46±1.17 (in 84 days) | 30 ˚C and non-aerated (flasks F21 & F22) | 14.96±0.69 (in 84 days) |
| 30 ˚C and aerated (flasks F27-3 & F27-4) | 0.079 | 28.31±2.48 (in 84 days) | 30 ˚C and aerated (flasks F25 & F26) | 22.40±1.33 (in 63 days) |

## Figures

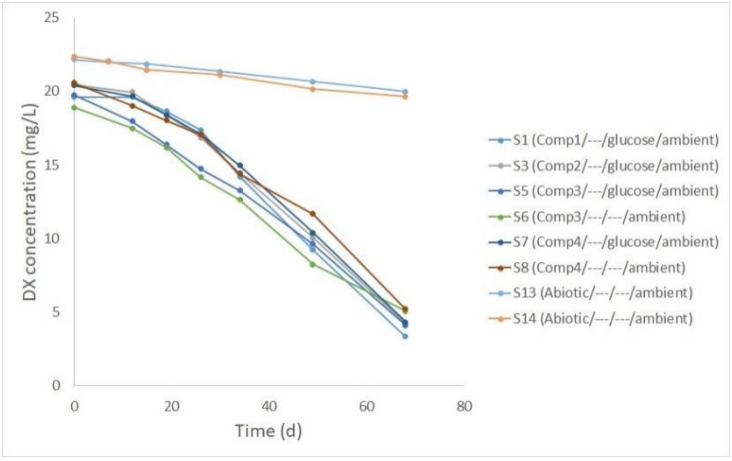


(A)

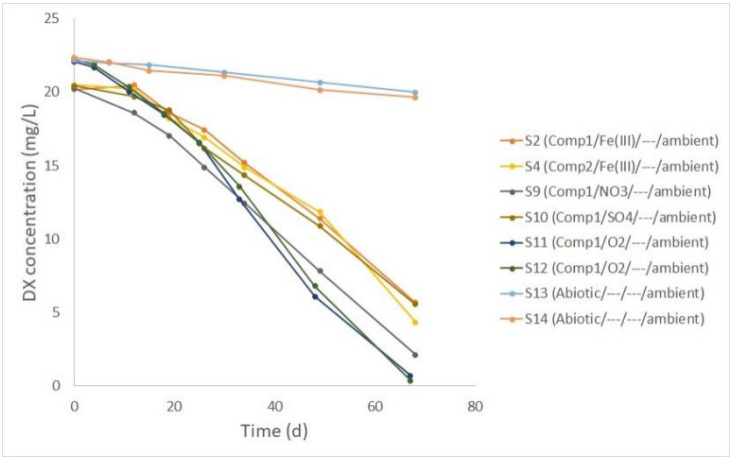


(B)

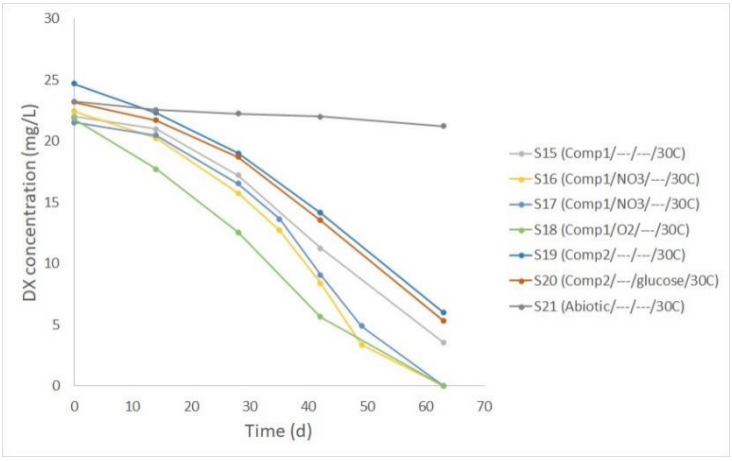


(C)

**Figure S1** DX biodegradation results of the acclimatization stage: (A) flasks at ambient condition with no added electron acceptor; (B) flasks at ambient condition with electron acceptors; (C) flasks at 30 ˚C.

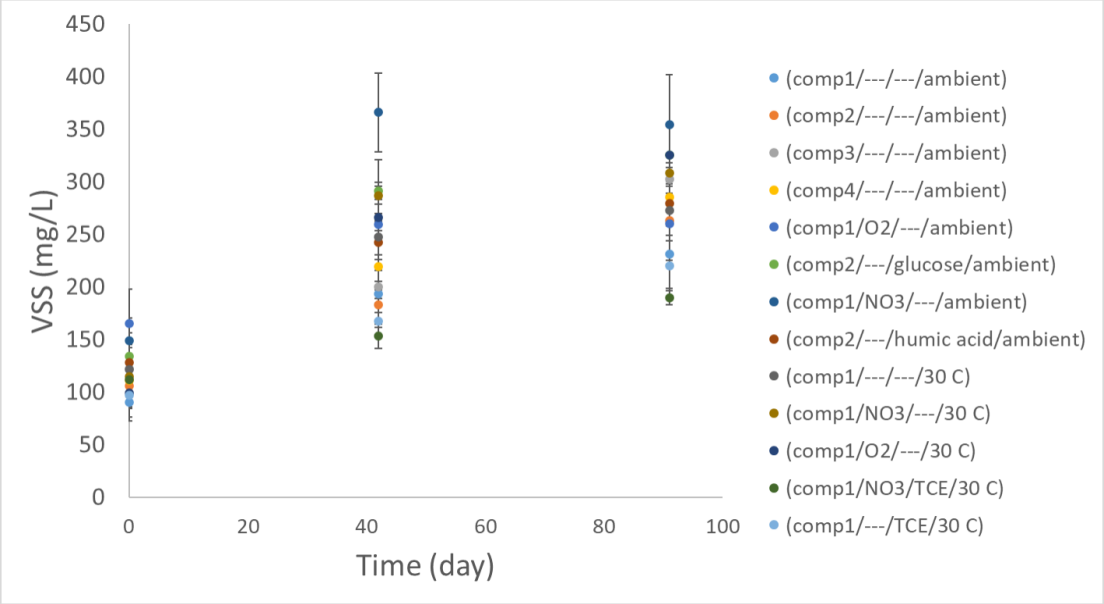


**Figure S2** Volatile suspended solids (VSS) concentration during the biodegradation stage.

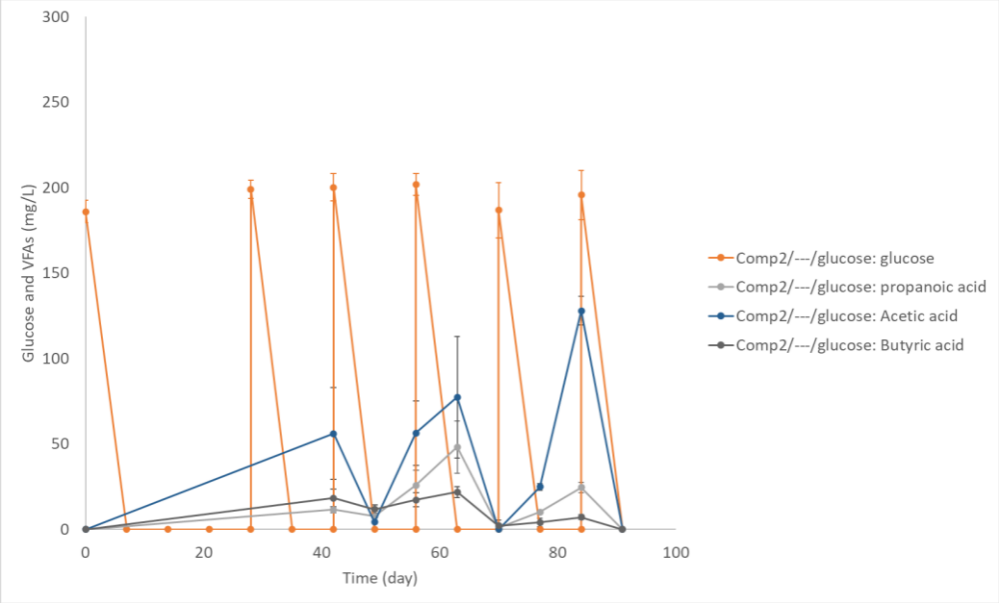


**Figure S3** Glucose, acetic acid, propanoic acid and butyric acid concentrations in the glucose-amended flasks (F11 and F12).

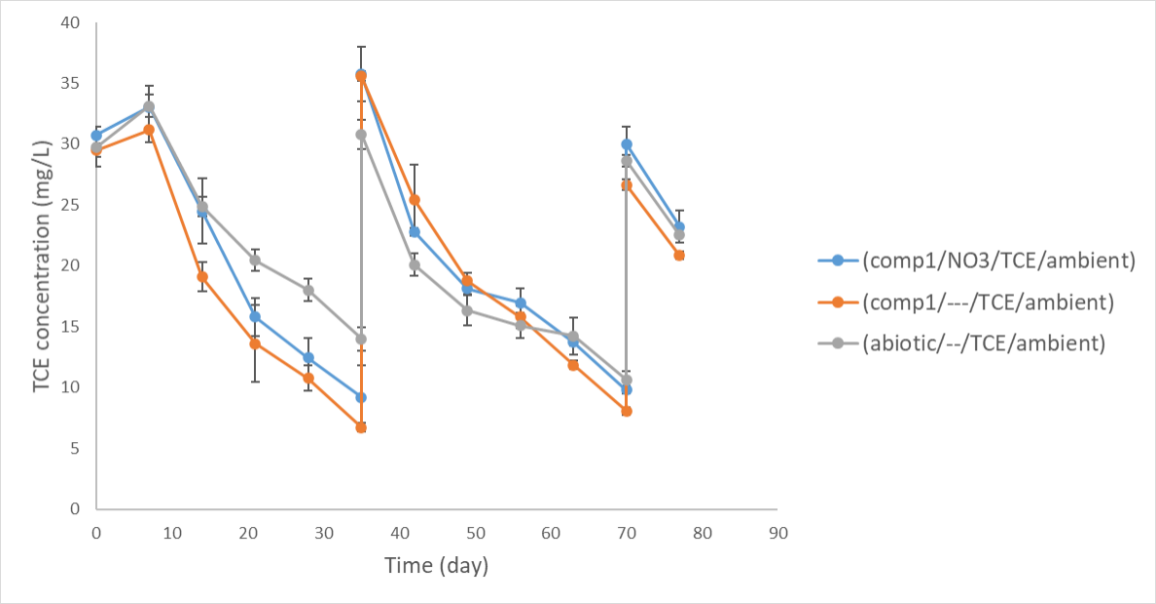


**Figure S4** TCE concentration during the biodegradation stage. TCE concentration in both inoculated and abiotic flasks decreased continuously due to evaporation. When its concentration reached below 10 mg/L, more TCE was added to bring the concentration to 30 mg/L, which is the concentration that TCE shows co-contaminant effect (Zhang et al., 2016).

# Appendix C Supplementary information for Chapter 4

**Table S1** Surface roughness parameters of the wood samples: Rq: root mean square roughness, Ra: Roughness Average, Rmax: arithmetic average roughness.

| Wood sample | Rq (µm) | Ra (µm) | Rmax (µm) |
|---|---|---|---|
| Untreated | 5.34-7.24 | 3.73-5.29 | 47.53-51.26 |
| Treated A | 10.17-12.35 | 8.12-9.54 | 75.99-82.36 |
| Treated B | 12.35-19.78 | 9.54-19.46 | 106.84-111.42 |

**Note:** Roughness parameters were measured on several areas of the wood samples, and the range of measurements are reported. The measurement uncertainty of the profilometer was 0.13 µm in the roughness range of wood samples.

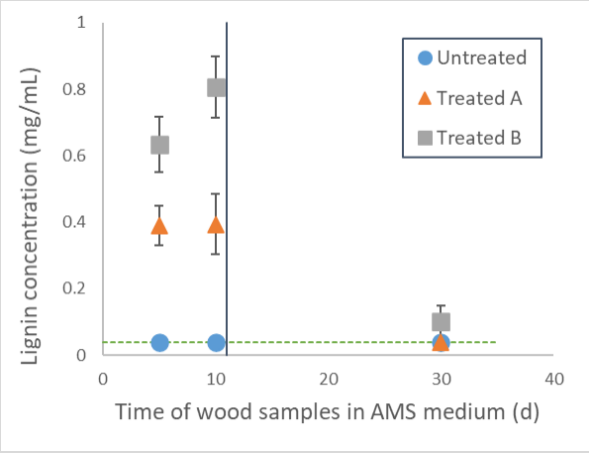


**Figure S1** Measurement of lignin concentration in the medium in the 10-days abiotic period followed by 20-days biofilm formation period.

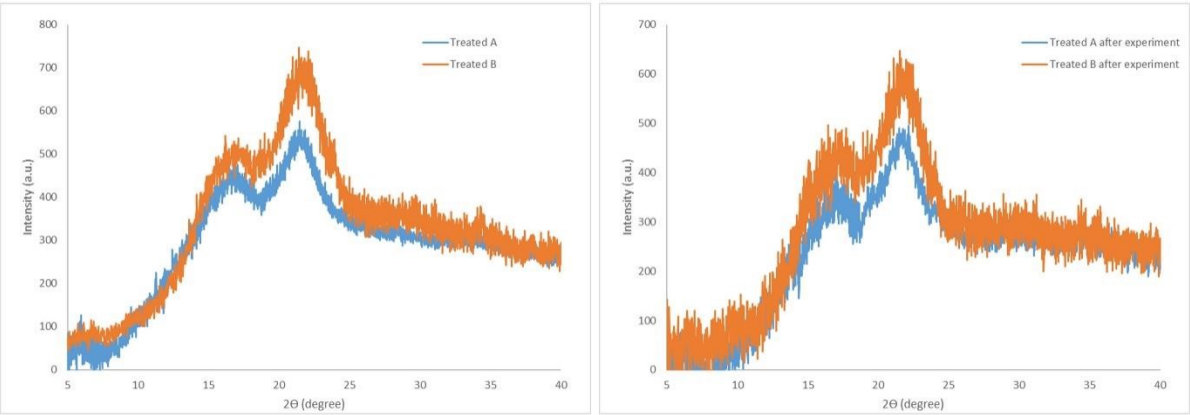


**Figure S2** XRD analysis of treated A and B wood samples (A) before and (B) after of the biofilm formation experiment.

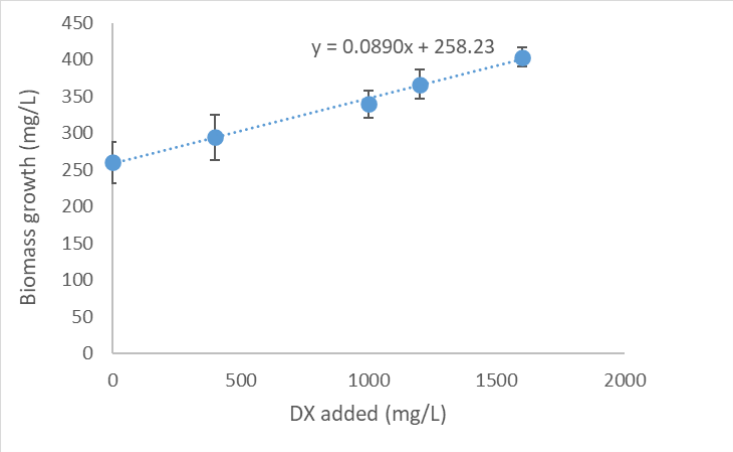


**Figure S3** Calculation of the yield for bacterial biomass based on mgVSS/L measurements versus total DX added.

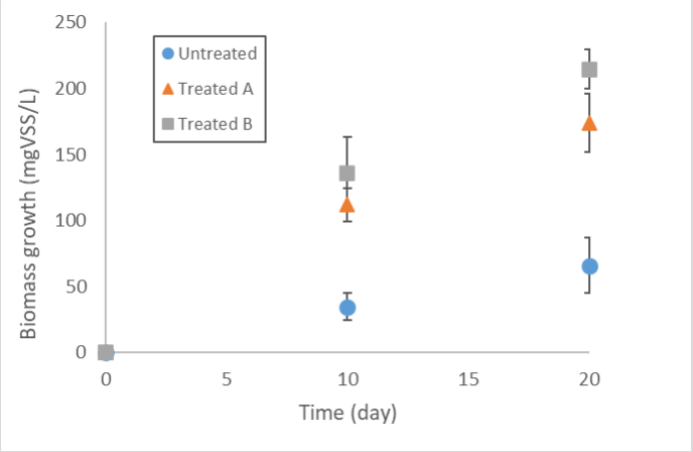


**Figure S4** Growth of bacterial biofilm on the untreated and treated wood samples during the biofilm formation period.

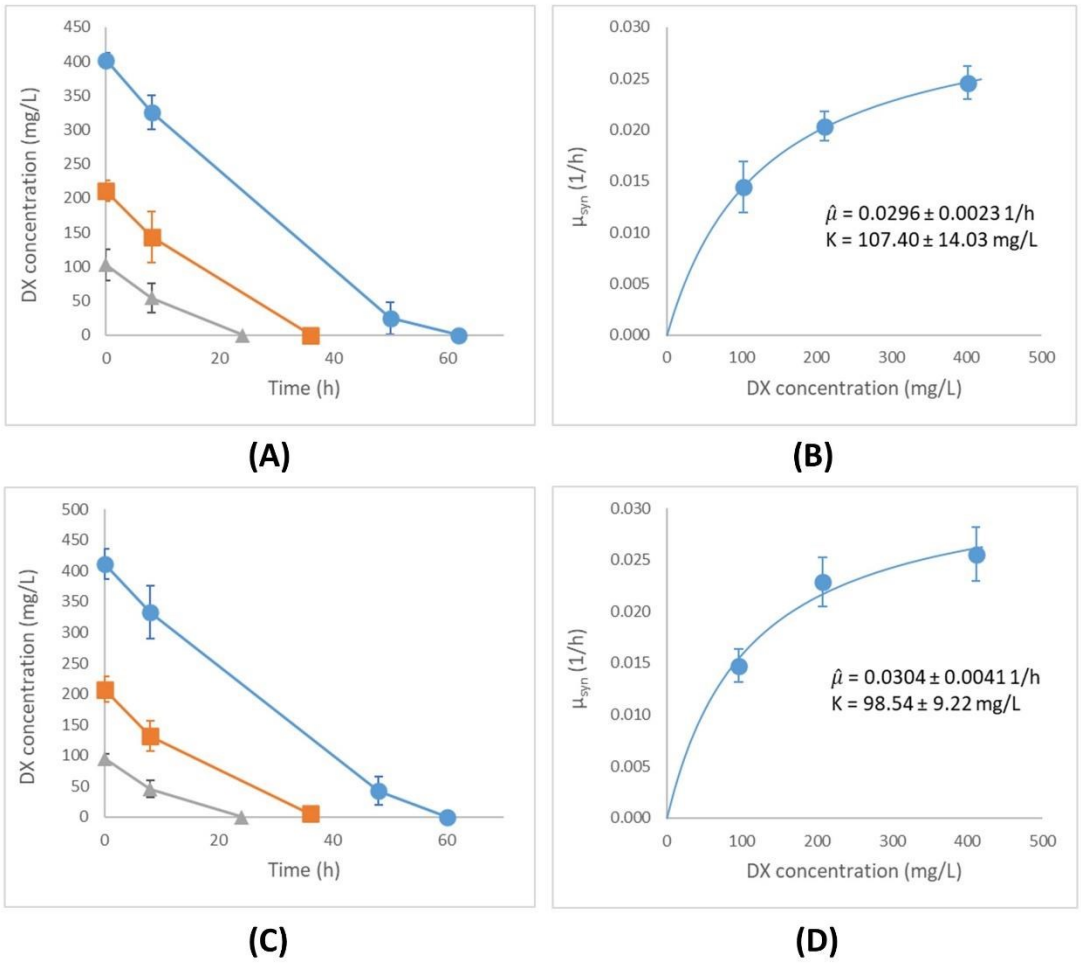


**Figure S5 (A)** DX biodegradation at various concentrations by biofilm on treated B wood samples and (B) Monod plot by biofilm on treated B wood samples; (C) DX biodegradation at various concentrations by regenerated biofilm on treated B wood samples and (D) Monod plot by regenerated biofilm on treated B wood samples.

# Appendix D Supplementary information for Chapter 5

**Table S1** Details of mass balance on the biomass based on mgVSS in the anode chamber of BER during the 110 days operation.

| Day | A. Sum of biomass formed on carrier (mgVSS/g Carrier) | B. Sum of biomass formed on carrier (mgVSS) | C. Sum of biomass removed from the system through effluent (mgVSS) | D. Sum of biomass formed on the membrane (mgVSS) | E. Sum of DX degraded (mg) | F. Sum of biomass removed from system through sampling (mgVSS) | G. Sum of biomass added to the system (mgVSS) | H. Sum of biomass removed from the system (mgVSS) | I. Total biomass measured in the system (mgVSS) |
|---|---|---|---|---|---|---|---|---|---|
| **BER operation with CB1190** | | | | | | | | | |
| 0 | 0 | 0 | 0 | 0 | 0 | 0 | 0 | 0 | 1629 |
| 10 | 0.03 | 2.9 | 28.8 | --- | 39.3 | 5.3 | 5.2 | 34.1 | --- |
| 25 | 0.12 | 11.1 | 72.0 | --- | 103.7 | 9.7 | 17.0 | 81.7 | --- |
| 41 | 0.26 | 23.8 | 118.1 | --- | 178.1 | 13.2 | 33.5 | 131.3 | --- |
| 71 | 0.57 | 51.1 | 204.5 | --- | 321.2 | 16.7 | 67.9 | 221.2 | --- |
| 82 | 0.64 | 57.7 | 236.2 | --- | 381.7 | 20.1 | 77.1 | 256.2 | --- |
| 97 | 0.70 | 63.2 | 279.4 | --- | 498.7 | 22.9 | 86.1 | 302.3 | --- |
| 110 | 0.75 | 67.1 | 316.8 | 26 | 607.5 | 25.9 | 93.1 | 342.7 | 1346 |
| **BER operation with microbial community on conductive carriers** | | | | | | | | | |
| 0 | 0 | 0 | 0 | 0 | 0 | 0 | 0 | 0 | 1492 |
| 16 | 0.05 | 4.32 | 63.8 | --- | 65.3 | 4.5 | 7.3 | 68.3 | --- |
| 31 | 0.10 | 9.30 | 123.5 | --- | 126.6 | 9.4 | 15.1 | 132.9 | --- |
| 37 | 0.16 | 14.0 | 147.4 | --- | 151.1 | 14.8 | 20.9 | 162.2 | --- |
| 50 | 0.20 | 18.3 | 199.2 | --- | 204.2 | 20.0 | 27.7 | 219.2 | --- |
| 64 | 0.26 | 23.1 | 255.0 | 12 | 261.4 | 25.0 | 35.2 | 280.0 | 1235 |
| **BER operation with microbial community on non-conductive carriers** | | | | | | | | | |
| 0 | 0 | 0 | 0 | 0 | 0 | 0 | 0 | 0 | 1571 |
| 10 | 0.5 | 4.5 | 26.2 | --- | 36.7 | 8.4 | 6.6 | 34.6 | --- |
| 27 | 1.2 | 10.8 | 44.3 | --- | 98.1 | 17.5 | 16.5 | 60.8 | --- |
| 47 | 2.1 | 18.9 | 122.5 | 10 | 185.4 | 29.1 | 28.9 | 151.4 | 1510 |

Mass balance equations (parameters are defined in the above table):

$$B\ (mgVSS) = A\ (\frac{mgVSS}{gCarrier}) \times (90\ g\ in\ case\ of\ conductive\ or\ 9\ g\ in\ case\ of\ non-conductive)$$

$$C\ (mgVSS) = day\ (d) \times 0.1\frac{mL}{min} \times 60 \times 24\frac{min}{d} \times average\ of\ biomass\ concentration\ in\ effluent\ (\frac{mgVSS}{L}) \times \frac{1L}{10\,00mL}$$

$$E\ (mg) = day\ (d) \times 0.1\frac{mL}{min} \times 60\ \times 24\frac{min}{d} \times average\ of\ (DX\ concentration\ in\ effluent - DX\ concentration\ in\ influent)\frac{mg}{L} \times \frac{1L}{1000mL}$$

$$G\ (mgVSS) = B(mgVSS) + D(mgVSS) \times \frac{day(d)}{total\ operation\ time\ (d)}$$

$$H\ (mgVSS) = C\ (mgVSS) + F\ (mgVSS)$$

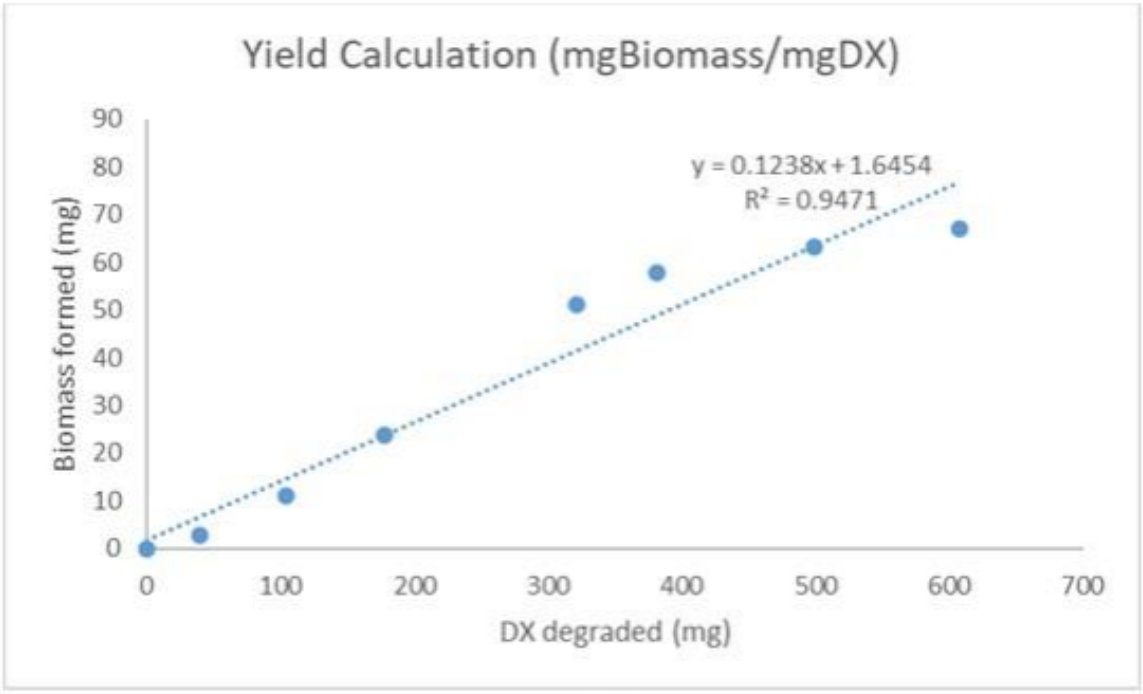


**(A)**

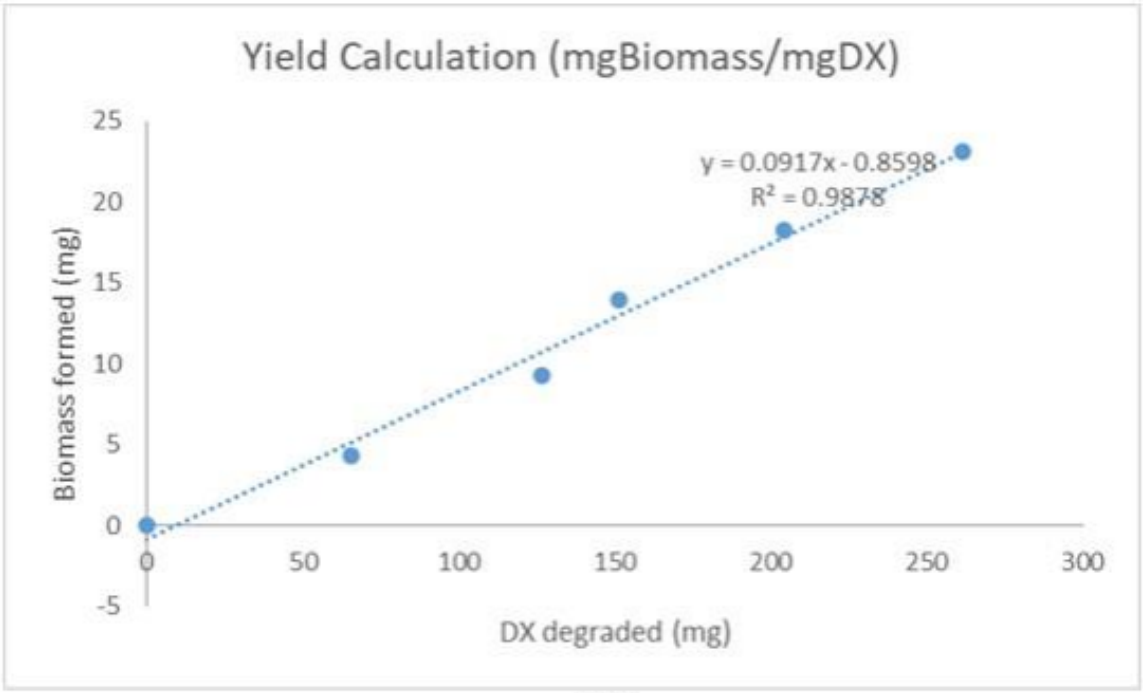


**(B)**

**Figure S1** Yield of biomass per DX degraded (mgVSS/mgDX) during the BER's operation with (A) CB1190 and (B) microbial community.

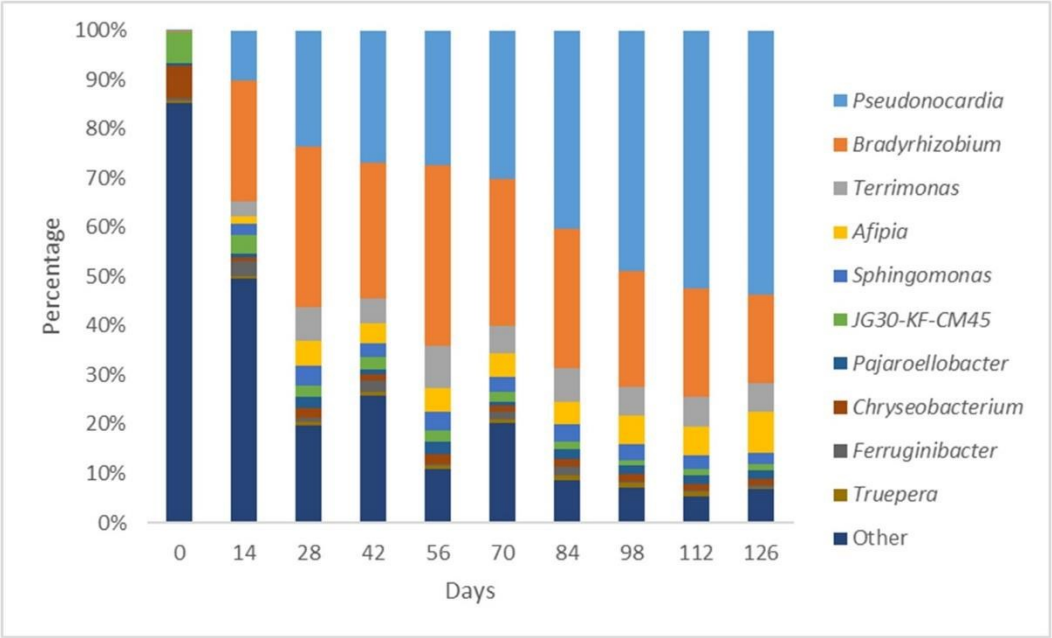


**Figure S2** Transition of the microbial community during the 18 weeks period of acclimation to DX.

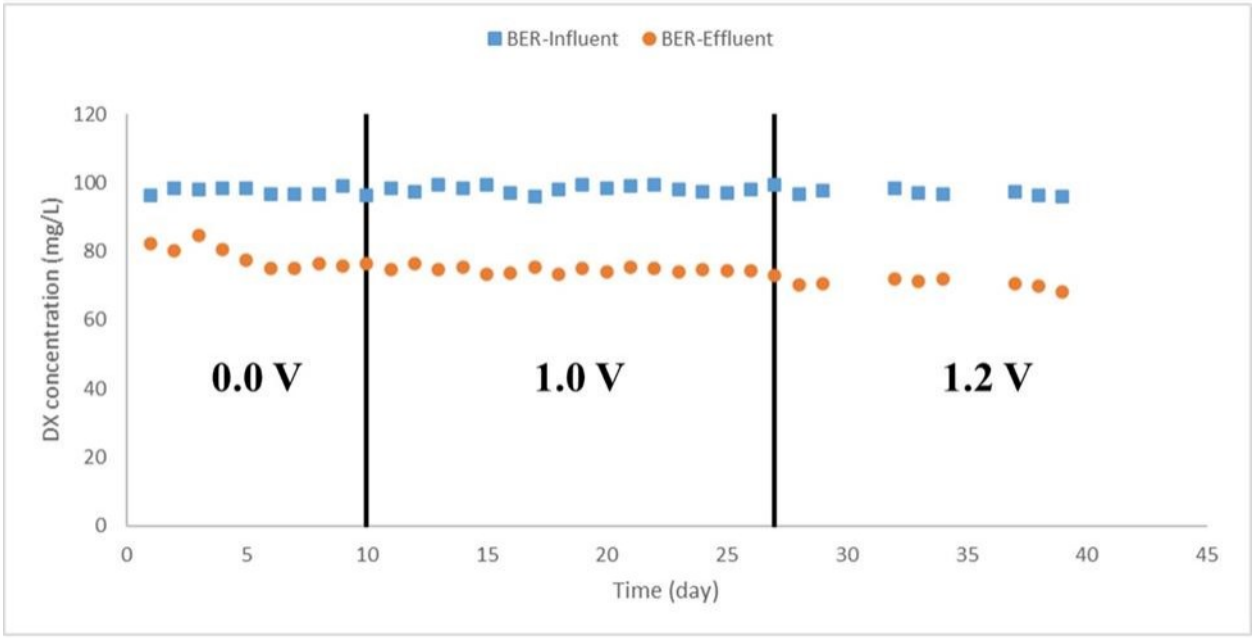


**Figure S3** DX concentration in the influent and effluent of the anode chamber of BER during its biological operation with microbial community biofilm on non-conductive carriers.

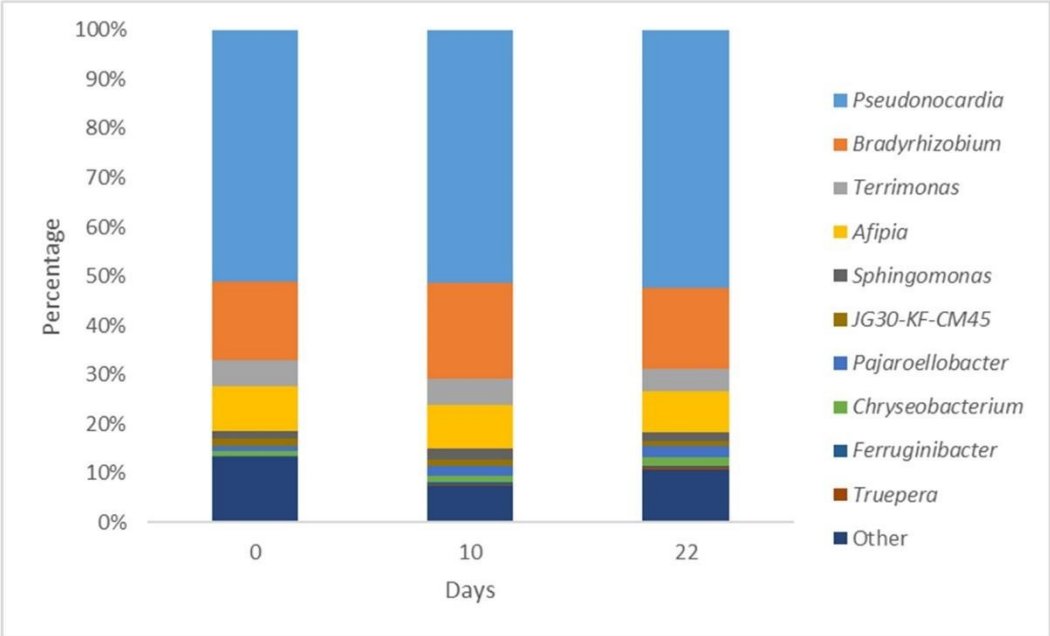


**Figure S4** Transition of microbial community during the BER's biological operation with microbial community biofilm on non-conductive carriers.